



UPPSALA  
UNIVERSITET

UPTEC W 21016

Examensarbete 30 hp

April 2021

# Opportunities for increased nutrient recovery at centralised wastewater treatment plants through urine separation

---

Hanna Gustavsson



## ABSTRACT

### Opportunities for increased nutrient recovery at centralised wastewater treatment plants through urine separation

*Hanna Gustavsson*

Municipal wastewater contains a significant amount of nutrients such as phosphorus (P) and nitrogen (N). Therefore have the interest of recovering these nutrients at wastewater treatment plants (WWTP) increased. Nutrient recovery would generate revenue for the WWTP, as it is possible to sell the products as fertiliser. Today, there are several techniques on the market to recover P as magnesium ammonium phosphate (MAP) and N as ammonium sulphate (AMS). Urine is the fraction contributing with the highest concentration of nutrients. Techniques to separate urine from the rest of the wastewater have been developed. These techniques enable the possibility to recover nutrients from the urine fraction separately; this is beneficial since the nutrient concentration would be higher. The purpose with this study was to examine the possibility for increased nutrient recovery at centralised WWTPs through urine separation.

Different techniques for nutrient recovery were compared by their recovery efficiency, chemical demand, and hydraulic retention time (HRT). A WWTP with enhanced biological P removal was modelled with Danish Hydraulic Institute's (DHI) software WEST. Eight scenarios, with different percentage of the population equivalents using urine separation techniques, were simulated. The P recovery was calculated from phosphate (PO<sub>4</sub>) in the hydrolysed excess sludge and the separated urine. The N recovery was calculated from the ammonium (NH<sub>4</sub>) in the supernatant from the anaerobe digester. The theoretical biogas production was also calculated, from the modelled sludge.

The comparison of P recovery techniques showed no substantial differences in their recovery efficiency, chemical demand, and HRT. The comparison of N recovery techniques showed three techniques with a higher efficiency than the other methods. Ekobalans Fenix AB, CMI Europe Environment, and Organics developed these techniques. To determine which method to use, requests for proposal from different providers are recommended. As the urine separation increased, the influent P and N load decreased. When the urine separation increased and the operational parameters were kept constant, the effluent concentration of P and N decreased. The ratio of total Kjeldahl nitrogen (TKN) and total nitrogen (TN) however increased as the urine separation increased. The total MAP production calculated from the modelled hydrolysis showed that the production increased as the urine separation increased. On the other hand, the total MAP production from calculated hydrolysis showed a decrease in production as the urine separation increased. The difference in these results could be because of the performance of the modelled hydrolysis was better with a smaller nutrient load, resulting in a larger release of PO<sub>4</sub> as the urine separation increased. The total AMS production increased as the urine separation increased. This, due to the increase of the TKN:TN ratio. The biogas production was not substantially affected by the increased urine separation.

**Keywords:** Nutrient recovery, urine separation, magnesium ammonium phosphate, MAP, ammonium sulphate, AMS, and DHI's WEST

*Department of Information Technology, Uppsala University  
Box 337, SE-751 05 Uppsala, Sweden*

## REFERAT

### Möjligheter till ökad näringsåtervinning vid centraliserade avloppsreningsverk genom urinsortering

*Hanna Gustavsson*

Avloppsvatten innehåller en stor del näring i form av fosfor och kväve. Intresset för att återvinna den näringen som kommer in till avloppsreningsverken (ARVen) har ökat. Den återvunna näringen skulle kunna användas och säljas som gödningsmedel, vilket genererar en inkomst för ARVen samt minskar behovet av att importera mineralgödsel för jordbruken. På marknaden finns nu ett flertal tekniker för att ARV ska kunna återvinna fosfor till struvit (magnesiumammoniumfosfat, MAP) och kväve till ammoniumsulfat (AMS). Eftersom urin innehåller mest näring har även tekniker för att separera urinen från resten av avloppsvattnet utvecklats. Urinsorteringen möjliggör återvinning av näring från enbart urinfraktionen där näringen är mer koncentrerad. Syftet med detta arbete var att undersöka möjligheten att återvinna fosfor och kväve vid ett ARV då urinsorteringen ökar i dess verksamhetsområde.

En jämförelse av olika tekniker för näringsåtervinning genomfördes utifrån deras återvinningseffektivitet, kemikalieåtgång och hydrauliska retentionstid (HRT). Därefter modellerades ett ARV med biologisk fosforering med Danmarks hydrologiska instituts (DHI) program WEST med inflöden motsvarande olika procent av personekvivalenter med urinsortering. Fosforåtervinningen hos ARV beräknades för tre olika mängder av fosfat i överskottsslammet; efter en modellerad hydrolys och efter två beräknade hydrolyser. Kväveåtervinningen beräknades från ammoniumet i rejektvattnet från röt-kammaren. I den totala, teoretiskt möjliga, näringsåtervinningen ingår även näringsåtervinningen från den separerade urinen. Biogasproduktionen beräknades utifrån det simulerade primärslammet och överskottsslammet.

Jämförelsen mellan de undersökta teknikerna för fosforutvinning visade inte någon större skillnad i effektivitet, kemikalieåtgång eller HRT. Jämförelsen mellan de undersökta teknikerna för AMS-produktion visade tre tekniker som hade högre effektivitet än de andra. Dessa tekniker kom från Ekobalans Fenix AB, CMI Europe Environment och Organics. För att slutligen bestämma metod krävs ytterligare information kring kostnader, därför rekommenderas att anbud skickas till de olika företagen. Då urinsorteringen ökade i ett ARVs verksamhetsområde minskade inkommande fosfor och kväve. Flödet, COD (eng. Chemical Oxygen Demand) och total suspenderat material (eng. total suspended solids, TSS) minskade däremot inte nämnvärt. Då driftparametrarna hölls konstanta för ARV, minskade koncentrationen av fosfor och kväve i utflödet då urinsorteringen ökade. Däremot ökade förhållandet mellan totala Kjeldahlkvävet (TKN) (ammonium och organiskt kväve) och totala kvävehalten (TN) i utflödet då urinsorteringen ökade. MAP-produktionen utifrån den modellerade hydrolysen visade att produktionen ökade då urinsorteringen ökade. Produktionen utifrån den beräknade hydrolysen visade tvärtom. Skillnaden i resultaten kan bero på att den modellerade hydrolysen fungerade bättre då det var mindre näring in till reaktorn och mer fosfat kunde frigöras. Den totala AMS-produktionen ökade då urinsorteringen ökade detta tack vare att TKN:TN-halten ökade och det gynnar AMS-produktionen av bioslammet. Biogasproduktionen påverkades inte nämnvärt av ökad urinsortering.

**Nyckelord:** Näringsåtervinning, urinsortering, struvit, MAP, ammoniumsulfat, AMS, DHI's WEST

*Institutionen för informationsteknologi, Uppsala University  
Box 337, SE-751 05 Uppsala, Sverige*

## PREFACE

My brother always says in Swedish “Det löser sig,” when an obstacle comes his way. This translates to “Everything works out in the end” or as Google translated it: It dissolves. And so it did this time as well even though the obstacles in this thesis sometime seemed greater than they were. I should have learned that by now. This Master’s Thesis completes the final part of the MSc in Environmental and Water Engineering at Uppsala University and the Swedish University of Agricultural Science (SLU). The Thesis corresponds to 30 ECTS Credits and was a project from Sweden Water Research in Lund.

I want to thank my main supervisor PhD David Gustavsson at Sweden Water Research/VA SYD for the opportunity to do this project. I also want to say thanks for the guidance, support and patience through this project. I want to thank my co-supervisors Associate Professor Ulf Jeppsson at Lund University and Senior Adviser Håkan Jönsson at SLU for being available if any question or obstacle would come my way. I want to thank my academic supervisor Professor Bengt Carlsson at Uppsala University for your support and patience through out this project.

I want to say thanks Sten Blomgren at Danish Hydraulic Institute for the student software license to use WEST, it have been a pleasure to learn the program.

Last but not least I want to thank my family and friends for the unbelievable support you have shown me during this crazy time and throughout my studies. I could not have done it without you. Thank you for bringing me back to reality when my head was overwhelmed by this project. Please keep reminding me that everything works out in the end.

*Hanna Gustavsson  
Uppsala 2018*

Copyright © Hanna Gustavsson and Department of Information Technology, Uppsala University Box 337, SE-751 05 Uppsala, Sweden  
UPTEC W 21 016. ISSN 1401-5765  
Published digitally in DiVA, 2021, by the Department of Earth Sciences, Uppsala University, Uppsala. (<http://www.diva-portal.org/>)

## POPULÄRVETENSKAPLIG SAMMANFATTNING

### Möjligheter till ökad näringsåtervinning vid centraliserade avloppsreningsverk genom urinsortering

*Hanna Gustavsson*

I avloppsvattnet som kommer in till ett avloppsreningsverk finns stora mängder med näring så som fosfor och kväve. Denna näring kommer till största delen från den mat som vi människor äter. Näringen i maten kommer från den åkermark som maten växt på. Under lång tid har avloppsreningsverk endast fokuserat på att rena vattnet från näringen för att skydda det vattendrag som det reade avloppsvattnet släpps ut till. Men för att sluta kretsloppet för näringen och återföra den till den mark som den en gång försvann ifrån så har tekniker för att återvinna näringen i avloppsvattnet utvecklats. Avloppsreningsverken kan tjäna på att återvinna näringen genom att sälja det som gödningsmedel. Det innebär att vi i Sverige inte behöver vara lika beroende av att importera mineralgödsel.

Eftersom urin är den del av avloppsvattnet som har högst koncentration av näring så har även tekniker för att sortera bort urinen från resten av avloppsvattnet utvecklats. Den näringen från urinen som sorteras bort kan också återvinnas till gödningsmedel. Urinsorteringen leder till mindre näring in till avloppsreningsverket, vilket kan bidra till en enklare rening av vattnet. Genom att sortera ut och återvinna urinen för sig kan eventuellt den totala återvinningen av näring från allt avloppsvatten öka. Ett annat scenario är att den totala återvinningen minskar och det inte är lönsamt för avloppsreningsverket att investera i tekniker för näringsåtervinning om urinsorteringen i dess verksamhetsområde skulle öka. Syftet med detta arbete var att undersöka möjligheten till näringsåtervinning vid ett avloppsreningsverk då urinsorteringen bland de anslutna hushållen ökade. Samt studera hur biogasproduktionen påverkas av urinsorteringen.

Ett konceptuellt avloppsreningsverk modellerades i ett simuleringsprogram som heter WEST från Danmarks hydrologiska institut. Avloppsvattnet till modellerade avloppsreningsverket varierades för att visa olika scenarion med olika många personer som använder urinsortering. Totalt testades åtta olika scenarion. Scenarion var då 0 %, 1 %, 5 %, 10 %, 25 %, 50 %, 75 % och 90 % av de anslutna personerna använder sig av urinsortering. Då urinsorteringen ökar minskar mängden fosfor och kväve in i det modellerade avloppsreningsverket. Avloppsreningsverket bestod av en biologisk fosforrening. Biologisk fosforrening innebär att mikroorganismer, som bildar ett slam, renar vattnet från fosfor. Då slammet befinner sig i en tank som är utan syre kan fosfat-ackumulerande mikroorganismerna lagra flyktiga fettsyror, som finns i avloppsvattnet, för att få energi. Men för att kunna göra det måste de samtidigt frigöra fosfat som de har lagrat inom sig. När slammet sedan transporteras in i en tank med syre kommer de mikroorganismerna att använda de lagrade fettsyrorna till att växa. När de använt sig av fettsyrorna kan de lagra på sig fosfaten som nu finns i avloppsvattnet igen. De fosfor-ackumulerande mikroorganismerna kan lagra mycket fosfat då de kan spara den näringen till senare behov. I första tanken utan syre ökar först fosfaten i avloppsvattnet för att sedan minska när det kommer in i en tank med syre. I en välfungerande biologisk fosforrening kommer det bli en nettominskning av fosfor. Slammet separeras från vattnet när mikroorganismerna har som mest fosfor lagrat inom sig. En del av slammet kommer att cirkulera tillbaka till första tanken utan syre men eftersom mikroorganismerna växer behövs en del att tas bort. Den delen av slammet som tas bort kallas överskottsslam. Det är från överskottsslammet som näringen sedan kommer återvinnas från. För att kunna återvinna

fosfor från överskottsslammet behöver det behandlas i en tank utan syre för att mikroorganismerna ska släppa ifrån sig den lagrade fosfor igen. Från och med nu kallas den process för P-släpp. Även en tank för P-släpp ingick i det modellerade avloppsreningsverket.

Då det finns flera olika tekniker för fosfor- och kväveåtervinning genomfördes en jämförelse av ett antal teknikers återvinningseffektivitet, kemikalieåtgång och uppehållstiden i tanken (HRT, eng. hydraulic retention time). Alla metoder kunde inte jämföras på grund av tidsramen av projektet. Ett krav på de tekniker som jämfördes var att de fanns i implementerade i full skala. Jämförelsen av tekniker för fosforåtervinning visar ingen större skillnad mellan deras återvinningseffektivitet, kemikalieåtgång eller uppehållstiden. Effektiviteten är generellt 90 %, vilket betyder att 90 % av fosfaten som kommer in i återvinningstanken återvinns till magnesiumammoniumfosfat (MAP). MAP fungerar som ett gödningsmedel. När teknikerna för kväveåtervinning jämfördes visade det sig att tre tekniker hade en bättre återvinningseffektivitet än de andra. Dessa tekniker är utvecklade av Ekobalans Fenix AB, CMI Europe Environment och Organics. Effektiviteten för dessa är generellt 90 %, och slutprodukten blir ammoniumsulfat (AMS). Men för att ta ett slutgiltigt beslut över vilken metod som bör investeras i bör anbud skickas ut till samtliga företag för att få mer specifik information över deras lösningar.

Då urinsorteringen ökar så minskar koncentrationen av totalfosfor och totalkväve i utflödet från avloppsreningsverket nämnvärt. Däremot så ökar koncentrationen av totala Kjeldahlkvävet (TKN). Totala Kjeldahlkvävet är ett samlingsnamn för ammonium och kväve bundet till organiskt material och partiklar; TKN är en del av totalkvävet. Att TKN ökar men totalkvävet minskar betyder att förhållandet mellan dem ökar när urinsorteringen ökar. Ökningen av TKN då urinsorteringen ökar beror på att mängden mikroorganismer som tar hand om kvävet i ARV minskar.

Det modellerade P-släppet är inte lika effektivt som litteraturvärden visade. Med en P-släppsenhet från Ostara Nutrient Recovery Technologies Inc, Kanada, kan det antas att 70 % av fosfor i överskottsslammet frigörs. En annan enhet från Ekobalans Fenix AB visade ett P-släpp på 50 %. Därför beräknades produktionen av MAP för de tre olika P-släppen. Då den totala MAP-produktionen från både fosfor från modellerade P-släppet och den separerade delen urin beräknades visade det sig att MAP-produktionen ökar då urinsorteringen ökar. Totala MAP-produktionen för de beräknade P-släppen och fosfor från den separerade urinen visade att MAP-produktionen minskar då urinsorteringen ökar. Skillnaden kan bero på att det modellerade P-släppet fungerade bättre då mindre näring kom in till enheten, vilket i sin tur leder till ökad P-släpp då urinsorteringen ökar. Den totala AMS-produktionen ökar då urinsorteringen ökar. Detta beror på att TKN:TN-halten i avloppsreningsverket ökar då urinsorteringen ökar, vilket gynnar AMS-produktionen. Biogasproduktionen förändras inte nämnvärt då urinsorteringen i verksamhetsområdet ökar.

## TERMINOLOGY

1Q	First quartile
3Q	Third quartile
AMS	Ammonium sulphate. Its chemical formula is $(\text{NH}_4)_2\text{SO}_4$
AS	Activated sludge
BOD	Biochemical oxygen demand
COD	Chemical oxygen demand
DHI	Danish Hydraulic Institute
EBPR	Enhanced biological phosphorus removal
IQR	Interquartile range. The range between the first and third quartile
MAP	Magnesium ammonium phosphate also called struvite. Its chemical formula is $\text{MgNH}_4\text{PO}_4 \cdot 6\text{H}_2\text{O}$ .
N	Nitrogen
NH <sub>4</sub>	Ammonium
P	Phosphorus
PO <sub>4</sub>	Phosphate
PAO	Polyphosphate accumulating organisms
PE	Population equivalent
Q	Flow rate, given in m <sup>3</sup> /day if nothing else is noted.
SOR	Surface overflow rate
SRT	Solids retention time
TKN	Total Kjeldahl Nitrogen
TSS	Total suspended solids
VFA	Volatile fatty acids (i.e. acetate acid)
WAS	Waste activated sludge
WWTP	Wastewater treatment plant

# TABLE OF CONTENT

<b>1</b>	<b>INTRODUCTION</b>	<b>1</b>
1.1	OBJECTIVE	1
1.2	DELIMITATIONS	2
<b>2</b>	<b>THEORY</b>	<b>2</b>
2.1	MUNICIPAL WASTEWATER	2
2.1.1	Characteristics of municipal wastewater	2
2.2	WASTEWATER TREATMENT PLANTS	4
2.2.1	Mechanical treatment processes	4
2.2.2	Activated sludge process and enhanced biological phosphorus removal	5
2.2.3	Sludge treatment	6
2.2.4	Effects of urine separation on wastewater treatment plants	6
2.3	ACTIVATED SLUDGE MODEL NUMBER 2d	6
2.3.1	COD components	7
2.3.2	Phosphorus components	8
2.3.3	Nitrogen components	8
2.4	NUTRIENT RECOVERY	8
2.5	MAGNESIUM AMMONIUM PHOSPHATE	9
2.5.1	Methods with an included unit for hydrolysis of PO <sub>4</sub>	10
2.5.2	Methods that require an extra treatment step for hydrolysis of PO <sub>4</sub>	12
2.5.3	Comparison of the methods	14
2.6	AMMONIA STRIPPING	15
2.6.1	Methods for ammonium recovery	16
2.6.2	Comparison of the methods	17
<b>3</b>	<b>METHOD</b>	<b>19</b>
3.1	THE CONCEPTUAL WASTEWATER TREATMENT PLANT	19
3.2	INPUT DATA	19
3.2.1	Measured data	19
3.2.2	Input data for scenarios with urine separation	20
3.3	MODEL IN DHI'S SOFTWARE WEST	21
3.4	THEORETICAL MAP PRODUCTION	29
3.5	THEORETICAL AMS PRODUCTION	29
3.6	THEORETICAL BIOGAS PRODUCTION	30
3.7	CALIBRATION	30
3.7.1	Mass balance	30
<b>4</b>	<b>RESULTS</b>	<b>31</b>
4.1	DATA SERIES	31
4.2	THE FULL WWTP MODEL	33
4.2.1	Final fractionation and wastewater characterisation	35
4.2.2	Calibrated primary clarifier	36
4.2.3	Calibrated ASUs	37
4.2.4	Calibrated secondary clarifier	37
4.3	EFFECTS OF URINE DIVERSION ON THE WWTP	37
4.3.1	Influent	37
4.3.2	Effluent	40
4.4	RECOVERED P AND MAP PRODUCTION	47

4.5	RECOVERED N AND AMS PRODUCTION .....	51
4.6	BIOGAS PRODUCTION .....	53
<b>5</b>	<b>DISCUSSION .....</b>	<b>53</b>
5.1	INPUT DATA .....	53
5.2	WWTP MODEL.....	54
5.3	EFFECTS OF URINE SEPARATION ON THE WWTP .....	54
5.4	RECOVERED P AND MAP PRODUCTION.....	55
5.5	RECOVERED N AND AMS PRODUCTION.....	56
5.6	BIOGAS PRODUCTION .....	56
5.7	METHODS FOR NUTRIENT RECOVERY .....	57
5.8	IMPLICATIONS OF THIS STUDY .....	57
<b>6</b>	<b>CONCLUSION.....</b>	<b>58</b>
6.1	FUTURE STUDIES AND APPLICATIONS.....	58
	<b>REFERENCES .....</b>	<b>60</b>
	<b>APPENDIX .....</b>	<b>65</b>
A.	MODELLED VS. MEASURED INFLUENT FOR SCENARIO 0.....	65
B.	INPUT DATA FOR SCENARIO 0.....	67

# 1 INTRODUCTION

Already in the 1990's the scarcity of phosphate ores was discussed. Steen (1998) examined how the global reserves would change in the future. Back then, the annual global phosphate production was around 40 million tonnes phosphorus pentoxide ( $P_2O_5$ ) and 80% of it was used in the mineral fertiliser industry. It was known that the non-renewable phosphorus (P) supply was being depleted, especially the high quality reserves. A lower concentration of phosphate in the rock results in a lower quality product when mining and in more waste products. This also leads to higher costs and chemicals required. Another problem with the mineral fertiliser discussed by Steen (1998) was the fact that twelve out of thirty countries producing phosphate rock control 95% of the total global production. USA, China and Morocco are controlling 50% of the global production. As the population grows, the agricultural demand and production will increase, which in turn will increase the fertiliser usage. Estimations of how long the mineral phosphate reserves will last have been presented through the years (Steen, 1998; Vaclav, 2000); e.g. Steen (1998) predicted that 50% of the high-quality reserves would be used up by year 2060–2070.

The wastewater excreted from humans contains nutrients, such as P, nitrogen (N), and potassium (Jönsson *et al.*, 2005). In Germany is the wastewater generated during a year estimated to contain the same amount of P as more than half of the imported fertiliser used per year (Angrick *et al.*, 2013). The aim of the wastewater treatment plants (WWTPs) has been to remove these nutrients from the water before releasing into a recipient (Tchobanoglous *et al.*, 2014b). The reports of the depletion of P ores and the uneven distribution of P reserves around the world have increased the interest of not only removing the nutrients at WWTPs but also recovering the nutrients. The recovered nutrients can be used as fertiliser, resulting in revenue for the WWTP and less dependence on imported mineral fertiliser.

Urine is the fraction containing the highest concentrations of nutrients. Therefore, development of techniques to separate the urine from the rest of the wastewater is interesting. Several new-development areas, often called eco-villages, around the world have implemented these solutions (Kvarnström *et al.*, 2006; Hood *et al.*, 2009). An increase in urine separation would lead to lower amounts of nutrients entering the WWTPs but if nutrient recovery techniques have been installed at WWTP it might no longer be profitable if there is not enough nutrients. Another possibility is that the nutrient recovery from the separated urine and from the sludge at the WWTP results in higher recovery than with no urine separation.

## 1.1 OBJECTIVE

The objective with this Master's thesis was to investigate the possibility of nutrient recovery at a centralised WWTP as the urine separation increases in its catchment area. Eight scenarios with different percentage of population equivalent (PE) using urine separation will be studied and compared by the amount of recovered P and N from the influent to the WWTP. The different scenarios studied will be 0%, 1%, 5%, 10%, 25%, 50%, 75% and 90% of the total PE using urine separation techniques. The conceptual WWTP includes methods for P and N recovery. Different recovery techniques will be compared. The main aim is to answer the following questions:

- How will the influents to the WWTP change for the different scenarios?
- How will the effluents from the WWTP change for the different scenarios?

- How much of phosphorus and nitrogen are possible to recover?
- How will the theoretical biogas production differ between the scenarios?
- Which method for phosphorus recovery is best regarding recovery efficiency, chemical demand, and hydraulic retention time?
- Which method for nitrogen recovery is best regarding recovery efficiency, chemical demand, and hydraulic retention time?

## 1.2 DELIMITATIONS

- The conceptual WWTP has no requirement of enhanced nitrogen removal.
- The number of nutrient recovery methods presented is limited. There are several methods that have not been mentioned due to limited time and information. One requirement of the methods mentioned is that they have been implemented in full-scale.
- The fertiliser production and biogas production are theoretical values.
- The dimensions and operational parameters for the modelled WWTP will not be changed for the different scenarios.

## 2 THEORY

### 2.1 MUNICIPAL WASTEWATER

Municipal wastewater is used water from households, public facilities and industries. Therefore, the wastewater contains human excreta, personal and household maintenance products (such as laundry detergent and soap), food waste, and other organic and inorganic compounds. It is common to divide wastewater from households and public facilities into fractions such as urine, faecal, greywater and flush water. Each fraction has different physical properties, and chemical and biological constituents (Tchobanoglous *et al.*, 2014b).

#### 2.1.1 Characteristics of municipal wastewater

The characteristics of wastewater and each fraction vary depending on its origin; however, some generalisations values for each fraction can be made. Jönsson *et al.* (2005) have studied and summarised values for different compounds in each fraction. The default values in the report from Jönsson *et al.* (2005) was estimated from how much of different compounds that would be released from human activities per day. The values are only meant to be used under Swedish conditions. Compounds found in each fraction can be solids, heavy metals, nutrients (such as P and N) and other organic and inorganic compounds. In Table 1 the concentrations of H<sub>2</sub>O, total solids (TS), total suspended solids (TSS), volatile solids (VS), chemical oxygen demand (COD<sub>tot</sub>), biological oxygen demand (BOD<sub>7</sub>), total Kjeldahl nitrogen (TKN), and total P (TP) are presented for each fraction as well as the sum of each compound for the entire household wastewater. The TKN is calculated from the total N concentration by subtracting the nitrate- and nitrite-nitrogen concentration (Tchobanoglous *et al.*, 2014b). Jönsson *et al.* (2005) have taken into account the fact that a person generates around 30% extra greywater when away from the household. Therefore, the concentration of TP in household greywater retrieved from Ek *et al.* (2011) is increased with 30%.

Table 1: Amount of H<sub>2</sub>O, TS, TSS, VS, COD<sub>tot</sub>, BOD<sub>7</sub>, TKN, and TP in the urine, faecal, and greywater fraction of municipal wastewater and the sum of each fraction constituting the household wastewater generated per PE and day. The values origin from Jönsson et al. (2005) if nothing else is noted.

Compound	Urine	Faecal	Greywater	Household wastewater	Unit
H <sub>2</sub> O	1487	110.6	129766*	131363.6	g PE <sup>-1</sup> day <sup>-1</sup>
TS	20	53.1	71.2	144.3	g PE <sup>-1</sup> day <sup>-2</sup>
TSS	0.76	48.0	17.6	66.36	g PE <sup>-1</sup> day <sup>-3</sup>
VS	7.4	46.4	41.6	95.4	g PE <sup>-1</sup> day <sup>-4</sup>
COD <sub>tot</sub>	8.5	64.1	62.4	135	g PE <sup>-1</sup> day <sup>-5</sup>
BOD <sub>7</sub>	5.0	34.1	33.8	72.9	g PE <sup>-1</sup> day <sup>-6</sup>
TKN	11.0	1.5	1.52	14.03	g PE <sup>-1</sup> day <sup>-7</sup>
TP	0.9	0.5	0.156**	1.556	g PE <sup>-1</sup> day <sup>-8</sup>

\* calculated from 130 l PE<sup>-1</sup> day<sup>-1</sup> (Jönsson et al. 2015) times 998.2 g l<sup>-1</sup>, which is the density of water at 20°C (Aylward & Findlay 2008)

\*\* 130% of 0.12 g PE<sup>-1</sup> day<sup>-1</sup>, which is retrieved from Ek et al. 2011

Urine is the fraction with highest concentration of P and TKN, with a value of 0.9 and 11.0 g/PE, day, respectively as seen in Table 1. According to Jönsson et al. (2005) is 91% of the P in urine inorganic, mainly phosphate (PO<sub>4</sub>), where the rest can be assumed to be particulate P, and 95% of the incoming TKN can be assumed to be ammonium (NH<sub>4</sub>). The average number of flushes, containing urine, is 6.5 times per PE and day.

Jönsson et al. (2005) defines the faecal fraction as faeces along with toilet paper. The number of flushes, with this fraction, is assumed to be 1–2 times per PE and day. Out of the total amount of N, 1.53 g/PE, day, is approximately 50% soluble in water. The P is mainly in the form of calcium phosphate granules and the dissolved P is recommended to be set to 20% out of the total P.

In order to more clearly see how the household wastewater is constituted by each fraction, the percentages of each compounds originated from each fraction are calculated from the values in Table 1. Table 2 below displays each compound's fractionation.

Table 2: The percentage of compounds each fraction contributes to the total household wastewater. Calculated from values in Table 1.

Compound	Urine	Faecal	Greywater	Household wastewater
H <sub>2</sub> O	1.13	0.0842	98.8	100
TS	13.9	36.8	49.3	100
TSS	1.15	72.3	26.5	100
VS	7.76	48.6	43.6	100
COD <sub>tot</sub>	6.30	47.5	46.2	100
BOD <sub>7</sub>	6.86	46.8	46.4	100
TKN	78.4	10.7	10.9	100
TP	57.8	32.1	10.0	100

Table 2 shows that urine is the fraction that contributes to most of the P and N found in the wastewater. The faecal fraction however contributes to most of the BOD and COD.

## **2.2 WASTEWATER TREATMENT PLANTS**

Before wastewater can be released into a recipient, it needs to be treated in order to not affect the recipient and the environment negatively. It should be treated to avoid eutrophication and spreading of heavy metals and pathogens (Tchobanoglous *et al.*, 2014b). The common method to clean wastewater from such compounds is to combine mechanical treatment processes with biological and chemical treatment processes and let the wastewater flow through each step (Tchobanoglous *et al.*, 2014a). It is possible to remove P through either a biological treatment process, called enhanced biological phosphorus removal (EBPR), or through chemical treatment processes (Smolders *et al.*, 1994). The conceptual WWTP studied in this report has no chemical treatment process; thus will the chemical treatment processes not be explained further.

### **2.2.1 Mechanical treatment processes**

There are mechanical treatment methods that aim to remove small particles but still large enough to settle. These particles are removed with sedimentation basins. The basin is designed for the particles to settle at the bottom of the basin before the water reaches the outlet at the end of the basin. A sedimentation basin is usually found in the beginning of the WWTP, called primary clarifier, and after a biological or chemical treatment process, called secondary clarifier. The purpose of the primary clarifier is to remove particles that can disturb the following treatment steps. The purpose of the secondary clarifier is to separate the activated sludge generated in the biological treatment from the water (Water Environment Federation, 2005).

Takács *et al.* (1991) developed a dynamic model in order to describe the processes found in a clarifier. Solid-liquid separation processes can be divided into four types: discrete particle settling, flocculent particle settling, hindered settling and compression settling. The discrete particle settling is the process of particles able to settle individually without interaction with other particles. This process is related to the removal of coarse particle and grit. Flocculent particle settling is defined as the settling of solid particles through flocculation of them as they settle down. This process is found in primary clarifiers and in the top layer of the secondary clarifier. The third process, hindered settling, is described as the process where the mass of solid particle settles as a unit; this occurs due to inter-particle forces hindering the settling of individual particles. Compression settling is solid-liquid separation through compression. The compression of the mass of the particles is caused by the weight of particles added to the clarifier. The Takács' model is based on Vitasovic's model from 1986, which is based on a layered model. The models differ since the Takács' model includes a clarification component. Takács' model is also based on five different groups of layers: the top layer, layers above feed point, feed layers, layers under feed point and the bottom layer. The feed layer is where the inlet to the clarifier is positioned.

Takács' model is built on several parameters. Table 3 presents the values for each model parameter used for the steady-state simulations in Takács *et al.* (1991). Low load, medium load and high load represent a flow of 360, 450 and 600 m<sup>3</sup>/day, respectively.

Table 3: Parameter values used in the application of the model by Takács *et al.* (1991)

Parameter	Unit	Low Load	Medium Load	High load
$v_0$	m/d	214.2	370.0	172.8
$v_0'$	m/d	150.2	142.9	112.1
$r_p$	$m^3/g$	$5.71e^{-3}$	$2.86e^{-3}$	$2.70e^{-3}$
$r_h$	$m^3/g$	$3.64e^{-4}$	$3.78e^{-4}$	$2.93e^{-4}$
$f_{ns}$	-	$1.23e^{-3}$	$2.28e^{-3}$	$2.59e^{-3}$

The parameter  $v_0$  describes the maximum theoretical settling velocity and  $v_0'$  the maximum practical settling velocity; both given in m/day. Parameter,  $r_p$ , is a settling parameter related to the low concentration and slowly settling component of the suspension given in  $m^3/day$ , while  $r_h$  is related to the hindered settling component of settling velocity equation also given in  $m^3/day$ . The last parameter,  $f_{ns}$ , is the non-settleable fraction of the incoming TSS.

### 2.2.2 Activated sludge process and enhanced biological phosphorus removal

The activated sludge (AS) process is a biological treatment process and it is through this process an EBPR is possible (Smolders *et al.*, 1994). The objectives with the AS process can be divided into three categories, which are to transform biodegradable substrate in the water to acceptable end products, form settable biological flocs with in-captured suspended non-settable colloidal solids and last but not least remove nutrients. This treatment depends on microorganisms, which constitute the AS. The microorganisms require a source of energy, carbon and nutrients in order to function properly and grow new biomass. Their source of energy and carbon are usually referred to as substrate. It is desirable to have a wide range of microorganisms competing for substrate. The population of microorganisms is dynamic and will be determined by natural selection under the specific conditions in the tank (Tchobanoglous *et al.*, 2014c).

Smolders *et al.* (1994) studied the EBPR process and the conditions required in the AS unit in order to achieve the P removal. The AS has to pass through anaerobic conditions first and then aerobic condition with recirculation of the sludge. This type of conditions will benefit polyphosphate-accumulating organisms (PAOs). The PAOs are able to store volatile fatty acids (VFA) where no other electron acceptor is available, which is the case under anaerobic conditions. The energy used to store the VFA originates from the hydrolysis of assimilated polyphosphate. There will be an increase of  $PO_4$  in the wastewater as the PAOs store VFA and release stored  $PO_4$  into the wastewater. When the activated sludge then goes through the aerobic conditions are the PAOs able to utilise the stored VFA as energy source for their growth; at the same time will the PAOs assimilate the  $PO_4$  in the wastewater as polyphosphate. The PAO's biomass will increase and the dissolved P in the wastewater decreases. The P in the wastewater decreases as the P-rich sludge is separated from the water stream. Most of the sludge will be returned to the anaerobic unit but some will be removed from the system as waste activated sludge (WAS).

For the EBPR process to function properly the flow of return sludge has to be large enough. The return sludge flow has to keep the biomass high enough to treat the incoming nutrient and substrate, but low enough to not overflow the units. This can be controlled by the solids retention time (SRT). Smolders *et al.* (1994) kept the SRT in a sequencing batch reactor at

nine days to study the EBPR process. Another recommendation from Olsson et al. (2005) for an appropriate SRT for EBPR is between 5–12 days. When Aspegren (1995) evaluated a high loaded AS process for EBPR in a pilot system at Sjölanda WWTP in Malmö, Sweden, the results showed that the anaerobic SRT should be higher than 0.5 days and the aerobic SRT should be longer than 2.5 days in order to achieve a well-functioned EBPR even at 10 °C.

### **2.2.3 Sludge treatment**

The WAS generated from the AS processes is removed from the main stream through a sedimentation basin. The WAS can thereafter be treated through anaerobic digestion to produce biogas and release nutrients (de Lemos Chernicharo, 2007). The anaerobic digestion can be divided into two steps: hydrolysis, where microorganisms convert complex compounds into VFAs, carbon dioxide (CO<sub>2</sub>) and hydrogen gases and the second step is the methane production. A specific group of microorganism, called methanogens, then transform the VFA and hydrogen into methane (CH<sub>4</sub>) and CO<sub>2</sub>. To produce 16 g of CH<sub>4</sub> requires 64 g of COD. The methane production will vary depending on the composition of the incoming sludge to the anaerobic digester and the conditions, such as the temperature, pH, and alkalinity. There is a release of N in the anaerobic digester from organically bound to ammonia. It is theoretically possible to release all the TKN into ammonia (de Lemos Chernicharo, 2007).

### **2.2.4 Effects of urine separation on wastewater treatment plants**

From section 2.1 above, it is shown that the wastewater fraction containing most of the nitrogen and phosphorus is urine. Table 2, shows that urine contributes with very small volume. Wilsenach and van Loosdrecht (2003) studied the impacts of urine separation on a WWTP with biological chemical P and N removal. If 100% of urine was collected separately would the total N in the influent to the WWTP decrease from 50 g N/m<sup>3</sup> to 11.4 g N/m<sup>3</sup>. The effect of 100% urine separation for the influent total P was a decrease of 2.7 g P/m<sup>3</sup> and for COD was it only a small decrease. The result of Wilsenach and van Loosdrecht's (2003) study showed that the ammonium concentration in the effluent from the WWTP increases as the urine separation increases. This could be explained by the fact that the number of nitrifying bacteria decreases as the urine separation increases; the effluent nitrate concentration however decrease (Wilsenach & van Loosdrecht, 2003). The conclusions made was that significant improvement of advanced biological nutrient removal processes was noticed up to around 60% urine separation; higher separation efficiency would not improve the effluent much further.

## **2.3 ACTIVATED SLUDGE MODEL NUMBER 2d**

The mathematical model used to resemble the EBPR process is the Activated Sludge Model 2d (ASM2d) developed by Henze et al. (1999). This model is an extension of the ASM2, which in turn is a development of the ASM1. The AS processes are described with kinetic and stoichiometric parameters, and process rate equations. Some of these processes are growth of biomass, decay of biomass, hydrolysis of particulate organic substrate, nitrification and chemical precipitation of P. The ASM2d also includes mathematical equations to describe the processes related to the EBPR, such as the cell internal storage of P and VFA as well as the process related to the denitrification by PAOs. One principle used in the model is the conservation equation for COD, N, P and electrical charges. This means that no elements, electrons, COD or net electrical charges can be formed or destroyed. However, they can transform into different components (Henze *et al.*, 1999). Components used in the ASM2d are divided into two categories particulate (X) and soluble (S). The particulate components constitute the AS and can be separated from the water through sedimentation. Soluble components can only be transported via water. In Table 4, all the components of the ASM2d are listed (Henze *et al.*, 1999).

Table 4: The model components used in the ASM2d, presented in groups of soluble and particulate components. Each component's unit and description is also listed (Henze et al. 1999).

Component	Unit	Description
<b>Soluble components</b>		
$S_{O_2}$	gO <sub>2</sub>	Dissolved oxygen
$S_F$	gCOD	Readily biodegradable substrate
$S_A$	gCOD	Volatile acids
$S_{NH_4}$	gN	Ammonium
$S_{NO_3}$	gN	Nitrate and nitrite
$S_{PO_4}$	gP	Phosphate
$S_I$	gCOD	Inert, non-biodegradable organics
$S_{Alk}$	mole HCO <sub>3</sub> <sup>-</sup>	Alkalinity of the wastewater
$S_{N_2}$	gN	Dinitrogen
<b>Particulate components</b>		
$X_I$	gCOD	Inert, non-biodegradable organics
$X_S$	gCOD	Slowly biodegradable organics
$X_H$	gCOD	Heterotrophic biomass
$X_{PAO}$	gCOD	PAOs
$X_{PP}$	gP	Poly-phosphate
$X_{PHA}$	gCOD	Primarily poly-hydroxy-alkanoates (PHA)
$X_{AUT}$	gCOD	Autrophic, nitrifying biomass
$X_{TSS}$	gTSS	Total suspended solids
$X_{MEOH}$	gTSS	Metal-hydroxides
$X_{MeP}$	gTSS	Metal-phosphate

### 2.3.1 COD components

The total COD found in the wastewater can be divided into smaller fractions describing the different characteristics of the COD. A typical wastewater characterisation presented by Henze et al. (1999) shows that the soluble COD ( $S\_COD$ ) is approximately 31% of the total COD, consequently is the percentage of particulate COD ( $X\_COD$ ) 69% of the total COD.

The soluble COD can be categorised into three fractions: readily biodegradable organic substrate  $S_F$ , volatile acids  $S_A$ , and inert, non-biodegradable organic substrate  $S_I$ . The fraction of  $S_F$  is described as the part of the  $S\_COD$  that is available for biodegradation of the heterotrophic organism. The  $S_I$  fraction is the  $S\_COD$  is the substrate that cannot be degraded any further; hence is it the minimal COD concentration possible to achieve in the effluent from the WWTP. This fraction is a part of the influent but can also be produced during the AS as the biodegradable substrate is further degraded. The final fraction of the  $S\_COD$  is the  $S_A$  that represents the fermentations products in the model, in the form of acetate. In the report from Henze et al. (1999), following suggestion for the fractionation of  $S\_COD$  is presented:  $S_F$  and  $S_I$  constitutes 37.5% each of the  $S\_COD$ , and the rest, 25%, is assumed to be  $S_A$ .

Particulate COD can also be categorised in three main fractions; slowly biodegradable substrate  $X_S$ , heterotrophic organisms  $X_H$ , and inert organic material  $X_I$ . The slowly biodegradable fraction is only available for the organisms after a cell external hydrolysis, which the fraction of heterotrophic organisms is responsible for. The fraction of  $X_I$  is part of the influent and can also be increase as the biomass decay. In the ASM2d is also a part of the  $X_{COD}$  in the AS described as the PAOs,  $X_{PAO}$ , as the cell internal storage product in the PAOs,  $X_{PHA}$ , and as the nitrifying organisms  $X_{AUT}$ . For typical influent water is the fractionation of  $X_{COD}$  suggested by Henze et al. (1999) as following: 69% is  $X_S$ , 14% is  $X_I$ , and 17% is the  $X_H$ . The fraction of  $X_{PAO}$ ,  $X_{PHA}$ , and  $X_{AUT}$  is considered to in the influent is considered so small that it is negligible.

### 2.3.2 Phosphorus components

In the ASM2d the EBPR process can be described through components as  $X_{PAO}$ ,  $X_{PP}$ , and  $X_{PHA}$ . The  $X_{PAO}$  is the biomass of the PAOs in the system and  $X_{PHA}$  is a functional component for the cell internal storage products within the PAOs, which is not included in the  $X_{PAO}$ . The  $X_{PP}$  component represents the poly-phosphate within the PAOs. The soluble phosphorus,  $S_{PO_4}$ , in the model is assumed to be phosphate ( $PO_4$ ). The fraction of  $S_{PO_4}$  of the influent water in the report by Henze et al. (1999) is 60% of the total P. Organic phosphorus is not a component in the model, it is however calculated from the fraction of P within the different COD components. Another P component is the  $X_{MeP}$  describing the metal-phosphate.

### 2.3.3 Nitrogen components

The nitrogen in the model is described as soluble and particulate nitrogen. The soluble nitrogen is represented as  $S_{NH_4}$ ,  $S_{NO_3}$ , and  $S_{N_2}$ , which are the ammonium, nitrate and nitrite, and the dinitrogen, respectively. As for the organic phosphorus is also the organic nitrogen calculated from the fraction of N within the different COD components (Henze *et al.*, 1999).

## 2.4 NUTRIENT RECOVERY

Most of the nutrients in the influent to the WWTP derive from the food we eat (Jönsson *et al.*, 2005), which is originally from the soil where the food was grown. A desirable goal is to recirculate the nutrients back to the soil to minimise the use of imported mineral fertilisers.

Mehta et al. (2015) reviewed different technologies to recover nutrients from wastewater streams. They suggest a framework to maximise the amount of nutrient recovered. The framework is built on three steps: nutrient accumulation, then nutrient release and last nutrient extraction. The framework is supposed to simplify the nutrient recovery process; each step can be optimised and calibrated separately to achieve the best nutrient recovery. Nutrient accumulation technologies aim to accumulate as much soluble nutrients as possible to meet the effluent targets for the WWTP but also recover as much of the nutrient as possible. EBPR is one example of nutrient accumulation technologies. According to Mehta et al. (2015) is the accumulation step most important when the concentrations of nutrients in the wastewater are low and the flow rate is high. Once the nutrients are accumulated and removed from the water stream the nutrient release takes place. The aim of this process is to release the accumulated nutrient back to soluble form or directly into recovered product. Anaerobic digestion is one treatment for nutrient release. The WAS enhanced release process is another (Baur, 2009). The WAS enhanced release process is placed prior to the anaerobic digester to release P and magnesium (Mg) through hydrolysis. The process consists of an anaerobic reactor and dewatering unit. An addition of VFA prior to the anaerobic reactor is possible to add, to increase the efficiency of the release of nutrients. Baur (2009) recommends an addition of 5–8 g VFA per gram planned  $PO_4$  release to keep the HRT short. For a HRT between 36–96h

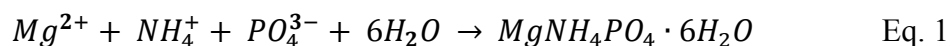
however is there no need of extra VFA source. A study of side stream hydrolysis was performed at Duvbackens WWTP in Gävle, Sweden, by Kumpulainen (2013). This study showed that the EBPR at Duvbacken WWTP was efficient enough not to require an extra VFA source for the hydrolysis. After the anaerobic reactor in the WAS enhanced release process by Baur (2009) is the water separated from the sludge. The sludge goes through the anaerobic digester while the supernatant from the dewatering unit is P- and Mg- rich and suitable for the next step in the framework created by Mehta et al. (2015). The final step in the framework is the nutrient extraction and recovery technologies. Two technologies presented, are the precipitation/crystallisation of P into struvite/magnesium ammonium phosphate (MAP) and liquid/gas stripping of N into ammonium sulphate (AMS) (Mehta *et al.*, 2015).

The chemical formula for MAP is  $MgNH_4PO_4 \cdot 6H_2O$ . It can be used as a slow-release fertiliser since it has low water solubility. This characteristic in a fertiliser generate advantages such as the fact that the loss of nutrients due to surface runoff and groundwater percolation is small, leading to fewer nutrients into recipients, and the possibility of too high nutrient concentration around the root structure is low. These advantages have made the market for slow-release fertiliser increase and the struvite production in WWTP to be considered an asset (Tchobanoglous *et al.*, 2014d).

The nitrogen found in the supernatant from the dewatering after the anaerobic digester can be recovered as ammonium sulphate ( $(NH_4)_2SO_4$ ). AMS can be used as a fertiliser however the market for WWTP-produced AMS is not fully established. The AMS found in fertiliser is usually obtained from other industries where AMS is a by-product. In order to increase the market of AMS from WWTP the quality and consistency needs to be high and meet the market and buyers specifications (Tchobanoglous *et al.*, 2014d).

## 2.5 MAGNESIUM AMMONIUM PHOSPHATE

The phosphorus in the wastewater and sludge can be transformed to MAP through a crystallisation process. In order for a crystallisation to occur there are essential stages within the reactor, such as supersaturated ion concentrations, nucleation processes and crystal growth. Under supersaturated ion molar concentrations of the desired product will ions aggregate into solid form when their solubility at a given pH and temperature is exceeded. The solids will dissolve and aggregate alternately until they form an aggregate with a stable enough surface for crystal growth; this cycle is the nucleation process. The crystal growth takes place when the nuclei are formed with stable surfaces. Aggregates will attach to each other's surfaces. The dimensions of the crystal will increase until it reaches its limit for the specific hydrodynamics conditions inside the reactor. When the crystal reaches a size where its density is higher than the liquid will it settle. This is desirable since it allows for the mineral to be separated more easily. In equation 1 below the formation of struvite is described by the stoichiometry reaction (Tchobanoglous *et al.*, 2014d),



where the reactants are magnesium ion (Mg), ammonium (NH<sub>4</sub>), phosphate (PO<sub>4</sub>) and water and the product is MAP. Most wastewaters do not contain high enough concentrations of the ion molar concentrations of MAP and therefore magnesium salt is added in order for the crystallisation process to occur (Tchobanoglous *et al.*, 2014d). The molar ratio of Mg:N:P has to be 1:1:1 in order to precipitate MAP (Egle *et al.*, 2015).

For optimal struvite precipitation there are several operational factors to take into consideration. If so, it is possible to receive a purer and higher quality product. The factors can be summarised as pre-treatment, pH and temperature control, chemical requirements, seed requirements and finally mixing and hydraulics. The pre-treatment of the side stream aims to reduce total suspended solids and colloidal materials. If the pH and temperature are controlled the purity of the final product will be higher. Increasing the pH, decreases the solubility of MAP and decreases the crystal growth. A lower pH would require a longer retention time in the reactor in order to have the same efficiency as with a higher pH. To prevent calcium phosphate from precipitating instead of MAP the pH should range between 8–8.8. This range has shown a phosphorus recovery efficiency of 80% (Tchobanoglous *et al.*, 2014d).

Phosphorus can be recovered from several streams at a WWTP, for example the effluent of the secondary clarifier, sewage sludge and digester supernatant. In order to recover MAP from the liquid phase or the sewage sludge, the stream has to be treated to transform the P into dissolved P. This pre-treatment process can be anaerobic treatment, thermal hydrolysis or wet-chemical leaching. Phosphorus recovery by crystallisation and precipitation are the methods more established and exist in full-scale implementations. The final product from some MAP recovery methods are pellets while other methods results in a wet MAP that needs further treatment in order to be useful as a commercial product such as fertiliser (Egle *et al.*, 2015). The following sections will be focusing on methods that recover P from liquid phase; some techniques available for this is NuReSys<sup>®</sup>, Ostara WASSTRIP and Pearl, PHOSPAQ<sup>®</sup>, eco:P, PHOSTRIP and STRUVIA.

### **2.5.1 Methods with an included unit for hydrolysis of PO<sub>4</sub>**

#### ***Ostara WASSTRIP and Pearl***

WASSTRIP and Pearl are developed by Ostara in Vancouver, Canada. Ostara was founded in 2005 and have today 15 commercial installations of their product worldwide (Ostara Nutrient Recovery Technologies Inc., 2017a). WASSTRIP is an acronym for waste activated sludge stripping to recover internal phosphate. The WASSTRIP is a mixed tank holding anaerobic conditions in order to achieve a phosphate release. It is customised with a specific hydraulic retention time and feed to fit depending on the WWTP's capacity and demand. With WASSTRIP it is possible to a 70% P release (Ostara Nutrient Recovery Technologies Inc., 2017c). With Ostara's PEARL, the released nutrients from the WASSTRIP can be turned into fertiliser. The Pearl process is a fluidised bed reactor and turns the nutrient to MAP through controlled precipitation. Mg is added to the streams from the WASSTRIP to maximise the precipitation (Ostara Nutrient Recovery Technologies Inc., 2017b).

Cullen *et al.* (2013) have in a report evaluated the performance and experience of the Ostara Pearl and WASSTRIP during the first three years of operation at Clean Water Service's Durham Advanced WWTP. At first, only the Pearl was installed, it was not until July 2011 that the WASSTRIP was introduced. In the report, the design of the Pearl is described. It is a funnel-shaped reactor with 3 layers with different diameter. The top layer has the largest diameter and the bottom layer has the smallest diameter. Pearl reactor is bottom-fed creating an up-flow of the water and when reaching the top of the reactor it is recirculate to the bottom again. The incoming water to the reactor has a high P and N concentration, but in order to precipitate MAP is magnesium chloride (MgCl<sub>2</sub>) added to reach the correct molar ratios. The reactor is designed with a plug flow; the up-flow velocity is highest at the bottom layer and lowest in the top layer. This design with smallest section and highest flow at the bottom and the largest section with the lowest flow at the top results in a segregation of the particles according to size. The largest MAP particles settle down to the bottom layer and the water fed

from the bottom has a high reactant concentration, under this conditions can more MAP precipitate onto the existing particles. As the water moves up to the next layer, middle section with a larger diameter, decreases the flow velocity. The size of the particles accumulated in this section is smaller than in the bottom layer, but the overall surface area of the particles is larger. The larger surface area and longer contact time with the reactant results in precipitation of MAP, and growth of the particles size. At the top layer decreases the flow velocity further, generating an even longer contact time for between the residual reactant and the small particles accumulated in the top layer. The smallest MAP particles are found at the top layer, unable to settle down due to the up-flow until they grow larger. The Pearl is designed to precipitate MAP on existing particles rather the creating new particles, however it is require to add seeds when starting up an empty reactor to reduce start-up time. Thereafter the procedure does not require anything other than added  $MgCl_2$ . The MAP is harvested from the bottom; the final particle size depends on the chosen SRT. The MAP particles has to be dried and dewatered before they are ready to use as fertiliser; one benefit with using Ostara Pearl is that the ownership of the MAP is then passed on to Ostara, which in turn store it, distribute and sells it as Crystal Green<sup>®</sup> (Cullen *et al.*, 2013).

The results from Durham reported by Cullen *et al.* in 2013 shows that the installation of the Ostara Pearl and the nutrient recovery associated with it reduces the recycle P load by 85% and the ammonia load with 15%. After the installation of WASSTRIP in 2011 the MAP production was doubled from previous years, and 70% of the phosphorus into the Pearl reactor originated from the WASSTRIP. It also resulted in an increase in ortho-P, from 125 kg/day to 216 kg/day, this load was higher the design load of the Pearl reactor (204 kg/day). This high load forced the Pearl reactor to run on an average of 25% over its capacity; the consequences of running over the Pearl reactor capacity lead to an increase of the nutrient load with the recycled water. The conclusion made from the three years running this nutrient recovering processes at the WWTP was that it stabilised the EBPR at the WWTP, which led to less aeration needed and since the recycle load decreased did the capacity of the WWTP and its EBPR increase. Another benefit was the revenue gained from the MAP sold as fertiliser.

### ***PhoStrip***

Kaschka and Weyrer (1999) have in a handbook described the technical aspects of PhoStrip. This process was developed as an alternative to P removal but has later also been used for P recovery.

The process is found at the excess sludge stream. It constitutes of a pre-stripper, stripper tank, reactor, and separator. The pre-stripper is a recommendation to lower the nitrate concentration to around 1–2 mg/l; this concentration is acceptable for the main stripper. This tank is a denitrification tank. In order for this process for reduction of nitrate to work is some of the organic acids-rich sludge from the main stripper redirected back to the pre-stripper. The sludge and water then flows through to the main stripper tank. The objective with the stripper tank is to achieve a P release through anaerobic conditions and separate the P-rich water with the sludge. The main stripper tank is designed as a sedimentation basin, where the sludge exiting from the bottom is partly redirected to the back to the main stripper, the pre-stripper, the ASU, and the rest is excess sludge in need of further treatment. The recirculation back to the main stripper and the pre-stripper is required to achieve high enough VFA concentrations. The P-rich effluent from the stripper tank reaches a reactor where a precipitant is added to precipitate the P from the water. In the next step it is then P- rich product separated from the

water, which in turn is recirculate to the main stream of the WWTP (Kaschka & Weyrer, 1999). This process recovers the P as calcium phosphate (Levlin & Hultman, 2003).

## **2.5.2 Methods that require an extra treatment step for hydrolysis of PO<sub>4</sub>**

### ***PHOSPAQ***

PHOSPAQ is a P recovery process developed by the Dutch company Paques with full-scale experience since 2006. The P is recovered through precipitation of MAP in a continuously aerated tank. The water inlet is placed at the bottom of a cylindrical tank while the outlet is placed at the top of the tank. PHOSPAQ uses MgO as a Mg<sup>2+</sup> source to reach the appropriate ratio of reactants and to increase the pH. Within the tank there is a PHOSPAQ separator, which separate the MAP from the water and harvest it as it precipitate (Paques, n.d.). One client to Paques, using the PHOSPAQ, is AVIKO potato processing plant in Steenderen, in the Netherlands. Their wastewater is high in protein, starch and P; with a P concentration equivalent to the concentrations found in wastewaters from a population of 160 000 persons. The water was treated through an anaerobic pre-treatment and an upflow anaerobic sludge blanket (UASB) by the municipal STW Olburgen. However, the effluent from the UASB still contained high concentrations of both P and N, which resulted in high discharge costs. The sewage plant receiving the effluent was WWTP Waterstromen and due to new regulations in 2013 they had to find a solution to reduce the nutrients in the effluent. This solution would need to reach the regulations at a low total cost of ownership but still maximising sustainability (Schultz, 2009). According to Schultz (2009) was the solution found through a comprehensive feasibility study made by WWTP Waterstromen themselves. This study resulted in the implementation of the PHOSPAQ among another process recovering N. The installation of PHOSPAQ resulted in an 80% P reduction and a production of 363 tonnes MAP per year.

### ***NuReSys***

NuReSys is an acronym for Nutrient Recovery Systems, which is a Belgian company established since 2011. They have developed a process for struvite crystallisation under the same name, NuReSys. The produced MAP can be directly used as fertiliser and sold as BIO-STRU® developed by Schwing Bioset (NuReSys, n.d.).

Moerman et al. (2009) executed a pilot and full-scale experiments of MAP crystallisation in order to remove phosphorus from agricultural industry. The full-scale experiment, design and process, was the now marketed NuReSys. The units used were an air stripper, a top-loaded crystallisation reactor and a settling zone. By adding sodium hydroxide (NaOH) was the pH controlled and in order to reach the proper reactant ratio an Mg source is added, as MgCl<sub>2</sub>. When a batch experiment was carried out with a PO<sub>4</sub> concentration of 150 mg/l of the influent was there a decrease to 14.7 mg PO<sub>4</sub>/l for the effluent. The rest of the PO<sub>4</sub> would be captured as MAP. Moerman et al. (2009) reach the conclusions that the phosphate recovery by MAP formation had high value after an anaerobic treatment.

The NuReSys process can be placed post the anaerobic digester and dewatering unit to treat the reject liquor, which NuReSys call from centrate. With an extra unit for P hydrolysis prior to the anaerobic digester can the P be recovered from the PO<sub>4</sub>-rich water from the WAS, which NuReSys call recovering P from the filtrate. A combination of these can also be applied. Apeldoorn is a WWTP in the Netherlands using the NuReSys –hybrid since 2016. The hybrid means that the stripper unit is placed between the anaerobic digester and the dewatering unit and the crystallisation unit is placed after the dewatering unit. PO<sub>4</sub>-rich water from a hydrolysis tank prior to the anaerobic digester is added to the crystallisation tank.

Average MAP production per day is 1500 kg/day with an flow rate of 140 m<sup>3</sup>/h and PO<sub>4</sub>-concentration of 450 mg P/l into the crystallisation tank and the effluent PO<sub>4</sub>-concentration of 40 mg P/l (NuReSys, n.d.).

Another implementation of NuReSys was installed in 2015 at Land Van Cuijck in the Netherlands. The NuReSys process was installed to recover the P from the centrate. It is possible to also include a stream of PO<sub>4</sub>-rich water from an anaerobe unit prior to the digester when installing the NuReSys to treat the centrate. However is it not specified if Land Van Cuijck has this solution with an extra stream. The design flow to the NuReSys unit is 5 m<sup>3</sup>/h and the average PO<sub>4</sub>-P-concentration of the influent water is 650 mg P/l. This results in a MAP production of 400 kg/day and an effluent PO<sub>4</sub>-P-concentration of 88 mg P/l (NuReSys, n.d.).

### ***Eco:P***

Eco:P is the process for P recovery developed by Ekobalans Fenix AB in Lund, Sweden. It is a batch process with air stripping and MAP precipitation; the air stripping takes place first. The P rich water flows in a downward direction through a cylindrical tank, while the air flows in the opposite direction. This increases the pH. After the air stripping is the water led to a second cylindrical tank where the MAP precipitation takes place. A Mg source, in this case MgCl<sub>2</sub>, has to be added to attain the correct ratio of reactant. The MAP crystals are separated from the water with a hydrocyclone (a cone-shaped tank which separates particles from liquid) after the second tank. The extracted MAP is a microcrystalline powder ready to use as fertiliser or as a raw material for other fertiliser production. According to Ekobalans Fenix AB (2017) is it possible to extract 90% of the P coming into the eco:P as MAP. The traditional placement of the eco:P is after the anaerobic digester, this leads to around 25% recovered P out of the total amount of incoming P to the WWTP. If the excess sludge is treated through an extra ASU or tank with hydrolysis prior to the anaerobic digester is it possible to extract and recover more than 50% of the incoming P to the WWTP (Ekobalans Fenix AB, 2017).

### ***STRUVIA***

Struvia<sup>TM</sup> is a P recovery process developed by Veolia Water Technologies (Veolia). It consists of a continuous stirred tank reactor with a mixing system called Turbomix<sup>TM</sup> also developed by Veolia. The mixing system is used to aid the crystallisation and growth of MAP crystals through an optimum mixing of the reactants. The aim is to achieve an optimum use of the reactants under a short retention time because of the limited space of the tank reactor. To initiate the crystallisation is the pH is increased and a magnesium salt is added. Through a lamellar settler is the MAP crystals separated from the treated water; the water is led back to the main stream of the WWTP. The produced MAP is removed from the bottom of the Struvia tank with a pump (Veolia Water Technologies, 2015). The Struvia-produced MAP is similar to sand, both in particle size and shape (Brockmann, 2015).

Brockmann (2015) presented results from different trials with the Struvia process. From Struvia pilot plant was two different trials executed with two different centrate from the digester sludge dewatering. The centrate collected under period 1 and period 2 was from the summer 2014 and February 2015, respectively. The characteristics of the centrate from period 1 was following: pH = 8.5, SS < 50 mg/l, N-NH<sub>4</sub> = 1200 mg/l, P-PO<sub>4</sub> = 340 mg/l, Mg<sup>2+</sup> < 2 mg/l. For period 2 was the concentration slightly higher while the pH was 8.1. The pH of the centrates was adjusted to those values through adding NaOH. The Struvia pilot plant was operated with a SRT of 2–3 days and a HRT of 30–60 min. Under normal operational

conditions showed the Struvia pilot plant a 90% or higher P- recovery efficiency. The N removed through the MAP production was around 15%. The pilot trials showed that the start up of the process was quick and an eventual shut down took only a few minutes. Failures in the dosing pump adding the MgCl<sub>2</sub> showed significant effects on the performance of MAP production. Brockmann (2015) also presented a case where Veolia was installing a Struvia reactor at the Elsinore WWTP in Denmark. The start-up of the tank was planned for February 2016. And the Struvia process was dimensioned for a design flow of 60 m<sup>3</sup>/day and a PO<sub>4</sub> load of 250 mg P/l in the influent water. The P-recovery efficiency was expected to be 90% or higher. Held (2017) presented some results from the Elsinore WWTP during a meeting for the Swedish Water platform in December 2017. The total reactor volume is 2.2 m<sup>3</sup> and operated with a HRT of 30 min. Elsinore WWTP now produces around 100 kg MAP/day.

### 2.5.3 Comparison of the methods

In Table 5 below, each different P recovery technique is listed and its performance and efficiency defined by the possible P recovery in per cent, chemical demand and the molar ratio between Mg and P and finally the hydraulic retention time (HRT).

Table 5: A summary of each P recovery technique's efficiency related to the per cent recovered P, the chemical demand, the molar ratio Mg:P, and the hydraulic retention time (HRT).

Method	Need of extra hydrolysis unit	P recovery Related to P-flow	Mg:P	Chemical demand	HRT min
NuReSys®	Yes	90% <sup>1</sup>	1:1 <sup>1</sup>	MgCl <sub>2</sub> , NaOH <sup>6</sup>	30–60 <sup>2</sup>
PHOSPAQ®	Yes	> 80–90% <sup>7</sup>	1:1 <sup>1</sup>	MgO <sup>7</sup>	300–360 <sup>2</sup>
OSTARA Pearl & WASSTRIP	No	90% <sup>1</sup>	1:1 <sup>1</sup>	MgCl <sub>2</sub> , NaOH <sup>3</sup>	60 (Pearl) <sup>2</sup>
Eco:P	Yes	> 90% <sup>3</sup>	-	MgCl <sub>2</sub> <sup>3</sup>	“Short” <sup>3</sup>
Phostrip	No	99% <sup>1</sup>	1.5:1 <sup>1</sup>	Lime <sup>8</sup>	82 <sup>4</sup>
STRUVIA	Yes	> 90% <sup>5</sup>	1:1 <sup>1</sup>	NaOH, MgCl <sub>2</sub> <sup>5</sup>	30 <sup>5</sup>

<sup>1</sup> (Egle et al., 2015) <sup>2</sup> (Tchobanoglous et al., 2014d) <sup>3</sup> (Ekobalans Fenix AB, 2017) <sup>4</sup> (Salehi et al., 2018) <sup>5</sup> (Brockmann, 2015) <sup>6</sup> (Moerman et al., 2009) <sup>7</sup> (Paques, n.d.) <sup>8</sup> (Levlin & Hultman, 2003)

When studying Table 5, it is shown that the P recovery is similar for all the methods. They also required almost the same chemical, and for the same purpose increasing pH and an extra Mg source. The HRT is varying a little, where PHOSPAQ has the longest HRT. Otherwise it is difficult to differentiate the methods more.

PhoStrip is the method with the highest P recovery, up to 99%, related to the P concentration in the influent to the recovery reactors. Methods with both precipitation and crystallisation requires a higher molar concentration of Mg in relation to P, 1.5:1, which means that there is a higher chemical demand for Phostrip (Egle *et al.*, 2015). However, PHOSPAQ is not depended on any chemical to increase the pH of the influent and can therefore have a lower chemical demand than other methods. As seen in Table 5 is lime used for the precipitation, resulting in calcium phosphate instead of MAP.

Egle et al. (2016) have done a review of different P recovery techniques; one of their analysis aspects is the cost of P recovery. Their cost analysis shows that the main part of the cost for a WWTP to have recover P is dependent on the investment cost of the equipment. A larger

WWTP can reduce investment costs because the economy of scale. Savings can also be achieved as there will be a reduction of P backflow and less MAP encrustations leading to lower reduced consumption of flocking agents and maintenance costs, respectively. Nutrient recovery that reduces the sludge volume will also reduce the sludge disposal costs. The sludge disposal cost is usually one of the larger costs that a WWTP has. Egle *et al.* (2016) have, in their review, compared a reference WWTP with mono-incineration to WWTP with P recovery; the reference WWTP's annual cost have been calculated and compared to the reference WWTP with different P recovery techniques. With the Ostara<sup>®</sup>, their study showed that savings of 1–4% of the annual cost for the WWTP without P recovery can be achieved. Methods recovering P from liquid phase has approximately the same yearly cost (Egle *et al.*, 2016).

## 2.6 AMMONIA STRIPPING

The method of ammonia stripping consists of at least one ammonia-stripping column coupled with an ammonia-scrubber column. The stripper column removes the ammonium from the water and the scrubber column recovers N in the form of ammonia into fertiliser (Minocha & Rao, 1988). The supernatant from the anaerobe digester is treated with NaOH or lime at the influent point to the stripper column to increase the pH. The percentage unionised ammonia increases when the pH and temperature increases. The supernatant from a digester usually holds a temperature around 25 to 35 °C, which would then require a pH adjustment to a value of 11 to efficiently convert nearly all the ammonium to ammonia (Tchobanoglous *et al.*, 2014d). Inside the stripper column, the supernatant (with the increased pH) flows in one direction and in the opposite direction flows air. The stripper column is filled with a supporting media to better distribute the water and increase the contact area. As the air is introduced, the ammonium in the water will be converted into ammonia in gas phase. The air or steam flow with the ammonia gas is then fed into the scrubber column. The purpose of the scrubber column is to recover the ammonia from the gas phase. This achieved through absorption or adsorption for an air stripper (Minocha & Rao, 1988).

Temperature, pH and the airflow rate are three factors affecting the efficiency of the ammonia stripper. Liao, Chen and Lo (1995) studied the effects of these parameters on ammonia stripping; they found that with a pH lower than 10.5 does the removal efficiency increase as the temperature increase. When the pH is kept at a higher value than 10.5 is the temperature not as important (Liao *et al.*, 1995). Gustin and Marinsek-Logar (2011) also studied the effects of temperature on the ammonia stripper. As they varied the temperature (with a pH of 10) the efficiency did not change much, from an 80% ammonium removal at around 30 °C to a 92.8% at around 70°C (Guštin & Marinšek-Logar, 2011). The effects of the pH on the removal efficiency in the study by Liao, Chen and Lo (1995) showed that up to a pH of 10.5 does the an removal rate increase with an increasing pH no matter how long the HRT was. For a pH above 10.5 will the efficiency not be as dependent on the pH. A higher pH requires a higher chemical demand, which leads to higher operational costs. As Liao, Chen and Lo (1995) mentioned in their report, since there is no significant increase in the removal rate with a pH higher than 10.5 and the operational costs associated with the increase of pH there is little reason to increase the pH above 10.5. The result from Gustin and Marinsek-Logar (2011) showed that pH had the most effects on the ammonia stripping. At a pH of 8.5, the ammonium removal efficiency was only at 27.4% but when increasing the pH to 10.5–11 was the removal at 92.8%. When the airflow rate was increased from 65 to 90 l/min the ammonium removal rate increased no matter the pH according to Liao, Chen and Lo (1995). This increase of airflow also changed the air to liquid ratio from 52 to 73. However, when the airflow was increased but the air to liquid ratio was kept constant, was there no increase of removal efficiency. Gustin and Marinsek-Logar (2011) studied the effect of air to liquid ratio

instead of airflow rate. In their study they saw that this ratio had greater effect of the removal rate than when changing the temperature between 30–70°C. The removal efficiency increased a lot up to a ratio of 1500. An appropriate air to liquid ratio is between 1500 and 2000 according to Gustin and Marinsek-Logar (2011), resulting in around 90% ammonium removal.

The digester supernatant, with a pH range of 7.0–8.0, contains ammonium in the form of ammonium bicarbonate. The ammonia stripping is suitable for supernatant with higher ammonium concentration, around 2000 mg NH<sub>4</sub>-N/l (Mehta *et al.*, 2015). When converting the ammonium to ammonia in the stripper column, will there be a release of carbon dioxide (CO<sub>2</sub>). Since the stripper column usually is designed as a closed system will the release of carbon dioxide be retained and the concentration of carbon dioxide leads to a decrease in pH (Tchobanoglous *et al.*, 2014d). An improvement to this process is to add a carbon dioxide-stripping column with an off- gas stream as a pre-treatment. If the CO<sub>2</sub> is emitted in the CO<sub>2</sub> pre-stripper, the pH of the sludge liquid will instead increase before entering the ammonia stripper. This in return, leads to a reduced chemical demand to increase the pH in the ammonia stripper. This was implemented at WWTP Kloten-Opfikon in 2011 (Boehler *et al.*, 2015).

### **2.6.1 Methods for ammonium recovery**

There are several companies providing ammonia-stripping technologies around the world, some have their own trademark of the ammonia stripper while others are untitled. For some companies were the information about removal efficiency and operational parameters of their products not found. The companies are still mentioned, for acknowledgement.

#### ***Eco:N by Ekobalans***

Eco:N is a nitrogen recovery process developed by the Swedish company Ekobalans Fenix AB. It consists of an air-stripping column to remove the ammonium in the water and a crystalliser to recover the ammonia from the gas phase. Prior to the stripper column is the ammonium-rich water heated and the pH is increased by adding NaOH. The stripper column has a N removal efficiency of 80–95% (Ekobalans Fenix AB, n.d., 2017). The N is then recovered as AMS salts in the crystalliser by adding sulphuric acid (H<sub>2</sub>S). The AMS crystals from the recovery process contain 21% nitrogen. The Eco:N unit is available in three different sizes depending on the flow rate of the supernatant; one for a flow of 5m<sup>3</sup>/h, 10 m<sup>3</sup>/h and larger than 10 m<sup>3</sup>/h (Ekobalans Fenix AB, n.d.). Some benefits with the Eco:N process, compared to conventional nitrogen removal, are the recovery of N, decrease in sludge volume, and revenue from the produced fertiliser (Ekobalans Fenix AB, 2017).

#### ***AMFER by Colsen***

Colsen is a company in the Netherlands that developed an ammonia-stripping unit called AMFER<sup>®</sup>. It is either under a batch wise or continuous operation. AMFER is uses air and heat in the process to strip ammonia, with no addition of chemicals in the stripper column. The temperature in the unit should be around 60 °C. In the scrubber column is acid absorption used to recover the ammonia. AMFER produces AMS by adding sulphuric acid (H<sub>2</sub>SO<sub>4</sub>). The ammonium removal rate is up to 80% (Colsen, 2015).

#### ***ANAStrip by GNS***

GNS is a company located in Germany. They have developed an ammonia stripper where the ammonium is removed with only using exhaust heat from a combined heat and power plant. The stripper has no chemical demand. The specific heat consumption varies between 30–120 kWh/m<sup>3</sup>; the optimised heat consumption is 70 kWh/m<sup>3</sup>. GNS suggest FGD gypsum for

the adsorption of ammonia in the scrubber column (GNS, n.d.). Gypsum is another word for hydrous calcium sulphate (*gypsum, n.*). FGD gypsum is an acronym for flue gas desulfurization gypsum. The ammonium sulphate solution contains around 25% AMS. Using FGD gypsum also generate calcium carbonate ( $\text{CaCO}_3$ ). The amount of FGD gypsum required to scrub the ammonia is 6.1 kg/kg N removed in the stripper. GNS shows two cases where the stripper been implemented; both of the implementations has a removal efficiency of 80–85%. The implementation with a smaller supernatant input, at 5.5–12.6 m<sup>3</sup>/h and a ammonium concentration of 3– 6 g/l requires 370–820 kW heat and a FGD gypsum load of 5–10 t/day. The amount of AMS produced is 13–27 t/day (GNS, n.d.).

### ***Air stripping by CMI Europe Environment***

CMI Europe Environment (CMI) is a French company providing air-stripping solutions. Their ammonia recovery is called RECOV'AMMONIA<sup>TM</sup>. In their document they give examples of to implementations of the ammonia recovery. The first client has a supernatant with an ammonium concentration at 2.4 g/l and a flow of 102 kg/h. The operational parameters for this case is a liquid flow at 42 m<sup>3</sup>/h, temperature at 60 °C, and a pH value of 9. The airflow is 80 000 m<sup>3</sup>/h (CMI Environment, 2017), resulting in an air to liquid ratio of approximately 1 905. The ammonium removal efficiency for this unit is higher than 92%. A scrubber column, producing ammonium salts, recovers the ammonia. The concentration of ammonium salts in the solution is 40%. The other client treats water with an ammonium concentration at 0.5 g/l with a flow of 11 kg/h. The operational parameters in this case is a liquid flow at 22 m<sup>3</sup>/h, temperature of 65 °C, and a pH higher or equal to 10. With an airflow at 17 000 m<sup>3</sup>/h, the air to liquid ratio is around 773. The removal efficiency in this case is higher than 75%; this client does not recover the ammonia.

### ***Ammonia stripping by Organics***

Organics is a company in the UK with two different methods for ammonia stripping: one pH-driven and one thermally driven. For both of these methods are there a pre-treatment required to remove solids in the leachate; solids with a diameter larger than 2 mm has to be removed through filtration. The strippers are available in different sizes to treat flow rates of 50 to 5000 m<sup>3</sup>/day; the space required for a stripping unit treating a flow of 200 m<sup>3</sup>/day is approximately 120 m<sup>2</sup>. This is however just an indication, the space varies depending on the process capacity and the choice of stripping unit. The energy consumption is around 125 kWh/m<sup>3</sup> liquid treated. For both of the unit is it possible to recover the ammonia with acid absorption with sulphate. Their pH-driven ammonia stripper requires a pH around 12 (Organics, n.d.a).

Organics' thermally driven ammonia stripper was developed so it does not require an addition of chemicals to increase the pH. The only chemical it might need is a small dose of anti-foam agent. The process of ammonia stripping is instead dependent on heat; the heat can be from waste gases, engine exhaust gas or any other source of energy (Organics, n.d.b). The temperature of the ammonia stripper reaches to around 65–70 °C (Organics, n.d.a). The ammonia removal efficiency for this unit is 98.5% (Organics, n.d.b).

## **2.6.2 Comparison of the methods**

In Table 6 below, are the different companies providing ammonia-stripping units compiled and compared.

Table 6: A summary of each N recovery technique's efficiency related to the per cent removed, the pH, the chemical demand, the temperature and the energy consumption.

Company	Method	NH <sub>4</sub> <sup>+</sup> removal efficiency %	pH	Chemical demand	Temp. °C	Energy consumption
Ekobalans Fenix	Eco:N	80-95	-	NaOH, H <sub>2</sub> S	-	-
Colsen	AMFER	≤ 80	-	H <sub>2</sub> SO <sub>4</sub>	60	-
GNS	ANAStrip	80-85	-	6.1 kg FGD gypsum/kg N	80-100	30-120 kWh/m <sup>3</sup>
CMI Europe Environment	Air stripping RECOV'AMMONIA	> 90, >75	9, ≥10	H <sub>2</sub> S	60,65	-
Organics	pH-driven	-	12	sulphate ion	-	125 kWh/m <sup>3</sup>
Organics	Thermally driven	98.5	-	sulphate ion	65-70	125 kWh/m <sup>3</sup>

The values presented in Table 6 have all previously been mentioned under the description of each technology. A missing value has been denoted with a dash. Ekobalans Fenix AB, CMI Europe Environment and the thermally driven process from Organics, provides the technologies with the highest N removal efficiency. Comparing these three methods is difficult since data is missing. The required pH for Eco:N and Organics' thermally driven stripper and the energy consumption for Eco:N and RECOV'AMMONIA are missing from the open access data supplied by each company.

Zarebska et al. (2015) conducted a review of several different nitrogen recovery processes; one of them was air stripping. In this report, the general pH of an air stripper mentioned is around 10.5–11 and a temperature of 45°C. The pH reported by Zarebska et al. (2015) matches what was also reported by Liao, Chen and Lo (1995), and Gustin and Marinsek-Logar (2011). The pH for the three N recovery processes with highest removal efficiency could be assumed to be similar. Processes with higher temperatures do not need to increase the pH. However, the high temperature can cause odour from the supernatant, larger operational costs (depending on the source of energy) and water evaporation.

In the review by Zarebska et al. (2015) the general energy consumption discussed. Bauermeister et al. (2010) (as cited in Zarebska et al. (2015)) states an electric consumption of 2 kWh/m<sup>3</sup> feed. As they include the heating to 80°C the energy consumption increases to 94 kWh/m<sup>3</sup> feed. This demonstrates the temperature's affect on operational costs. Since the stripping process provided by CMI Europe Environment operates at a lower temperature than the thermally driven provided by Organics is it possible to assume that the energy consumption is slightly smaller when using CMI's unit. When Zarebska et al. (2015) compared air stripping to other methods they assumed an energy consumption of 4.18 kWh/m<sup>3</sup> feed.

The revenue from the produced AMS is up to € 90–120/ tonnes AMS (Colsen, 2015), which today is approximately 900–1200 SEK/ tonnes AMS. Mehta et al. (2015) mentions a cost gap for the N recovery at a WWTP because high operational costs. The operational cost constitutes of high chemical costs to increase the pH and for the thermally driven process is the energy cost high. The recovered N-products compete with cheaper alternatives. According to Mehta et al. (2015) might this change if the market for recovered N finds a specific niche market that can increase the value of recovered N.

### 3 METHOD

A literature review was performed to increase the understanding of the characteristics of municipal wastewater and the different functions of a WWTP but also to compare different methods for P and N recovery. The comparison was limited to factors as the recovery/removal efficiency, the chemical demand, and the HRT.

#### 3.1 THE CONCEPTUAL WASTEWATER TREATMENT PLANT

The conceptual WWTP and the flow chart of all the streams with in the WWTP are illustrated in Figure 1.

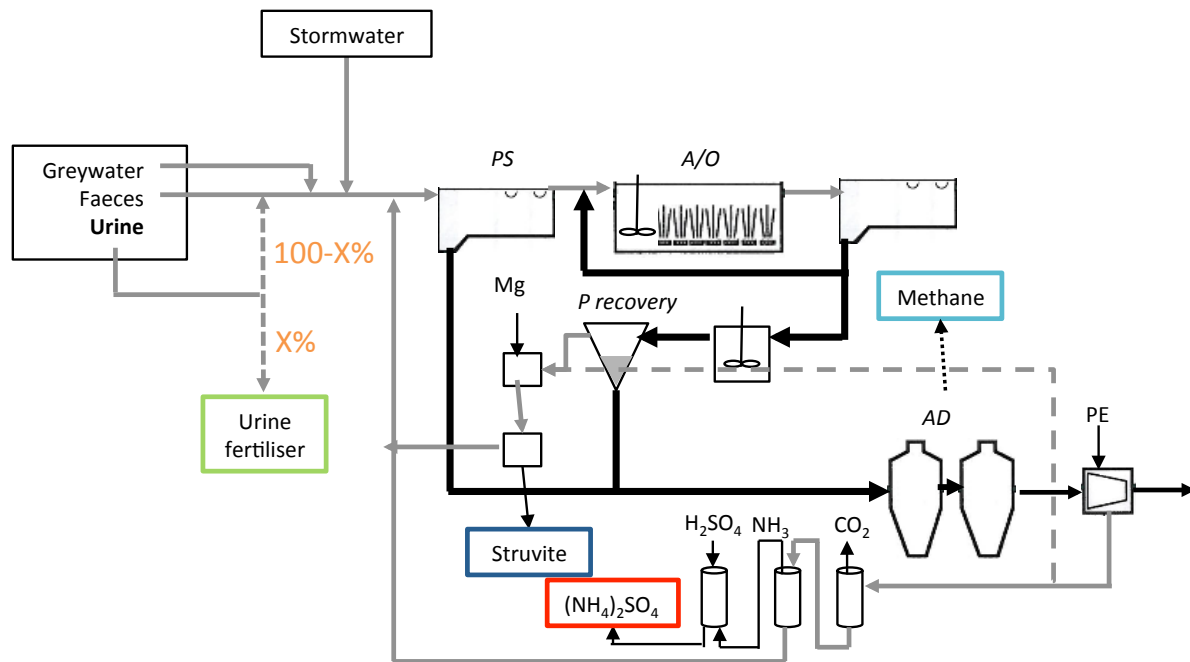


Figure 1: Flow scheme and layout of part of the conceptual WWTP (with permission from Gustavsson 2017).

The wastewater flows into the WWTP and reaches a pre-treatment in a sedimentation basin; the material, which settles, is led to the anaerobe digester. The next treatment process of the wastewater is an EBPR, with an anaerobe section followed by an aerobic section. The effluent from this treatment step is led to a second sedimentation basin where the AS can settle and returned to the biological treatment or led to the sludge treatment. Effluent wastewater from the second sedimentation basin is led to further treatments process before it is released into a recipient. This next treatment of the wastewater is not considered in this report. The side stream of the excess sludge flows through a MAP recovery process, with an anaerobe tank for P release in order to turn  $\text{PO}_4$  in to MAP. The excess sludge, now with less P concentration, is mixed with the stream from the pre-treatment and the treated in an anaerobe digester. The sludge is then dewatered and from that water is N recovered through ammonia stripping.

#### 3.2 INPUT DATA

##### 3.2.1 Measured data

A data series from 2015 from the Sjölanda WWTP in Malmö was used to define the incoming wastewater to the modelled WWTP. The data was received from VA SYD in Malmö through David Gustavsson. The measured data from Sjölanda contained the daily average flow in l/s, BOD, COD, filtered COD, TP, filtered TP, TN,  $\text{NH}_4^+\text{-N}$ ,  $\text{NO}_{2,3}\text{-N}$ , TSS in mg/l, and temperature in  $^\circ\text{C}$ . The incoming N had to be converted. It was converted to TKN by

subtracting the nitrate- and nitrite-nitrogen (NO<sub>2,3</sub>-N) from the TN. There were some values in the data series that seemed to differ quite a lot compared to the other for the same component. In order to find out if they could be considered outliers were some box plots created: one for the COD, and then for the TP:COD, TKN:COD and TSS:COD ratios. All the measurements from a day containing an extreme outlier were removed. The definition of an extreme outlier in this report was a value that was higher than the third quartile (3Q) plus three times the interquartile range (IQR) or lower than the first quartile (1Q) minus three times the IQR.

The filtered TP:TP and the NH<sub>4</sub><sup>+</sup>:TKN ratios were plotted. The filtered TP fraction of TP and the ammonium fraction of TKN were also calculated for each day.

The data series over 2015 was incomplete and interpolations for the missing values had to be done in order to use the data for modelling in DHI's software WEST. Interpolations were first made for the values representing the COD, next step was to look at the nutrient to COD ratio for each day and interpolate the ratios where they were missing. The missing values for the other components were thereafter calculated by multiplying the ratios and the COD amount.

The dimensions of each unit of the modelled WWTP were the same as the units from one of the twelve streamlines at Sjölanda; the flow was therefore divided by twelve. Thereafter was the units converted to the amount of each component per day, given by g/ day. The monthly average flow and amount of component per day in 2015 was also calculated. Incoming water to Sjölanda was a mix of both industrial wastewater and household wastewater, where the industrial wastewater contributes to higher COD concentrations into the WWTP at Sjölanda (Gustavsson, pers. contact). The industrial wastewater however has a low N concentration. It was therefore assumed that all the measured N origin from the household wastewater. By calculating the total COD:N ratio of the measured data and comparing it with the theoretical value for household wastewater presented by Jönsson et al. (2005) and Ek et al. (2011), was it possible to determine the percentage industrial wastewater of the total flow into Sjölanda. The household wastewater constituted 81% of the total COD. This meant that 81% of the COD origin from household wastewater and according to Jönsson et al. (2005) does a PE generate 135 g COD/day, which was assumed to be representative for the people connected to Sjölanda. The number of PE, from households, connected to the catchment area of the measured data was given by dividing the amount of COD from the household with the amount of COD generated by one person. The number of PE generating the wastewater from households was 27 516 PE. Given the number of PE was the number of PE with urine separation calculated for each scenario.

### 3.2.2 Input data for scenarios with urine separation

Theoretical values of the amount of each component and flow generated by one PE, from Table 1 under section 2.1.1, were used to estimate the total reduction when a number of PE changed to urine diversion toilets. Following equations describes the change in flow and amount of components such as COD, TKN, TP and TSS. The reduction of a component for a scenario was calculated according to equation 3,

$$X_{red} = 0.95nX_{perPE} \quad \text{Eq. 3}$$

where  $X_{red}$  is the amount of the component X that will have to be deducted from the original data given in g/day, 0.95 is the purification factor which describe that 95% of the urine will be separated,  $n$  is the number of PE with urine separation toilets, and  $X_{perPE}$  is the amount of

component generated through urine per PE and day. The flow was changed as the urine separation increased and is calculated according to equation 4,

$$Q_{red} = \frac{X_{red_{H2O}}}{998\ 200} \quad \text{Eq. 4}$$

where  $Q_{red}$  is the flow, given in  $m^3/day$ , which had to be deducted from the original data to simulate the scenario where  $n$  PE uses urine separation,  $X_{red_{H2O}}$  is the mass of the water in urine which would be removed given by  $g/day$ , and 998 200 is the density of water given in  $g/m^3$ . The flow was also assumed to be reduced by the fact that the number of flushes would decrease. The small amount of water to flush the separated urine is assumed to only dilute the separated urine and not be flushed down the same pipe as the faeces and regular flush water. The total reduction of flow is given by equation 5,

$$Q_{red_{tot}} = Q_{red} + n4.5 * 0.002 \quad \text{Eq. 5}$$

where  $Q_{red_{tot}}$  is the total reduction of flow, given in  $m^3/day$ , for  $n$  PE using urine separation,  $Q_{red}$  is the reduction of flow due to less urine in to the WWTP, and the other term describes the reduction of flow due to less number of flushes. It was assumed that each PE with urine separation would decrease the number of flushes per day by 4.5 times; multiplying that number with  $n$  PE and assuming each of those flushes to have been with containing  $0.002 m^3$  of water per flush generated the total decrease of flow generated by a decrease of flushes. Given the amount of reduction of component X and flow Q generated by  $n$  PE is the percentage calculated by equation 6,

$$\%red = \frac{X_{red}}{X_0}, \frac{Q_{red_{tot}}}{Q_0} \quad \text{Eq. 6}$$

where  $\%red$  is the percentage that the component  $X_0$  or flow  $Q_0$  from the data for the scenario with no urine separation has to be reduced to represent the amount of component X or flow Q generated with  $n$  PE using urine diversion toilets.

According to Jönsson et al. (2005) are the P and N in urine most in the form of phosphate and ammonium, respectively. So the reduction caused by urine diversion results in a shift of the PO4:TP and NH4:TKN ratios. The new ratios were calculated according to equation 7 and 8,

$$PO4:TP_i = \frac{PO4:TP_0 TP_{average,0} - 0.91(TP_{average,0} - TP_{average,i})}{TP_{average,i}} \quad \text{Eq. 7}$$

$$NH4:TKN_i = \frac{NH4:TKN_0 TKN_{average,0} - 0.95(TKN_{average,0} - TKN_{average,i})}{TKN_{average,i}} \quad \text{Eq. 8}$$

where  $X_{average,0}$  is the average influent concentration of TP or TKN for scenario 0 with no urine diversion. The parameter  $TP_{average, i}$  and  $TKN_{average, i}$  describes the average influent concentration of TP and TKN, respectively, for scenario  $i$ . The PO4:TP<sub>0</sub> and NH4:TKN<sub>0</sub> describes the ratios for scenario 0. The parameter 0.91 is the PO4 fraction of the TP in urine, and 0.95 the NH4 fraction of TKN.

### 3.3 MODEL IN DHI'S SOFTWARE WEST

The model of the WWTP was created with DHI's software WEST, and the simulation tool used was WESTforOPTIMIZATION. In this programme there is a library of blocks, representing different treatment units in a WWTP through known models. In order to replicate

an EBPR was the ASM2dModTemp instance chosen for the simulations. The blocks were assembled by drag and drop on to a layout sheet to create a flow scheme. The blocks were then connected to each other through their inflow or outflow connections. In Figure 2 is the first scheme of the WWTP's influent and main effluent illustrated, the items in this figure are an excerpt from WEST (DHI, 2017).

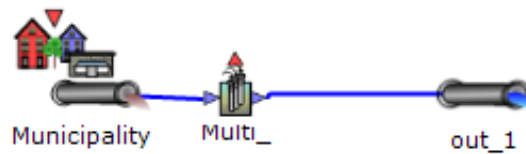


*Figure 2: The first step in the layout of the model. Furthest to the left is the influent block denoted Municipality; the middle block is a sensor denoted Multi\_ and the last block is the main effluent denoted out\_1.*

From the left in Figure 2, the incoming water origin from the “Municipality” block, then a sensor measuring the components in the generated wastewater and last an effluent block. This layout was used to fractionate the wastewater properly to resemble the measured data; this was the system boundary for the first mass balance. The “Municipality” block converts the input data Q, COD, TSS, TKN, and TP to the components used in the ASM2dModTemp instance developed for WEST by DHI (2017). The conversion is described by a fractionation scheme. For this instance was there no default fractionation scheme available and one was made with inspiration from the default fractionation schemes found for the ASMG2d and ASM2dM instance along with the description of the ASM2dModTemp found at the WEST models guide online (DHI, n.d.). In Figure 3 is the fractionation for the modelled wastewater illustrated. The left pointing arrows symbolise the input data and the right pointing arrows symbolise the ASM2dModTemp components.

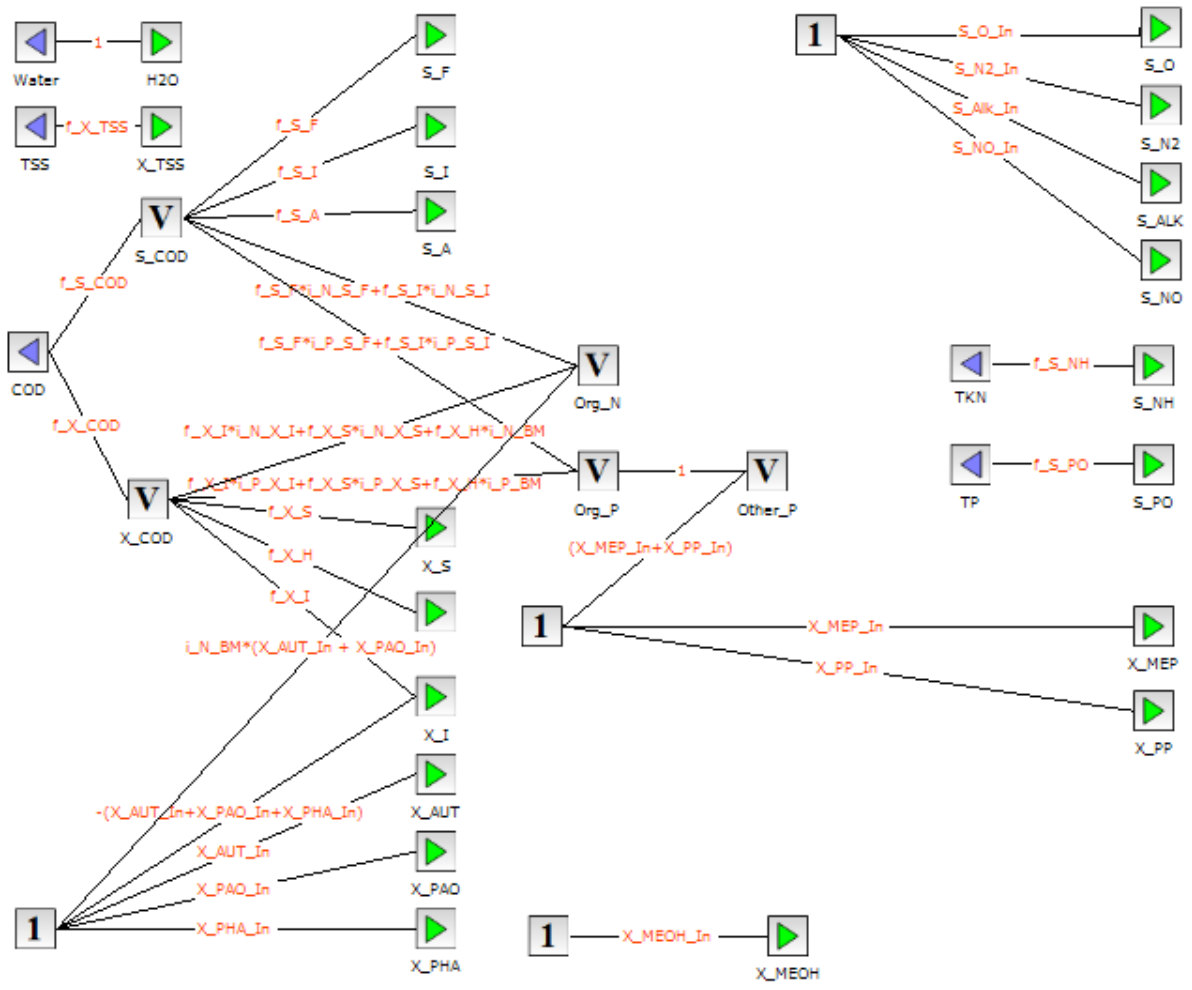


Figure 3: The fractionation of the measured data into model components. Left-pointing arrows symbolise the measured data and the right-pointing arrows the ASM2dModTemp components. This is an excerpt from DHI WEST.

A similar scheme was created for the effluent block. The purpose of this scheme was to transform the model components back to the variables of interest, in this case the same as the measured data. The scheme in Figure 4 below is a defractionation scheme.

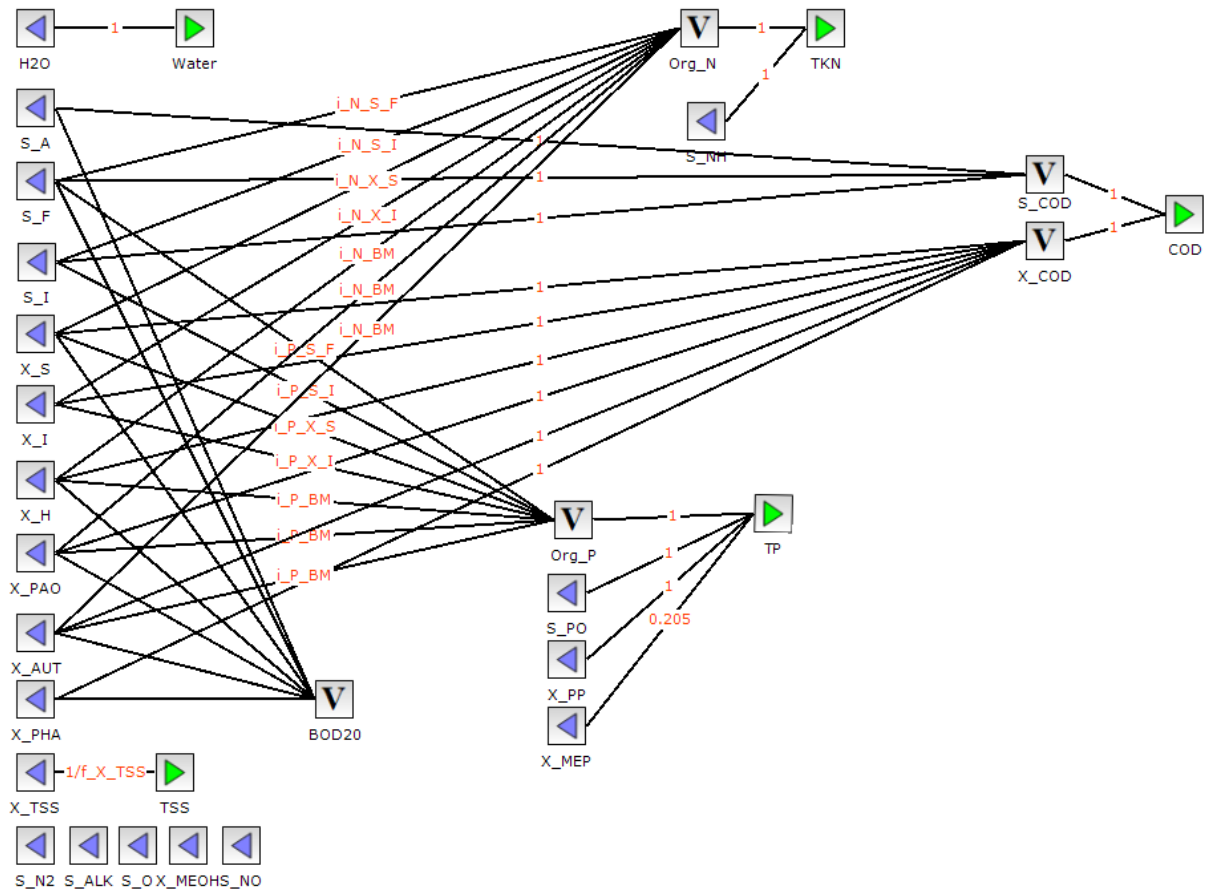


Figure 4: The defractionation scheme transforming the model components into the variables of interest. In this case are they the same as the measured data. Left-pointing arrows represent the model components and the right-pointing arrows the variables of interest. This is an excerpt from DHI WEST.

The fractionation scheme is a description how the data will be transformed and converted to the components used in the programme, and vice versa for the defractionation scheme. The lines between each box display how the input data and components are depended of each other. Each link was assigned a weight, which describes how the value of one box is depended of the box prior to it. The box with a “V” is a variable and the box with “1” is a so-called “dummy” for when the component is assigned a value directly. The weighting of components was set with the parameters described in the table below, Table 7, collected from the ASM2d model developed by Henze et al. (1999).

Table 7: Parameters used to fraction the measured data into model components. The default values are values presented in a characterisation done by Henze et al. (1999).

Parameter	Type	Description	Default value
f_X_COD	Fraction	Particulate COD fraction of total COD	0.69
f_S_COD	Fraction	Soluble COD fraction of total COD	0.31
f_S_F	Fraction	S <sub>F</sub> fraction of soluble COD	0.375
f_S_A	Fraction	S <sub>A</sub> fraction of soluble COD	0.25
f_S_I	Fraction	S <sub>I</sub> fraction of soluble COD	0.375
f_X_I	Fraction	X <sub>I</sub> fraction of particulate COD	0.14
f_X_S	Fraction	X <sub>S</sub> fraction of particulate COD	0.69
f_X_H	Fraction	X <sub>H</sub> fraction of particulate COD	0.17
f_S_PO	Fraction	S <sub>PO</sub> fraction of TP	0.6
f_S_NH	Fraction	S <sub>NH</sub> fraction of TKN	0.6
f_X_TSS	Conversion factor	Measured SS to X <sub>TSS</sub>	1.29

Henze et al. (2000) recommend increasing the measured value for suspended solids, often measured with a 1.6 µm filter, with a factor of 1.29. Hence the filter is too coarse and the colloidal part of X<sub>S</sub> will not be measured. The default values for parameters in the fractionation scheme generated a too high TP concentration for the modelled influent. To investigate this problem was the TP:COD and S<sub>PO</sub>:TP ratios of the wastewater used by Henze et al. (1999) compared with the ratios for the measured values from Sjölanda. The ratios are presented in Table 8 below.

Table 8: Comparison of the TP to COD, the S<sub>PO</sub> to TP, and the Other<sub>P</sub> to COD ratio between the wastewater used by Henze et al. (1999) and the wastewater used in this report from Sjölanda WWTP. Other<sub>P</sub> is a notation for the P in other forms than dissolved P in the system.

	Henze et al. (1999)	Sjölanda
<b>TP:COD</b>	2.31e-2	9.74e-3
<b>S<sub>PO</sub>:TP</b>	0,6	0,51
<b>Other<sub>P</sub>:COD</b>	9.23e-3	4.97e-3

When studying the ratios presented in Table 8 it was seen that the Other<sub>P</sub> to COD ratio for Sjölanda was about half of the ratio in the wastewater presented in Henze et al. (1999). Parameters in the ASM2dModTemp instance affecting these ratios, and the N and COD ratios, are presented in Table 9, along with a range of values for the parameters suggested by in the report from Henze et al. (2000).

Table 9: The table presents composition parameters describing the amount of N and P within the different fractions of COD. There is a short description for each composition parameter, as well as its unit and default value given by the DHI's WEST models guide (n.d) for the ASM2dModTemp instance, and the range given by Henze et al. (2000).

Parameter	Description	Unit	Default value	Range given by Henze et al. (2000)
i_N_BM	The N content of the biomass	gN/gCOD	0.07	0.05-0.07
i_N_S_F	The N content of the soluble substrate		0.03	0.02-0.04
i_N_S_I	The N content of the inert S_COD		0.01	0.01-0.02
i_N_X_I	The N content of the inert X_COD		0.03	0.005-0.01
i_N_X_S	The N content of the particulate substrate		0.04	0.02-0.04
i_P_BM	The P content of the biomass	gP/gCOD	0.02	0.01-0.02
i_P_S_F	The P content of the soluble substrate		0.01	0.01-0.015
i_P_S_I	The P content of the inert S_COD		0	0.002-0.008
i_P_X_I	The P content of the inert X_COD		0.01	0.005-0.01
i_P_X_S	The P content of the particulate substrate		0.01	0.01-0.015

Trials with different values within the range given by Henze et al. (2000) were executed, and an acceptable TKN concentration compared to the measured data was found. The parameters describing the P content in COD however, had to be set to lower values in order for the TP concentration in the model to decrease enough to be similar to the measured value.

After the fractionation scheme was set the input data was uploaded to the “Municipality” block and then the influent to the WWTP could be generated for both steady state and dynamic simulations.

The next block in the layout was the “primary clarifier”. This block is based on Takács primary clarifier model, which in turn is based on Vitasovic (DHI, n.d.). In Figure 5 below is the flow scheme updated with a primary clarifier block between the sensor and the effluent point. A second effluent point was also added to generate the primary sludge from the clarifier. The figure also shows the system for the second mass balance calibration.

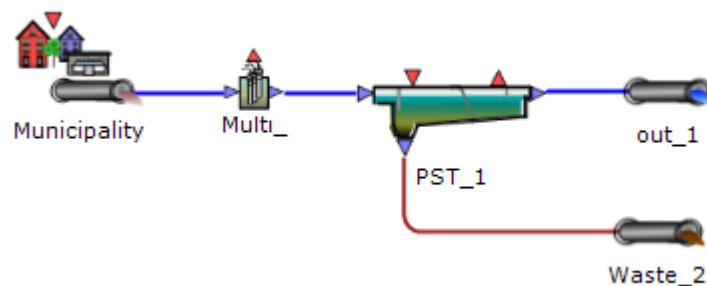


Figure 5: The second step in the layout of the model. Furthest to the left is the influent block denoted Municipality; the next block is a sensor denoted Multi\_; third block from the left is the primary clarifier denoted PST\_1 and from this block is the stream divided into one water stream and one sludge stream; the last block of the main stream of the water is the main effluent denoted out\_1. The sludge stream is collected in an effluent point for waste, denoted Waste\_2.

According to Swedish standard should the primary clarifier remove around 50–70% of the incoming TSS and 5–15% of the incoming P (Svenskt Vatten, 2013). The value of parameters used for the primary clarifier block was first the default values, which are presented in Table 10.

Table 10: The parameters included in the model for the primary clarifier block in DHI WEST (DHI, n.d.).

Parameter	Description	Unit	Default value
<b>A</b>	Surface area	m <sup>2</sup>	1500
<b>F_Energy_FlowRate</b>	Conversion factor	kWh/m <sup>3</sup>	0.04
<b>f_ns</b>	Non-settleable fraction of TSS	-	0.0024
<b>F_TSS_COD</b>	TSS:COD ratio	-	0.75
<b>H</b>	Height of the clarifier	m	4
<b>Q_Under</b>	Underflow rate	m <sup>3</sup> /d	200
<b>r_H</b>	Hindered settling parameter	m <sup>3</sup> /g	0.00019
<b>r_P</b>	Settling parameter for low conc.	m <sup>3</sup> /g	0.00286
<b>v0</b>	Max. theoretical settling velocity	m/d	474
<b>v00</b>	Max. practical settling velocity	m/d	250
<b>X_Lim</b>	Minimal conc. In sludge blanket	g/m <sup>3</sup>	900
<b>X_T</b>	Threshold suspended solids conc.	g/m <sup>3</sup>	3000

Those parameter values generated a too high removal rate for both TSS and TP. Through trials were some values changed to better fit the expected treatment efficiency. The default area of the primary clarifier was larger than required. Therefore was the dimension of the primary clarifier was set through some design parameters given by equation 9, from (Water Environment Federation, 2005),

$$SOR = \frac{Q_{PI}}{A_{PC}} \quad \text{Eq. 9}$$

where SOR is the surface overflow rate in m<sup>3</sup>/m<sup>2</sup>,day, Q<sub>PI</sub> is the flow rate of the water coming in to the primary clarifier given in m<sup>3</sup>/day, and A<sub>PC</sub> is the surface area of the primary clarifier. An appropriate SOR according to Water Environment Federation (WEF) is around 24.4–48.9 m<sup>3</sup>/m<sup>2</sup>, day. And by the yearly average flow rate at 9603.1 m<sup>3</sup>/day could the area of the primary clarifier be varied between 196.4–393.6 m<sup>2</sup>.

The parameter for the non-settleable fraction of TSS, *f<sub>ns</sub>*, results in higher removal rate the smaller the value is. Since the removal rate was too high was it assumed that the *f<sub>ns</sub>* for the used wastewater was higher than the given default value. Wahlberg (2006) studied the performance of primary clarifier for several WWTPs in US. The raw wastewater and its characterisation for all the WWTP is given in Wahlberg's report, and is used as a guide for the determination of *f<sub>ns</sub>* in this report. The non-settleable fraction of TSS and COD varied between 0.20–0.33 and 0.43–0.59, respectively (Wahlberg, 2006).

Takacs et al. (1991) presented a set of values for the parameter *v0*, *v00*, and *r<sub>P</sub>* depending on the flow and concentration of the wastewater used in a pilot scale trial of the Takacs model, presented earlier in Table 3. The trial with the highest flow and concentrations of components, such as COD and TP, had the lowest parameter values for those parameters, and vice versa for

the water with the lowest flow and load. Since the wastewater from Sjölanda had even higher flow and concentrations were those parameters set to even smaller values.

The next blocks, after the primary clarifier, were the ASUs making up the EBPR. The two first units were anaerobic and the three after have aerobic conditions. The ASU were denoted with numbers in the order they were reached by the water. The dimensions of an anaerobic ASU and an aerobic ASU are presented in Table 11 below, given by Martinello (2013). The ASU\_6 and ASU\_7 are also anaerobic but not a part of the EBPR. They are used for the hydrolysis of the excess sludge.

Table 11: The dimensions of the activated sludge units constituting the EBPR, the ASU used for the P release, and the secondary settler.

	Unit	Height m	Area m <sup>2</sup>	Volume m <sup>3</sup>
<b>Anaerobe reactors</b>	ASU_1, ASU_2, ASU_6 and ASU_7	3.8	54.3	206.25
<b>Aerobic reactors</b>	ASU_3, ASU_4 and ASU_5	3.8	108.6	412.5
<b>Total EBPR</b>	ASU_1 - ASU_5	3.8	434.2	1650
<b>Secondary settler</b>	SST_1	3.8	467	1783

The controllers connected to the ASUs with aerobic conditions were set to keep a dissolved oxygen (DO) concentration of 3 g/m<sup>3</sup> as in Aspegren (1995) study. The ASU block is a model describing the process of AS if there is a constant volume and it is ideally mixed (DHI, n.d.). A model of an EBPR processes in the WWTP was created with these conditions of the ASUs.

The “secondary clarifier” block was the block after the EBPR. This block is based on Takács SVI model developed by Takács et al. in 1991. The parameters, presented in Table 12, corresponding to this unit were modified in order to allow for a larger sludge production and removal of nutrients in the effluent through sedimentation.

Table 12: The parameters included in the model for the secondary settler block in DHI WEST ASM2dModTemp instance (DHI, n.d.).

Parameter	Description	Unit	Default value
<b>A</b>	Surface area	m <sup>2</sup>	1500
<b>F_Energy_FlowRate</b>	Conversion factor	kWh/m <sup>3</sup>	0.04
<b>f_ns</b>	Non-settleable fraction of TSS	-	0.0024
<b>F_TSS_COD</b>	TSS:COD ratio	-	0.75
<b>H</b>	Height of the clarifier	m	4
<b>Q_under</b>	Underflow rate	m <sup>3</sup> /d	200
<b>r_P</b>	Settling parameter for low conc.	m <sup>3</sup> /g	0.00228
<b>v0</b>	Max. theoretical settling velocity	m/d	474
<b>v00</b>	Max. practical settling velocity	m/d	250
<b>X_lim</b>	Min. conc. In the sludge blanket	g/m <sup>3</sup>	900
<b>X_T</b>	Threshold suspended solids conc.	g/m <sup>3</sup>	3000
<b>SVI</b>	Sludge volume index	-	100

The sludge flow from the secondary settler was controlled by two “on and off” controllers, which in turn was dependent on the flow rate of the incoming wastewater. If the flow of the incoming water increased over 20 000 m<sup>3</sup>/day the flow of the sludge increased from 4550 m<sup>3</sup>/day to 8000.

Guidelines showed that the SRT of an EBPR process should be between 5–12 days. Trials eventually led up to that the lowest P concentration in the effluent water was reached when SRT was 5 days. The mean SRT of the whole EBPR process was then kept at 5 days through a combination of a calculator and controller called Q\_WAS\_PI. The mean SRT was set to 5 days and then the controller was connected to the separation point redirecting the excess sludge from the return sludge. The excess sludge was treated through two anaerobe ASUs, ASU\_6 and ASU\_7. Since the flow of the excess sludge was varied to keep a SRT of 5 days was it necessary to add an “on and off” controller to change the Q\_WAS\_PI signal to 1 m<sup>3</sup>/day if the signal was lower than 1 m<sup>3</sup>/day. A signal lower than 1 m<sup>3</sup>/day into the ASU\_6 and ASU\_7 would generate an error message. The return sludge would be led back to the main stream prior to the EBPR.

The excess sludge was treated through two anaerobe ASUs to generate a PO<sub>4</sub> release for the nutrient recovery. In order to simulate this was the temperature kept at 20 °C. With hydrolysis of the excess sludge is it possible to transform 50–70% of the TP to PO<sub>4</sub> according to Ekobalans Fenix AB (2017) and Ostara Nutrient Recovery Technologies Inc (2017c). A dewatering unit was added after the ASU\_7 to separate most of the sludge from the water and the now dissolved P. This unit was a large simplification, with only two operational parameters. The percentages dry solids and the desired flow of sludge. These were set to 50% and an interval of 25–40 m<sup>3</sup>/day depending on the excess sludge flow, respectively.

### 3.4 THEORETICAL MAP PRODUCTION

According to the comparison of the methods producing MAP, Table 5, would approximately 90% of the PO<sub>4</sub> in the influent to the recovering process be recovered as MAP. The molar weight of phosphate is 94.97 g/mole and the total molar weight of MAP is 245.42 g/mole (Aylward & Findlay, 2008); phosphate constitutes around 39% of the total weight of MAP. The theoretical MAP production was calculated with equation 9 below,

$$MAP_{theoretical} = \frac{0.9PO_4}{0.39} \quad \text{Eq. 10}$$

where MAP<sub>theoretical</sub> is the possible amount of MAP that can be produced and PO<sub>4</sub> is the amount of phosphate in the influent.

### 3.5 THEORETICAL AMS PRODUCTION

According to the comparison of the methods producing AMS, Table 6, is approximately 90% of the N in the influent to the AMS recovery unit recovered. The molar weight of ammonium is 18.04 g/mole and the total molar weight of AMS is 132.14 g/mole (Aylward & Findlay, 2008); ammonia constitutes around 14% of the total weight of AMS. Under the assumption that 70% of TKN in the sludge was converted into ammonium in the anaerobic digester (Gustavsson, pers.contact) was the theoretical AMS production calculated with equation 11 below,

$$AMS_{theoretical} = \frac{0.9(0.7TKN)}{0.14} \quad \text{Eq. 11}$$

where  $AMS_{\text{theoretical}}$  is the possible amount of AMS that can be produced and TKN is the amount of TKN in the influent to the recovery unit.

### 3.6 THEORETICAL BIOGAS PRODUCTION

The theoretical biogas production (BgP) was calculated from the biodegradable COD found in the primary sludge and the WAS for each scenario. Biogas is a mixture of several different gases where  $CH_4$  is one of them. From the stoichiometric formula of producing methane, it is theoretically possible to produce  $0.35 \text{ m}^3 \text{ CH}_4 / \text{kg}$  biodegradable COD found in the sludge under normal temperature and pressure conditions. The fraction of  $CH_4$  in biogas usually varies between 70–80% (de Lemos Chernicharo, 2007). The theoretical biogas production would therefore be according to equation 12,

$$BgP_{\text{max}} = \frac{0.35}{0.70} COD = 0.5COD, \quad BgP_{\text{min}} = \frac{0.35}{0.80} COD = 0.438COD \quad \text{Eq. 12}$$

where  $BgP$  is the theoretical biogas production given in  $\text{m}^3$ , COD is the amount of COD in the sludge given in kg and the conversion factor is given in  $\text{m}^3 \text{ BgP/kg COD}$ .

### 3.7 CALIBRATION

Calibration of the model was done in several steps throughout building the layout of the model.

#### 3.7.1 Mass balance

The model was calibrated by studying the mass balance of COD, TSS, TKN and TP in the system, equation 13 describes the mass balance, given by Rieger et al. (2013),

$$C_{\text{input}} Q_{\text{input}} + Vr_v = \sum_n^1 C_{\text{output},i} Q_{\text{output},i} + Acc. \quad \text{Eq. 13}$$

where  $C_{\text{input}}$  is the concentration the component in the influent,  $Q_{\text{input}}$  is the influent flow,  $C_{\text{output},i}$  is the concentration of the component and  $Q_{\text{output},i}$  is the flow at the effluent point  $i$ , and  $n$  is the number of effluent points in the system. The term  $Vr_v$  describes the reactions happening within the system, where  $V$  is the volume of the system and  $r_v$  is the reaction rate. For the TP in a WWTP is there no reaction rate and this term can be set to 0. It can also be assumed that there are no reactions of COD, TKN and TSS within the primary clarifier and the secondary settler.  $Acc.$  is the accumulation of the component in the system. Under steady state conditions and a period longer than 2–3 times the SRT is the accumulation in the system minor and the term can be set to 0. An acceptable error in the mass balance is 5–10% (Rieger et al., 2013).

The different systems that was used for the mass balances was: around the primary clarifier, around the secondary clarifier, around the EBPR and secondary clarifier, around the hydrolysis of the excess sludge and the extra secondary clarifier, and last around the whole WWTP.

## 4 RESULTS

### 4.1 DATA SERIES

The box plot of the measured COD showed that there was one extreme outlier, with a value of 1400 mg/l. The data set from that day was removed. When studying the box plots of the different ratios only the TSS/COD ratio resulted in extreme outliers. In this case were there 4 measurements where the TSS was higher than the COD. These data sets were also removed. In the appendix is the data series for scenario 0 found, where the days that contained an extreme outlier are missing.

The calculated mean filtered TP fraction of TP was 0.54 and when studying the plot below, Figure 6, it shows a ratio of 0.51. It is assumed that the measured filtered TP is close to the PO<sub>4</sub> concentration.

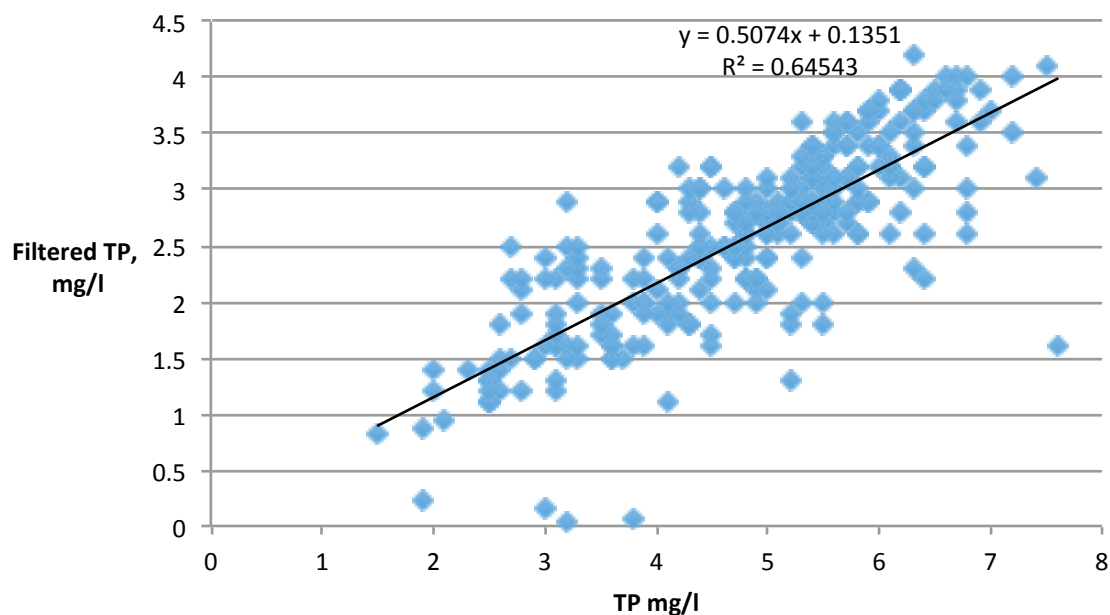


Figure 6: The relation between measured filtered TP (mg/l) and TP (mg/l) in the incoming wastewater at Sjöhlunda WWTP in 2015.

The calculated mean NH<sub>4</sub> fraction of TKN was 0.61 and the plot below, Figure 7, show a ratio of 0.56.

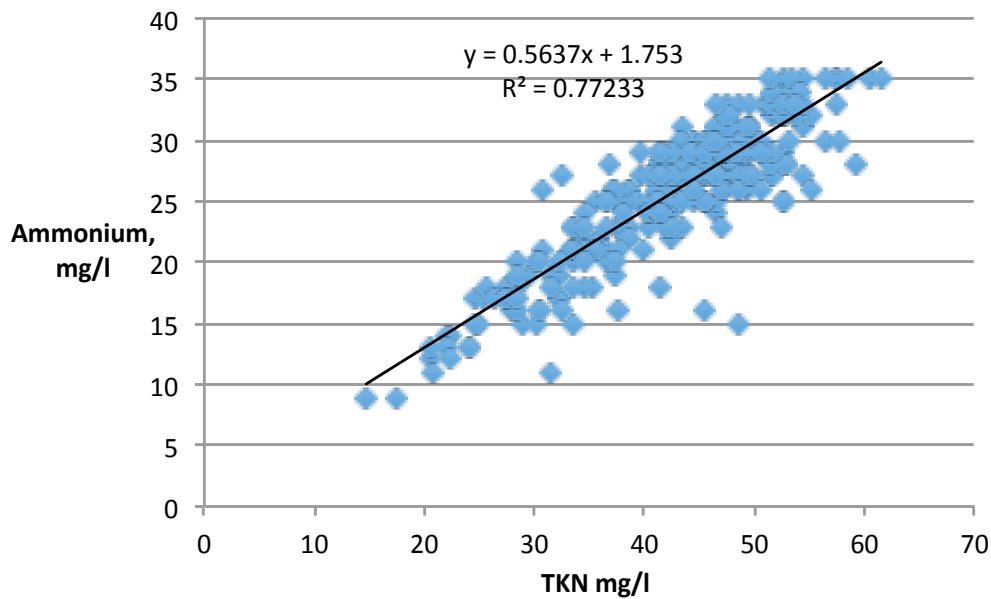


Figure 7: The relation between measured ammonium (mg/l) and TKN (mg/l) in the incoming wastewater at Sjölanda WWTP in 2015.

The table below, Table 13, presents the percentage each component and flow was reduced by in order to simulate an increasing urine separation in the WWTP's catchment area. By reducing each day with the same percentage are the seasonal variations of the original data kept.

Table 13: The reduction of components and flow from the original data with no urine separation given by percentage for each scenario of urine separation.

Scenario	Number of PE with urine separation	Q (%)	COD (%)	TP (%)	TKN (%)	TSS (%)
0 %	0	0	0	0	0	0
1 %	275	3.08e-2	4.94e-2	5.48e-1	7.51e-1	9.00e-3
5 %	1376	1.54e-1	2.47e-1	2.74	3.75	4.50e-2
10 %	2752	3.08e-1	4.94e-1	5.48	7.51	9.00e-2
25 %	6879	7.70e-1	1.23	13.7	18.8	2.25e-1
50 %	13758	1.54	2.47	27.4	37.5	4.50e-1
75 %	20637	2.17	3.70	41.1	56.3	6.75e-1
90 %	24764	2.77	4.44	49.3	67.6	8.10e-1

Table 13 shows that the components most affected by the urine separation are the incoming TP and TKN. The decrease in TP and TKN and the assumption that 91% of the TP removed was PO<sub>4</sub> and 95% of the removed TKN was NH<sub>4</sub> resulted in a change of the fraction of PO<sub>4</sub>:TP and NH<sub>4</sub>:TKN. The different fractions for the 8 scenarios are presented in Table 14 below.

Table 14: The fraction PO4 of the TP, denoted  $f_{S\_PO}$ , and the fraction NH4 of the TKN, denoted  $f_{S\_NH}$ , are presented for each scenario.

Scenario	$f_{S\_PO}$	$f_{S\_NH}$
0	0.515	0.61
1	0.513	0.607
5	0.504	0.597
10	0.492	0.582
25	0.452	0.531
50	0.366	0.406
75	0.239	0.172
90	0.131	0*

The value for  $f_{S\_NH}$  for scenario 90, with 90% urine diversion, is denoted with an asterisk. This is because when calculating this value with equation 8, mentioned earlier, was the result negative, -0.09. However, the range of a fraction is between 0 and 1. It was therefore set to the smallest value possible.

## 4.2 THE FULL WWTP MODEL

The full WWTP model is illustrated in Figure 8. The figure is an excerpt from DHI WEST (2017).

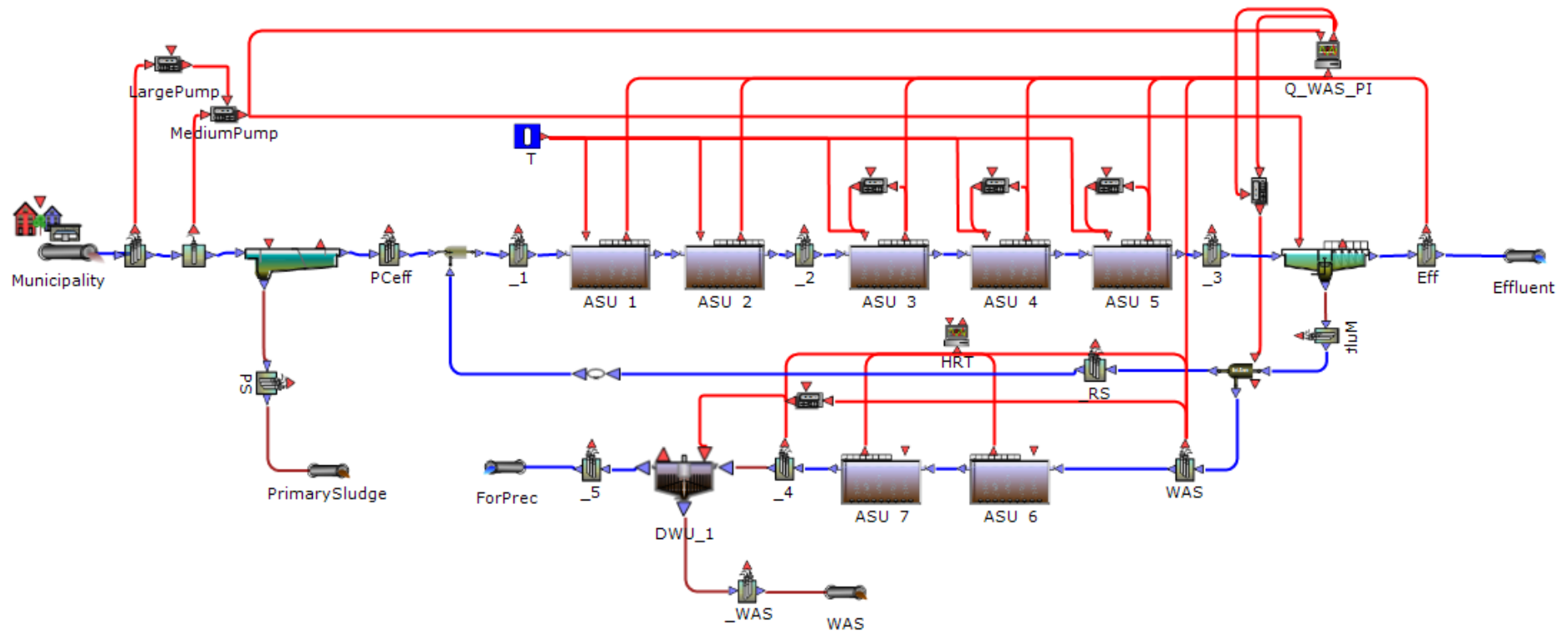


Figure 8: The full WWTP; an excerpt from DHI WEST. Furthest to the left is the influent to the WWTP, then the main streamline goes through a primary clarifier, two anaerobe ASUs (ASU\_1 and ASU\_2), three aerobe ASUs (ASU\_3-ASU\_5), a secondary settler and eventually to the effluent point furthest to the right. A sludge streamline is placed from the primary clarifier to generate the primary sludge. A second sludge streamline can be seen from the secondary settler. It splits up into two separate streams: the return sludge that is led back to the main stream and the excess sludge stream led to ASU\_6. The streamline representing the excess sludge contains two anaerobe ASUs (ASU\_6 and ASU\_7) and a dewatering unit separating the phosphate-rich water from the excess sludge. There are several controllers in the layout; the first controllers furthest to the left denoted LargePump and MediumPump controls the underflow rate of secondary clarifier and the parameter for the maximum flow of the excess sludge in the Q\_WAS\_PI controller. The Q\_WAS\_PI controller keeps the mean SRT to 5 days. Next is three PI controllers placed above the aerobe ASU to control the oxygen within the tanks. The blue box with a white mark on, attached to all ASUs in the EBPR, changes the temperature to match the measured temperatures from Sjölanda. The block denoted HRT is a calculator, it calculates the HRT of ASU\_6 and ASU\_7.

#### 4.2.1 Final fractionation and wastewater characterisation

The fractionation of the measured data variables to model components was changed back and forth until an acceptable mass balance was achieved between the modelled COD, TSS, TKN, TP, PO<sub>4</sub> and NH<sub>4</sub> and the measured values. A higher TSS than the measured value caused large indifferences in the mass balances and problems when running the model even though Henze et al. (2000) recommended an increase in TSS. The fraction  $f_{X\_TSS}$  was therefore set to 1. The fractionation of COD was set by studying fractionations from Henze et al. (2000) and Nobel (2015). The PO<sub>4</sub> fraction of TP and the NH<sub>4</sub> fraction of TKN were changed according to the calculated fractions presented in Table 14 presented earlier. In Table 15 below are the final values and the default values for each fraction in the Municipality block presented.

Table 15: The final values of the calibrated fractions in the fractionation scheme for the WWTP model along with the default values.

Parameter	Description	Default value	Final value
f_X_COD	Particulate COD fraction of total COD	0.69	0.69
f_S_COD	Soluble COD fraction of total COD	0.31	0.31
f_S_F	S <sub>F</sub> fraction of soluble COD	0.375	0.4
f_S_A	S <sub>A</sub> fraction of soluble COD	0.25	0.3
f_S_I	S <sub>I</sub> fraction of soluble COD	0.375	0.3
f_X_I	X <sub>I</sub> fraction of particulate COD	0.14	0.33
f_X_S	X <sub>S</sub> fraction of particulate COD	0.69	0.51
f_X_H	X <sub>H</sub> fraction of particulate COD	0.17	0.16
f_S_PO	S <sub>PO</sub> fraction of TP	0.6	0.515*
f_S_NH	S <sub>NH</sub> fraction of TKN	0.6	0.61*
f_X_TSS	Measured SS to X_TSS	1.29	1

\*scenario 0, changed for each scenario

The composition fractions describing the N and P content within the COD was changed to better fit the influent wastewater from Sjölanda. The parameters describing N was changed within the range presented by Henze et al. (2000). For the parameters describing P however, was it necessary to decrease the values even more. This due to the fact that the TP:COD ratio for Sjölanda was half of the ratio for typical wastewater presented by Henze et al. (2000). In Table 16 below are the final values of the composition fractions presented along with the default and range given by Henze et al. (2000).

Table 16: The final composition parameters for the P and N content of the COD along with the default values.

Parameter	Unit	Default value	Range given by Henze et al. (2000)	Final value
i_N_BM	gN/gCOD	0.07	0.05-0.07	0.07
i_N_S_F		0.03	0.02-0.04	0.04
i_N_S_I		0.01	0.01-0.02	0.02
i_N_X_I		0.03	0.005-0.01	0.01
i_N_X_S		0.04	0.02-0.04	0.04
i_P_BM	gP/gCOD	0.02	0.01-0.02	0.01
i_P_S_F		0.01	0.01-0.015	0.005
i_P_S_I		0	0.002-0.008	0
i_P_X_I		0.01	0.005-0.01	0.005
i_P_X_S		0.01	0.01-0.015	0.005

The composition parameters were set throughout the model; this includes the municipality block, the effluent points (both water and waste), sensors, and the ASUs.

#### 4.2.2 Calibrated primary clarifier

The parameters for the primary clarifier were changed in order to achieve a more realistic separation of TSS and TP. The default values caused a too high removal of TP and TSS. The aim was therefore to slow down the settling in the clarifier. Increasing the non-settable fraction, and decreasing the flow of primary sludge, settling velocities and parameters achieved this. The final values of the parameters describing the primary clarifier are presented in Table 17. The surface area results in a SOR of 38.4 m<sup>3</sup>/m<sup>2</sup>day for the mean flow, 9603.1 m<sup>3</sup>/day.

Table 17: The final values of the parameters found in the primary clarifier unit along with the default values.

Parameter	Unit	Default value	Final value
A	m <sup>2</sup>	1500	250
F_Energy_FlowRate	kWh/m <sup>3</sup>	0.04	0.04
f_ns	-	0.0024	0.44
F_TSS_COD	-	0.75	0.75
H	m	4	4
Q_under	m <sup>3</sup> /d	200	150
r_H	m <sup>3</sup> /g	0.00019	0.00019
r_P	m <sup>3</sup> /g	0.00286	0.001
v0	m/d	474	150
v00	m/d	250	45
X_lim	g/m <sup>3</sup>	900	900
X_T	g/m <sup>3</sup>	3000	3000

These parameters resulted in around 15% removal of TP and 35% removal of TSS. Several parameters combination were tried out, either the TSS removal was satisfying or the TP removal. A set of parameters resulting in a satisfying TP removal was chosen since the P recovering was of interest in this report.

### 4.2.3 Calibrated ASUs

The ASUs were changed as little as possible since the kinetics and stoichiometric parameters require more detailed and complex calculations to achieve better values than the default. However, it was seen that the amount of acetate in the ASU\_6 and ASU\_7 was low. The saturation factor for acetate was therefore increased from 4 to 5 g COD/m<sup>3</sup> in the ASUs describing the EBPR in order to spare some acetate for the ASU\_6 and ASU\_7. In the ASU\_6 and ASU\_7 were some parameters changed in order to achieve a better hydrolysis; according to Ekobalans Fenix AB is it possible to release 50% of the TP in the excess sludge in to PO<sub>4</sub>. The WASSTRIP from Ostara is supposed to release 70%. The parameters changed in the ASU\_6 and ASU\_7 was the temperature, which was set to 20 °C, the saturation parameter for the phosphorus, which was set from 0.01 to 0.3 g/m<sup>3</sup>. The latter mentioned parameter makes it possible for a larger PO<sub>4</sub> concentration in the tanks.

### 4.2.4 Calibrated secondary clarifier

The secondary clarifier was changed to settle faster than the default. This was done to achieve an acceptable effluent and to generate enough return and excess sludge. In the table below, Table 18, are the final values for each parameter in the secondary clarifier presented.

Table 18: The final values for the parameters describing the secondary settler along with the default values.

Parameter	Description	Unit	Default value	Final value
A	Surface area	m <sup>2</sup>	1500	467
F_Energy_FlowRate	Conversion factor	kWh/m <sup>3</sup>	0.04	0.04
f_ns	Non-settleable fraction of TSS	-	0.0024	0.002
F_TSS_COD	TSS:COD ratio	-	0.75	0.75
H	Height of the clarifier	m	4	3.8
Q_under	Underflow rate	m <sup>3</sup> /d	200	4550*
r_P	Settling parameter for low conc.	m <sup>3</sup> /g	0.00228	0.0035
v0	Max. theoretical settling velocity	m/d	474	900
v00	Max. practical settling velocity	m/d	250	500
X_lim	Min. conc. In the sludge blanket	g/m <sup>3</sup>	900	900
X_T	Threshold suspended solids conc.	g/m <sup>3</sup>	3000	3000
SVI	Sludge volume index	-	100	100

The final value of the  $Q_{underflow}$  is denoted with an asterisk. This is to note that the  $Q_{underflow}$  is changed by two “on and off”- controllers depending on the flow rate of the influent. If the flow rate falls below 8000 m<sup>3</sup>/day is the  $Q_{underflow}$  set to 1500 m<sup>3</sup>/day; if it is above 8500 is the “on and off” controller called LargePump activated and the  $Q_{underflow}$  is set to 4550 m<sup>3</sup>/day, and last if the flow rises up to 20 000 m<sup>3</sup>/day is the  $Q_{underflow}$  set to 8000 m<sup>3</sup>/day.

## 4.3 EFFECTS OF URINE DIVERSION ON THE WWTP

### 4.3.1 Influent

The modelled and measured influent flow rate, COD, TSS, TKN and TP for scenario 0 are found in Appendix A. The influent flows for each scenario are presented in Figure 9. The Figure 9 shows the monthly average flow for each scenario under a year.

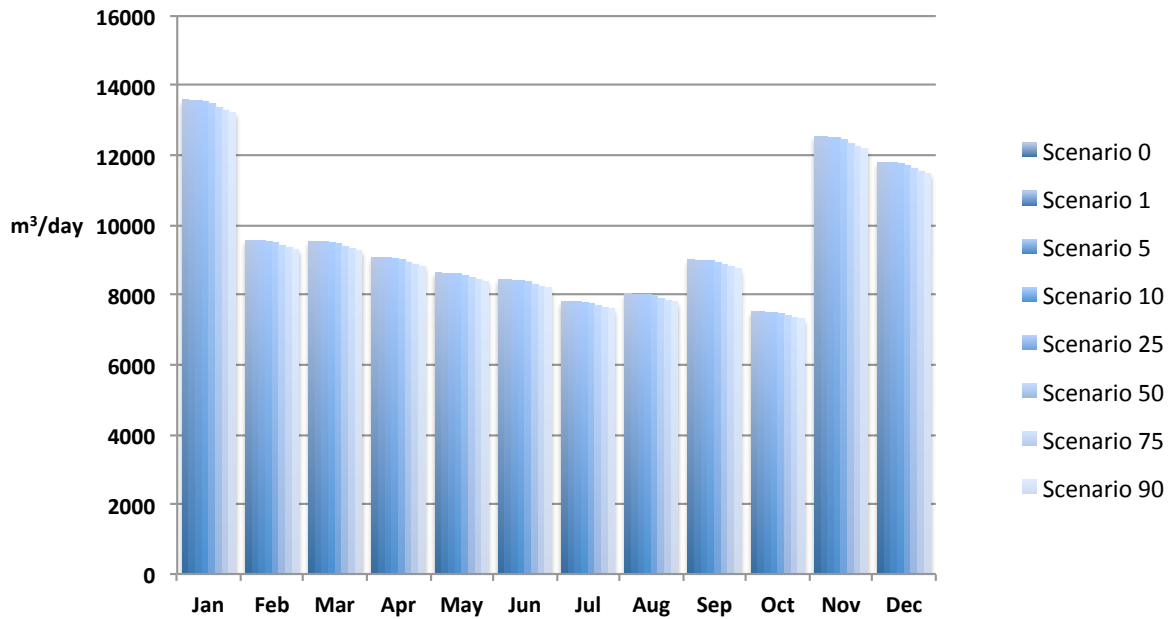


Figure 9: The graph shows the monthly average of the influent flow rate for each scenario. The darkest colour, furthest to the left in each column, represents scenario 0 with no urine diversion. The lightest colour, furthest to the right in each column, represents scenario 90 where 90% of the PE uses urine separation systems.

Figure 9, shows just a small difference in the flow even with 90% of the PE using urine separation systems. In Figure 10 is the change in the monthly average COD concentration for each scenario displayed.

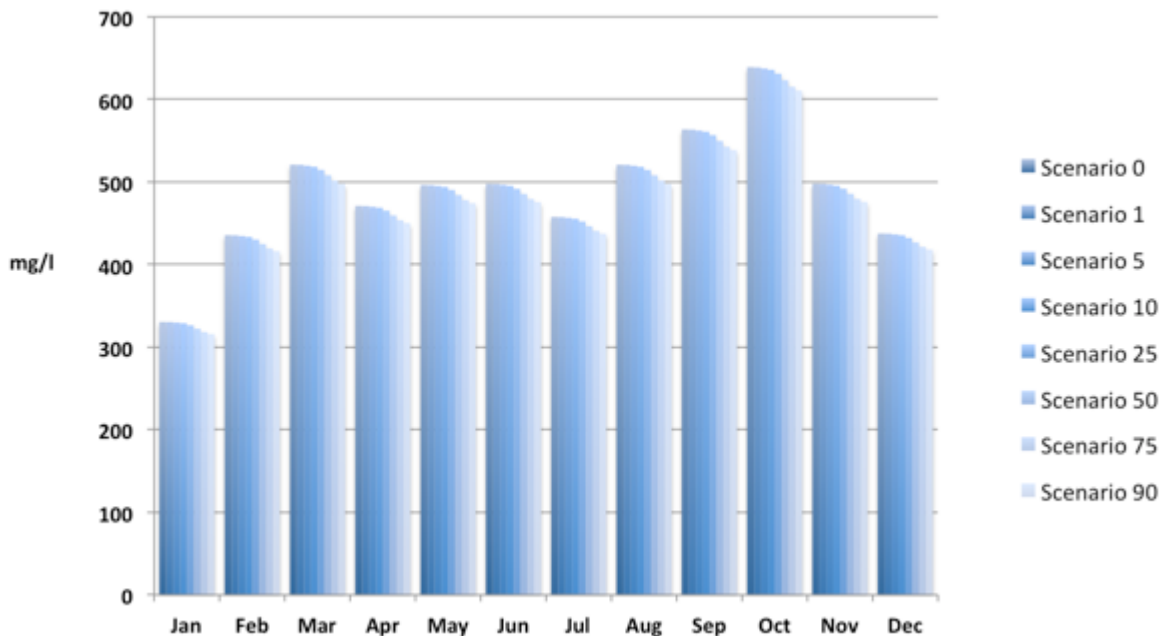


Figure 10: The graph shows the monthly average COD concentration into the modelled WWTP for each scenario. The darkest colour, furthest to the left in each column, represents scenario 0 with no urine diversion. The lightest colour, furthest to the right in each column, represents scenario 90 where 90% of the PE uses urine separation systems.

As for the flow rate, also the differences between the monthly average COD concentration for each scenario are small. In Figure 11 are the monthly average TSS concentrations for the different scenarios presented.

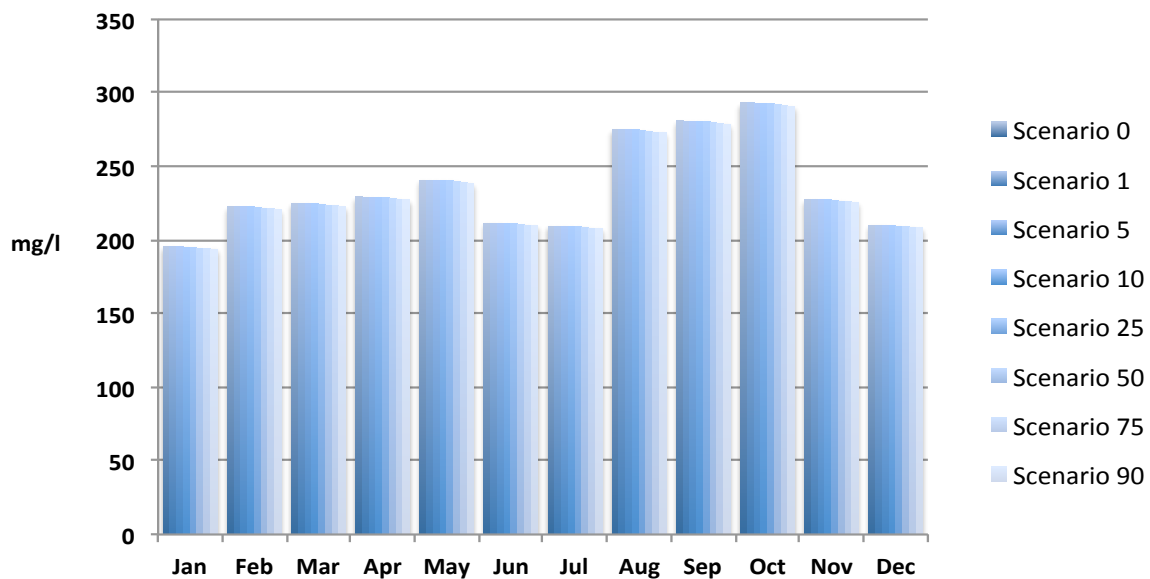


Figure 11: The graph shows the monthly average TSS concentration into the modelled WWTP for each scenario. The darkest colour, furthest to the left in each column, represents scenario 0 with no urine diversion. The lightest colour, furthest to the right in each column, represents scenario 90 where 90% of the PE uses urine separation systems.

Figure 11 shows that there is barely any change in the influent TSS when the urine diversion increases in the WWTP’s catchment area. In Figure 12 are the monthly average TKN concentrations for each scenario plotted for a whole year. There are significant differences in the TKN concentrations for the different scenarios. For example, in January the highest TKN concentration is between 20–30 mg/l for scenario 0 and between 0–10 mg/l for scenario 90.

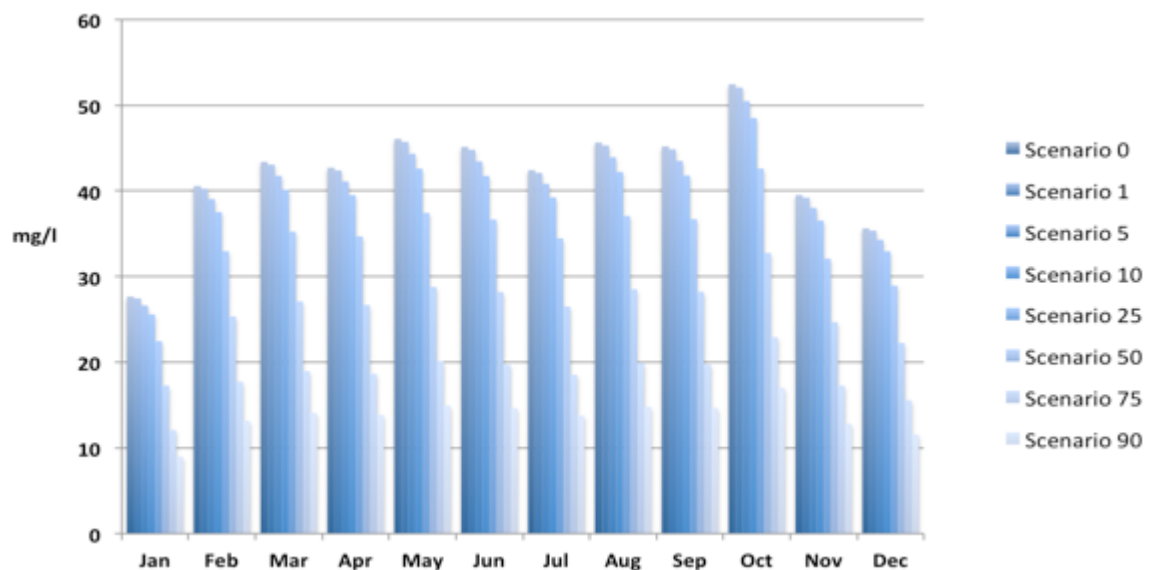


Figure 12: The graph shows the monthly average TKN concentration into the modelled WWTP for each scenario. The darkest colour, furthest to the left in each column, represents scenario 0 with no urine diversion. The lightest colour, furthest to the right in each column, represents scenario 90 where 90% of the PE uses urine separation systems.

The monthly average TP concentrations for each scenario are presented in Figure 13. There are also large differences in the TP concentrations for the different scenarios, as for the TKN concentrations.

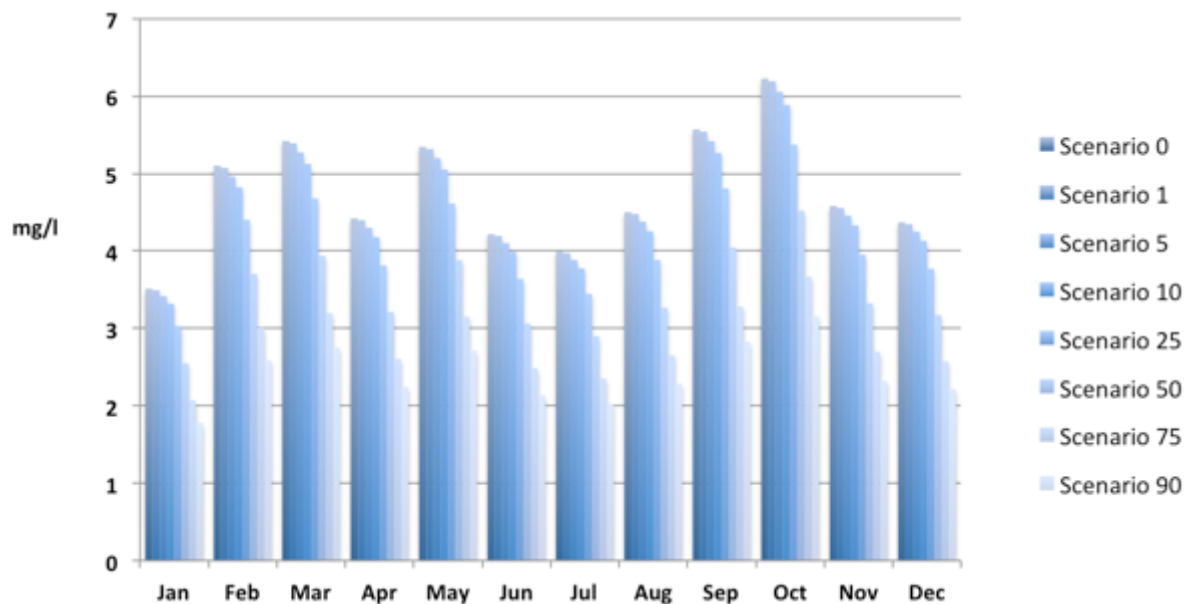


Figure 13: The graph shows the monthly average TP concentration into the modelled WWTP for each scenario. The darkest colour, furthest to the left in each column, represents scenario 0 with no urine diversion. The lightest colour, furthest to the right in each column, represents scenario 90 where 90% of the PE uses urine separation systems.

### 4.3.2 Effluent

The modelled effluent flow, given in  $\text{m}^3/\text{day}$ , for scenario 0 and the annual average is presented in Figure 14. The annual average is  $9374 \text{ m}^3/\text{day}$ .

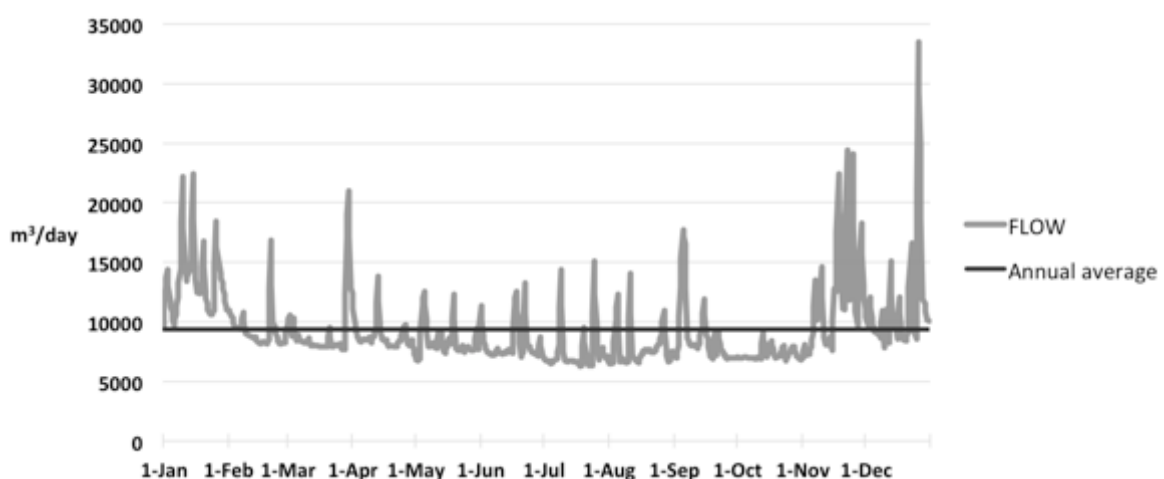


Figure 14: The grey line represents the effluent flow rate from the modelled WWTP over a year for scenario 0. The black, straight line represents the average flow rate over the year. The flow rate is given in  $\text{m}^3$  per day.

The difference in the effluent flow rate for each scenario is presented in Figure 15. As the influent flow rate does not change too much, neither does the effluent flow rate.

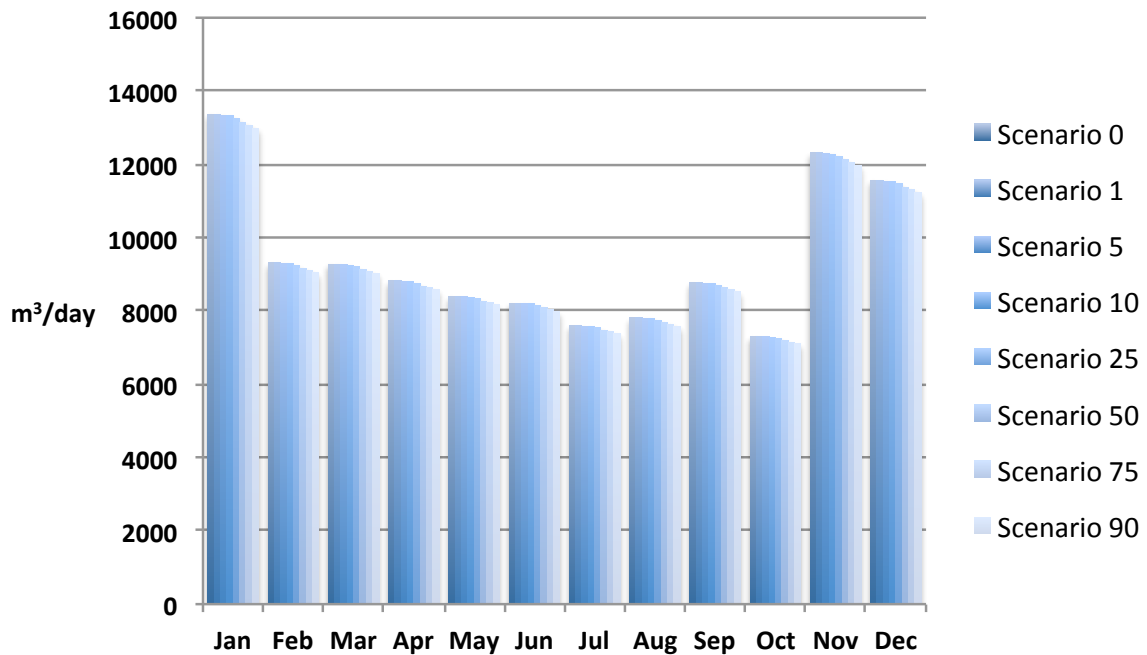


Figure 15: The monthly average of the effluent flow rate for each scenario. The darkest colour, furthest to the left in each column, represents scenario 0 with no urine diversion. The lightest colour, furthest to the right in each column, represents scenario 90 where 90% of the PE uses urine separation systems.

Figure 16 is a graph of the effluent COD concentration over a year for the scenario with no urine separation. The annual mean is 62.4 mg/l.

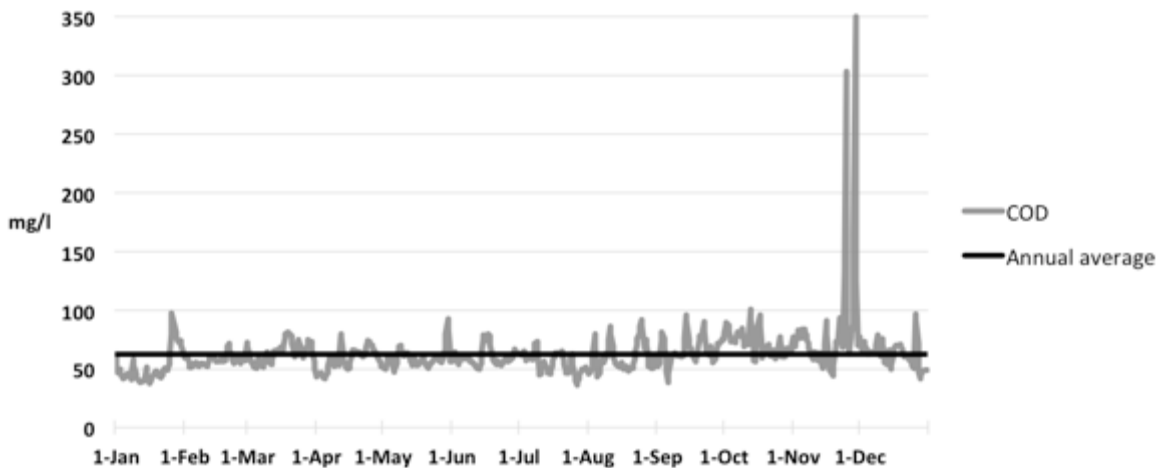


Figure 16: The grey line represents the effluent concentration of COD from the modelled WWTP over a year for scenario 0. The black, straight line represents the average effluent concentration over the year. The concentration is given in mg per litre.

In the end of the year is there a significant increase in the COD concentration. If the influent flow rate is studied, along with the influent COD concentration (both found in the Appendix) there is a higher load of COD into the WWTP for some period before the large increase in the

effluent COD concentration. Figure 17 illustrates the monthly mean COD concentration in the effluent for the different scenarios.

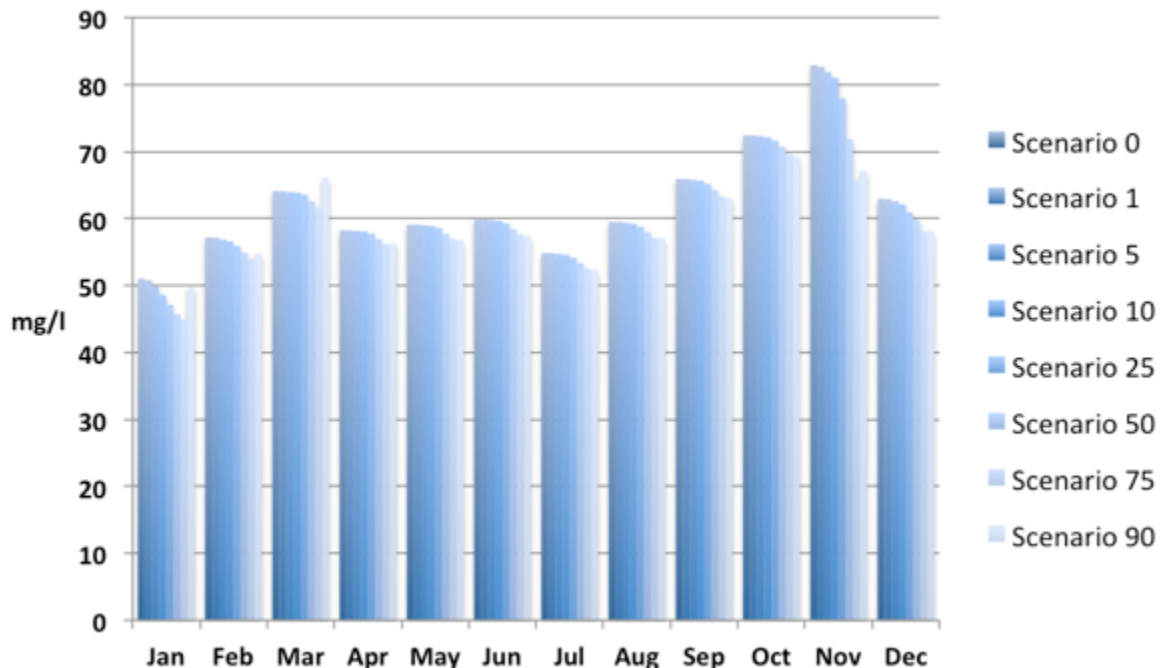


Figure 17: The monthly average of the effluent COD concentration for each scenario. The darkest colour, furthest to the left in each column, represents scenario 0 with no urine diversion. The lightest colour, furthest to the right in each column, represents scenario 90 where 90% of the PE uses urine separation systems.

The monthly mean of the effluent COD concentration does not change much between the different scenarios, which is also seen in the influent COD concentration so this could be expected. Figure 18 is a graph of the effluent TSS concentration over a year for the scenario with no urine separation. The annual mean is 13.3 mg/l.

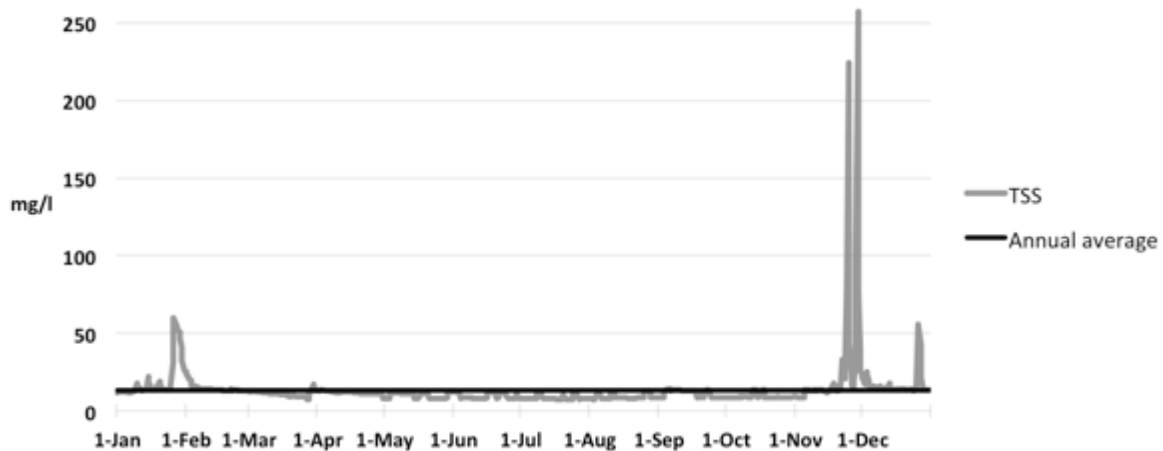


Figure 18: The grey line represents the effluent concentration of TSS from the modelled WWTP over a year for scenario 0. The black, straight line represents the average effluent concentration over the year. The concentration is given in mg per litre.

Also in Figure 18 is a large increase in the effluent concentration seen in the end of the year. This is correlated to the higher influent rates for some period prior to the peak in Figure 18, above. The change in the effluent TSS concentrations can be seen in Figure 19 below. Figure 19 illustrates the monthly mean, given in mg/l, for each scenario.

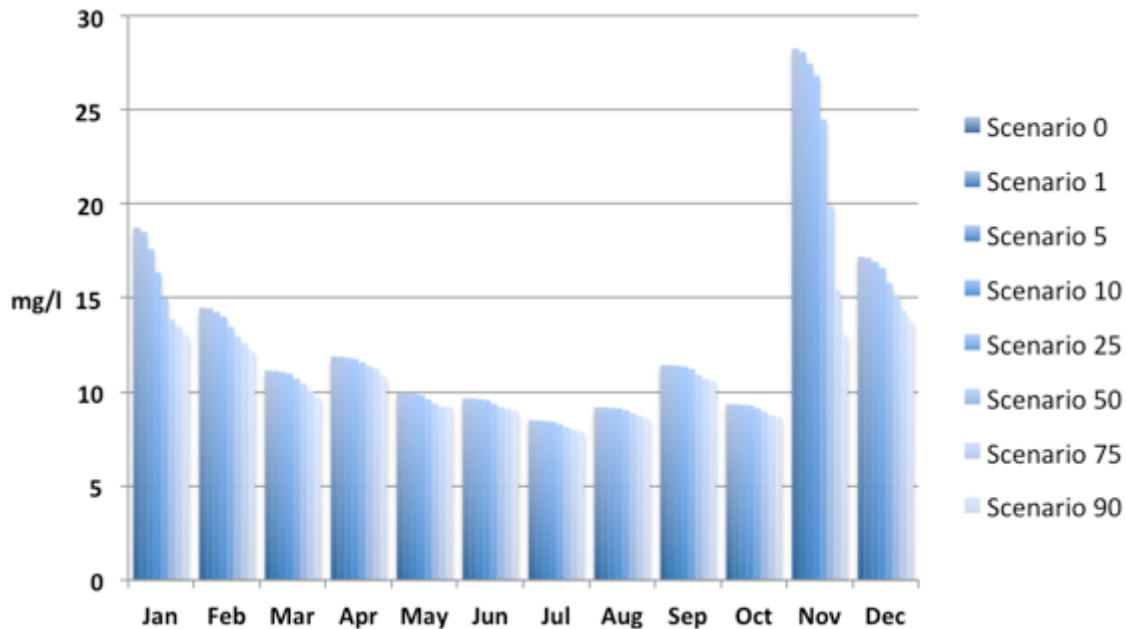


Figure 19: The monthly average of the effluent TSS concentration for each scenario. The darkest colour, furthest to the left in each column, represents scenario 0 with no urine diversion. The lightest colour, furthest to the right in each column, represents scenario 90 where 90% of the PE uses urine separation systems.

The largest differences the Figure 19 are in the end of the year where there is a peak. In Figure 20 is the effluent TKN concentration for scenario 0, with no urine diversion. This graph follows the same pattern as previous effluent graphs in this report. The annual TKN mean is 5.0 mg/l.

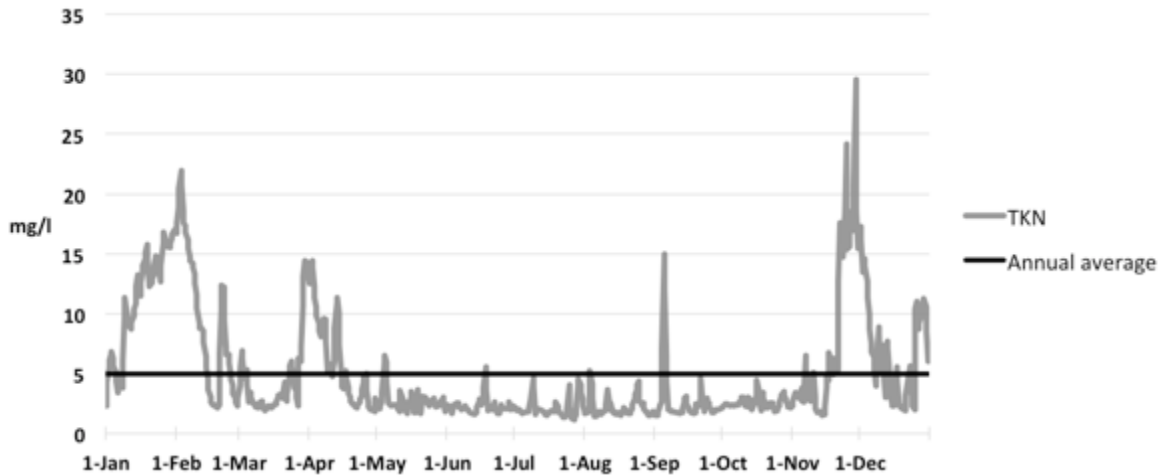


Figure 20: The grey line represents the effluent concentration of TKN from the modelled WWTP over a year for scenario 0. The black, straight line represents the average effluent concentration over the year. The concentration is given in mg per litre.

Figure 21 describes the change of TKN concentration for each scenario by plotting each scenarios monthly mean.

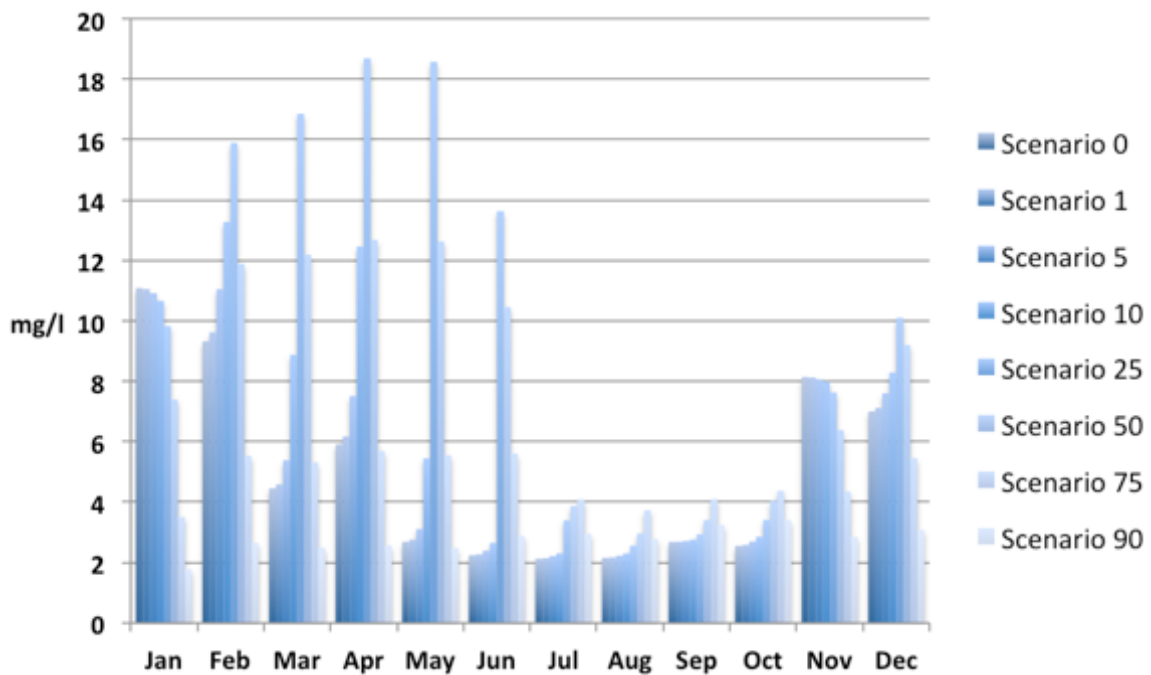


Figure 21: The monthly average of the effluent TKN concentration for each scenario. The darkest colour, furthest to the left in each column, represents scenario 0 with no urine diversion. The lightest colour, furthest to the right in each column, represents scenario 90 where 90% of the PE uses urine separation systems.

Figure 21 shows that the effluent TKN concentration generally increases for scenarios up to 75. Scenario 90 is the only scenario with continuously less effluent TKN than scenario 0. Due to the result in Figure 21, was the TN effluent studied. The effluent TN concentration for scenario 0 is presented in Figure 22, below. The annual mean is 21.21 mg/l.

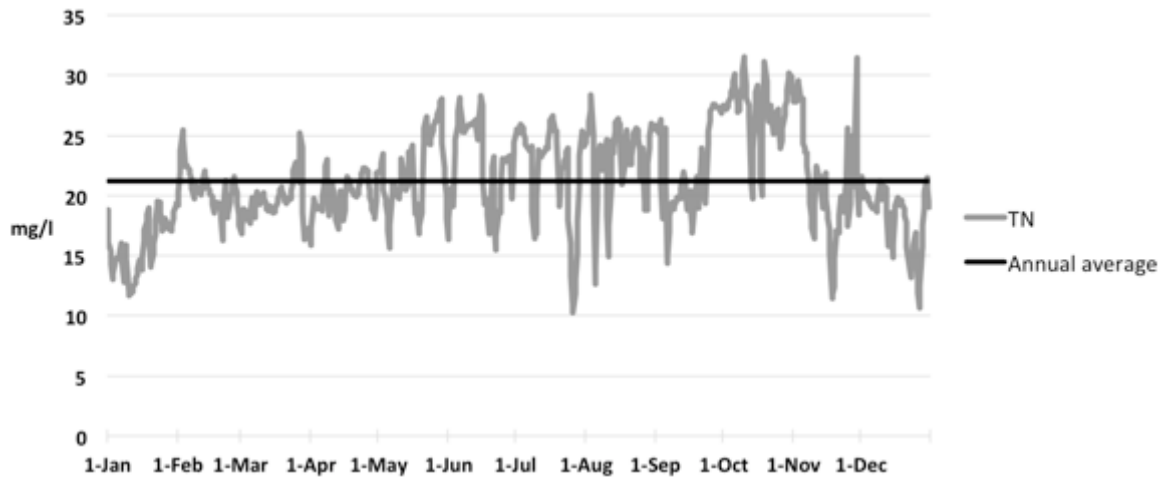


Figure 22: The grey line represents the effluent concentration of TN from the modelled WWTP over a year for scenario 0. The black, straight line represents the average effluent concentration over the year. The concentration is given in mg per litre.

In Figure 23, below, is the monthly mean for each scenario plotted. It is clearly seen that the effluent TN concentration is decreasing as the urine separation increases. This, coupled with the Figure 21, means that the TKN:TN ratio increase with an increasing population with urine diversion systems.

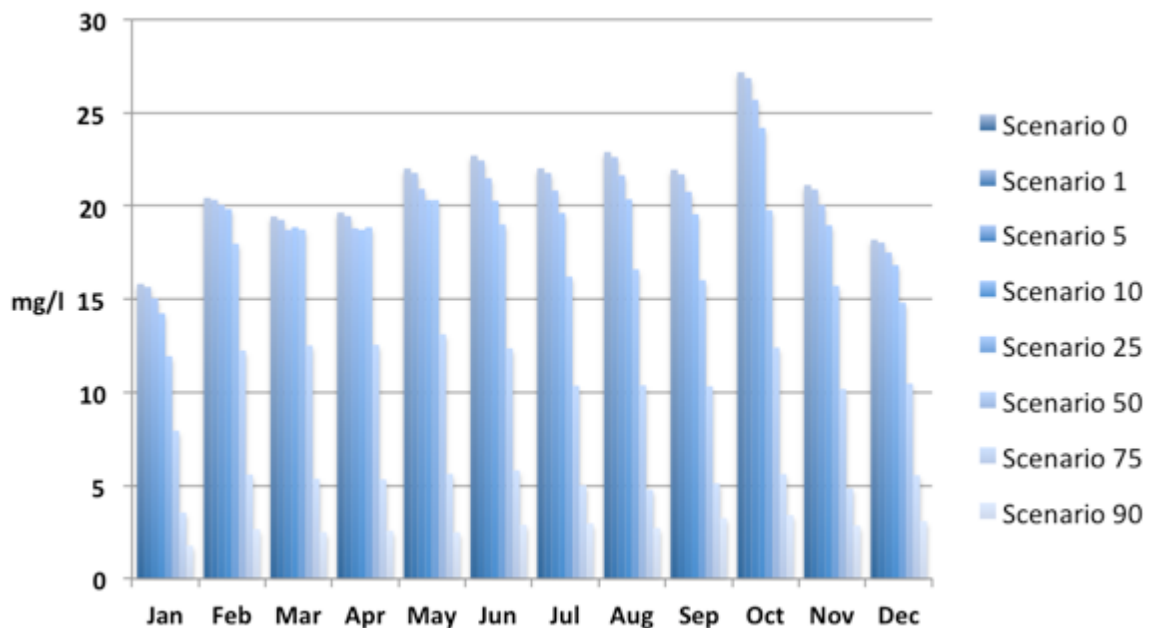


Figure 23: The monthly average of the effluent TN concentration for each scenario. The darkest colour, furthest to the left in each column, represents scenario 0 with no urine diversion. The lightest colour, furthest to the right in each column, represents scenario 90 where 90% of the PE uses urine separation systems.

In Figure 24, below, is the effluent TP concentration for the scenario with no urine diversion plotted. The annual mean for the TP concentration is 0.35 mg/l.

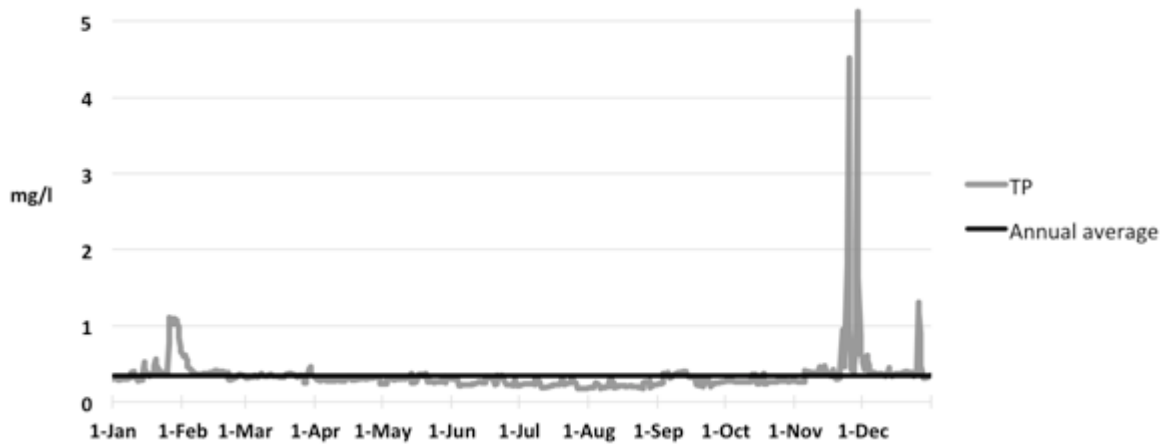


Figure 24: The grey line represents the effluent concentration of TP from the modelled WWTP over a year for scenario 0. The black, straight line represents the average effluent concentration over the year. The concentration is given in mg per litre.

The graph shows a peak at the end of the year, this seems to be the same for all the effluent components studied. This is due to a high influent flow, resulting in a higher load. The change of effluent TP concentration for the different scenarios is presented in the figure below, Figure 25. There is a significant decrease in the monthly average TP concentration between the different scenarios.

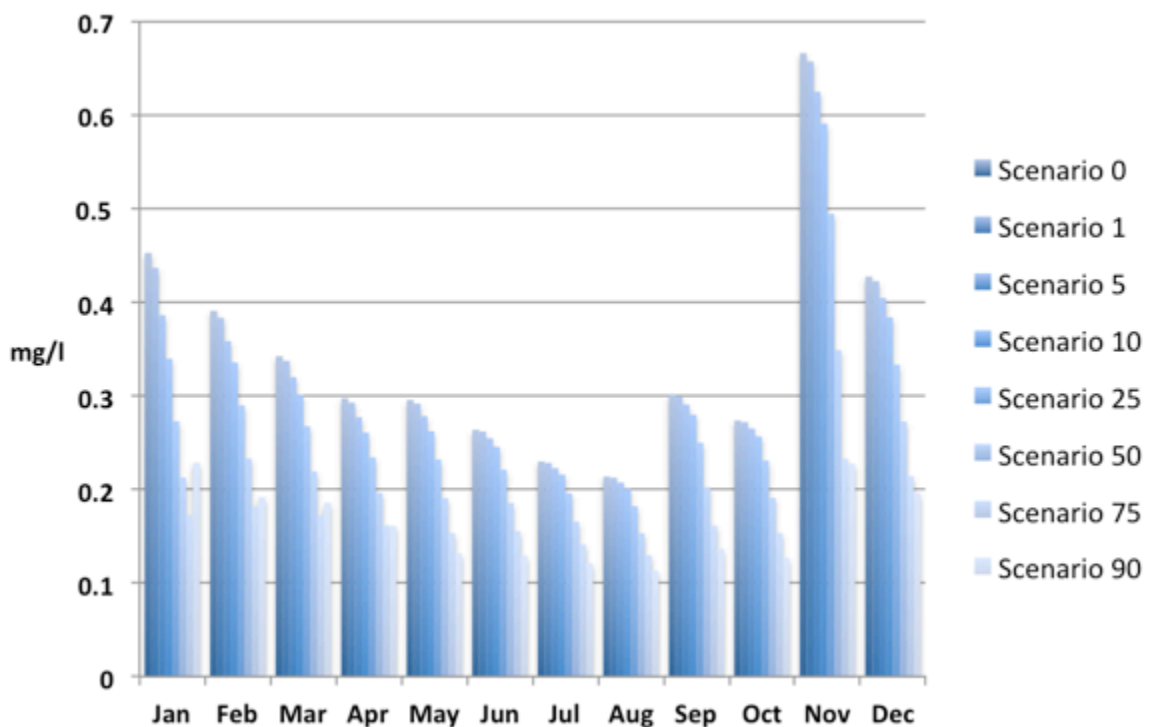


Figure 25: The monthly average of the effluent TP concentration for each scenario. The darkest colour, furthest to the left in each column, represents scenario 0 with no urine diversion. The lightest colour, furthest to the right in each column, represents scenario 90 where 90% of the PE uses urine separation systems.

#### 4.4 RECOVERED P AND MAP PRODUCTION

The P recovery from EBPR is dependent on an extra unit to generate a PO<sub>4</sub> release from the PAOs. Ekobalans Fenix AB have mentioned it is possible to release 50% of the TP in the excess sludge into PO<sub>4</sub>, Ostara's WASSTRIP is said to be able to release 70%. The two ASUs used in this modelled has not achieved this level of release. In Figure 26 below is the modelled PO<sub>4</sub> load, given in kg PO<sub>4</sub>/PE,year, after the hydrolysis and dewatering of the excess sludge presented for each scenario. The efficiency for the modelled PO<sub>4</sub> release increases up to scenario 25 and the PO<sub>4</sub> load after the hydrolysis is the highest for when there is 25% of the PE using urine diversion systems.

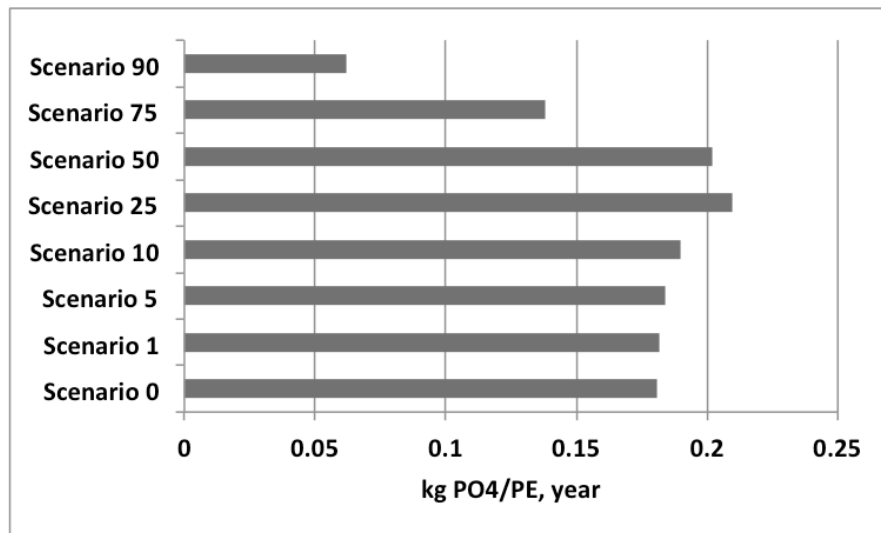


Figure 26: The columns show the modelled PO<sub>4</sub> release for each scenario given in kilograms PO<sub>4</sub> per PE and year, The darkest colour represent the modelled PO<sub>4</sub> release in ASU\_6 and ASU\_7,

As the modelled hydrolysis units did not achieve as high PO<sub>4</sub> release as units existing on the market are able to, calculation of a possible PO<sub>4</sub> release of the modelled stored P load within the PAOS in the excess sludge prior to the hydrolysis was executed. Figure 27 shows calculated PO<sub>4</sub> load, given a 50% and 70% release of PO<sub>4</sub>.

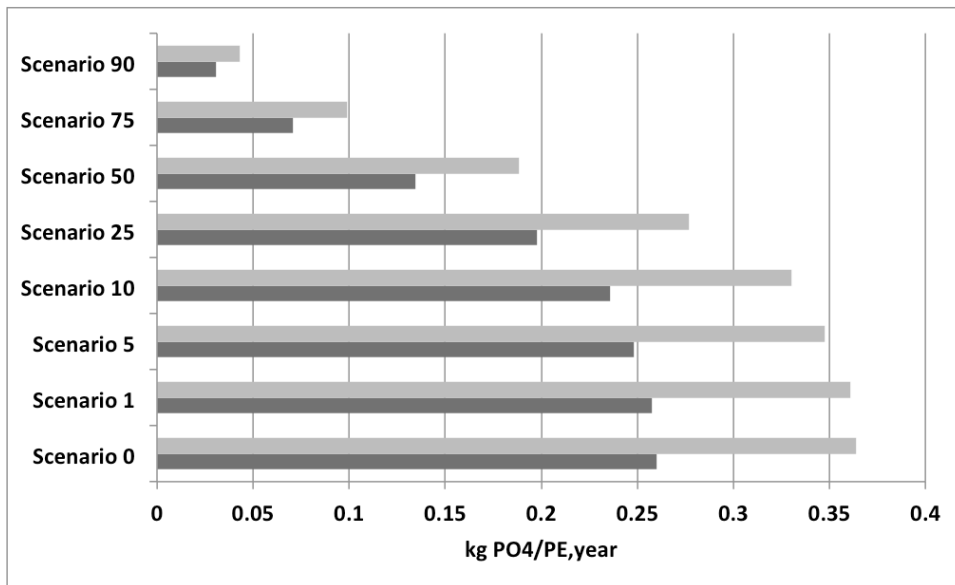


Figure 27: The columns show the calculated PO4 release for each scenario given in kilograms PO4 per PE and year. The light grey is the amount PO4 released with an efficiency of 70% out of the stored P load within the PAOs in the WAS, and the dark grey is calculated with a 50% P release efficiency.

Figure 27 represents more the amount of PO4 that could be expected in reality. However the trend shown in Figure 26 of the scenario 25 has the highest PO4 is not shown in Figure 27. In Figure 28 is the stored P within the PAO in the excess sludge prior to the hydrolysis units presented as kg P/PE,year.

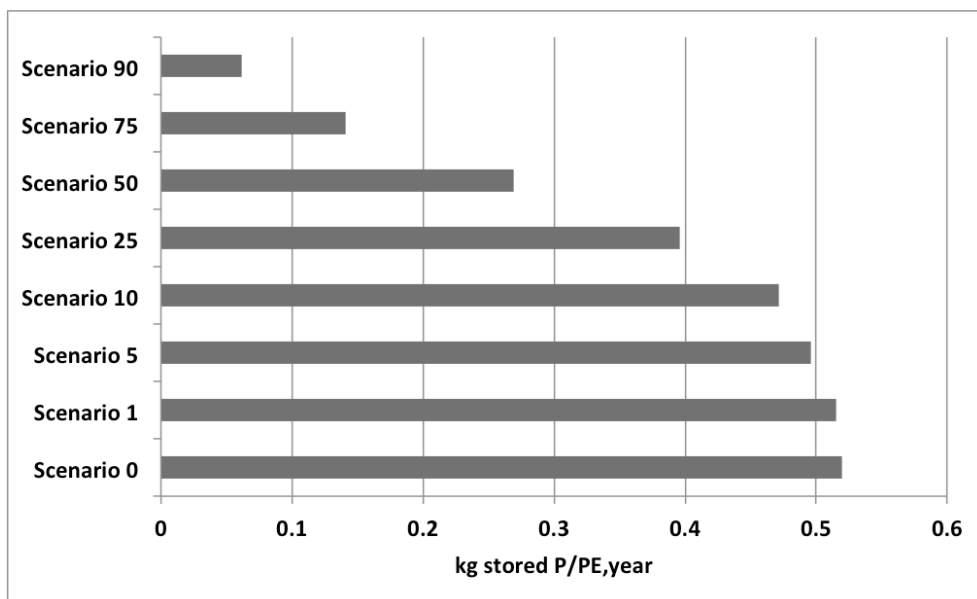


Figure 28: The columns show the modelled amount of stored P within the PAOs prior to the hydrolysis, given in kg P per PE and year, for each scenario.

As seen in Figure 28, the amount of P stored in the PAOs decreases as the urine diversion increase. From more than 0.5 kg stored/PE,year for scenario 0 to less than 0.1 kg stored P/PE,year for scenario 90.

The theoretical MAP production is calculated without taking the other reactants into account. The MAP productions in Figure 29 are therefore the MAP production without any limiting reactant other than the PO4. Figure 29 shows the possible MAP production, given in kg MAP/PE and year, for the modelled PO4 release.

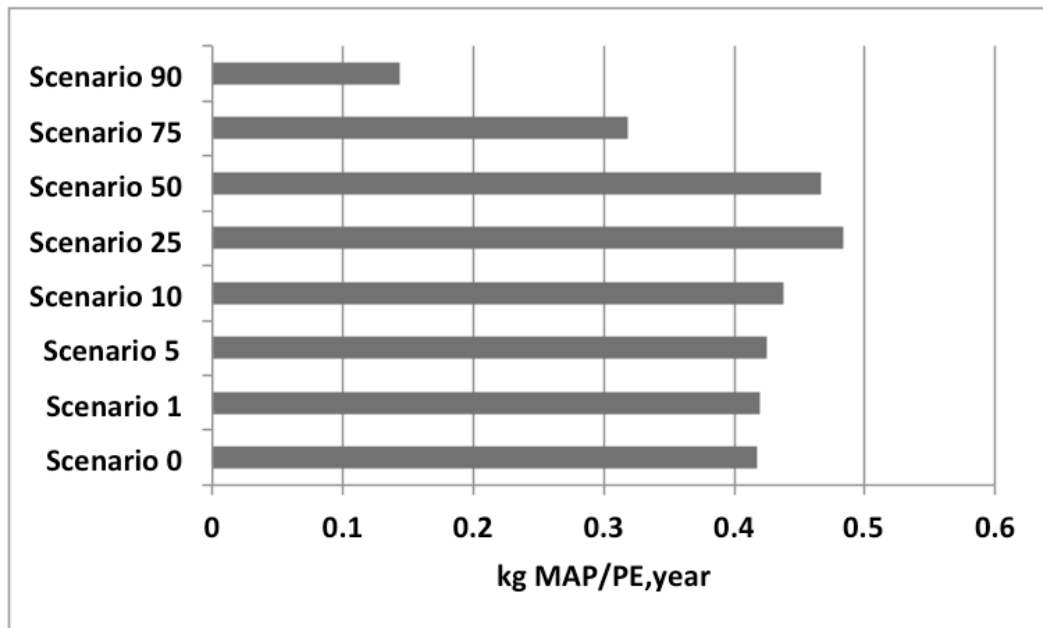


Figure 29: The columns show the MAP production from the modelled PO4 in the WAS for each scenario given in kilograms MAP per PE and year,

For the MAP production of the modelled PO4 release increases up to scenario 25, where it has the highest MAP production. Figure 30 shows the possible MAP production, given in kg MAP/PE and year, for the calculated PO4 release.

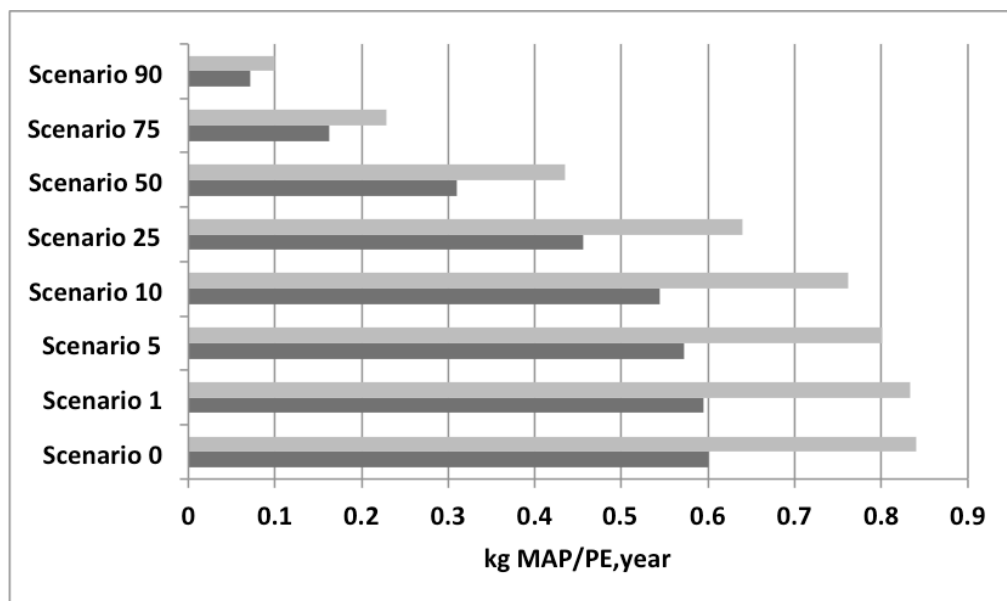


Figure 30: The columns show the MAP production from the calculated PO4 in the WAS for each scenario given in kilograms MAP per PE and year. The light grey is the MAP production with 70% P release, and the dark grey is calculated with a 50% P release efficiency.

Figure 31 presents the total amount of PO<sub>4</sub> per PE and year that could be recycled to the soil for each scenario from both the separated urine and the recovered modelled PO<sub>4</sub> within the MAP.

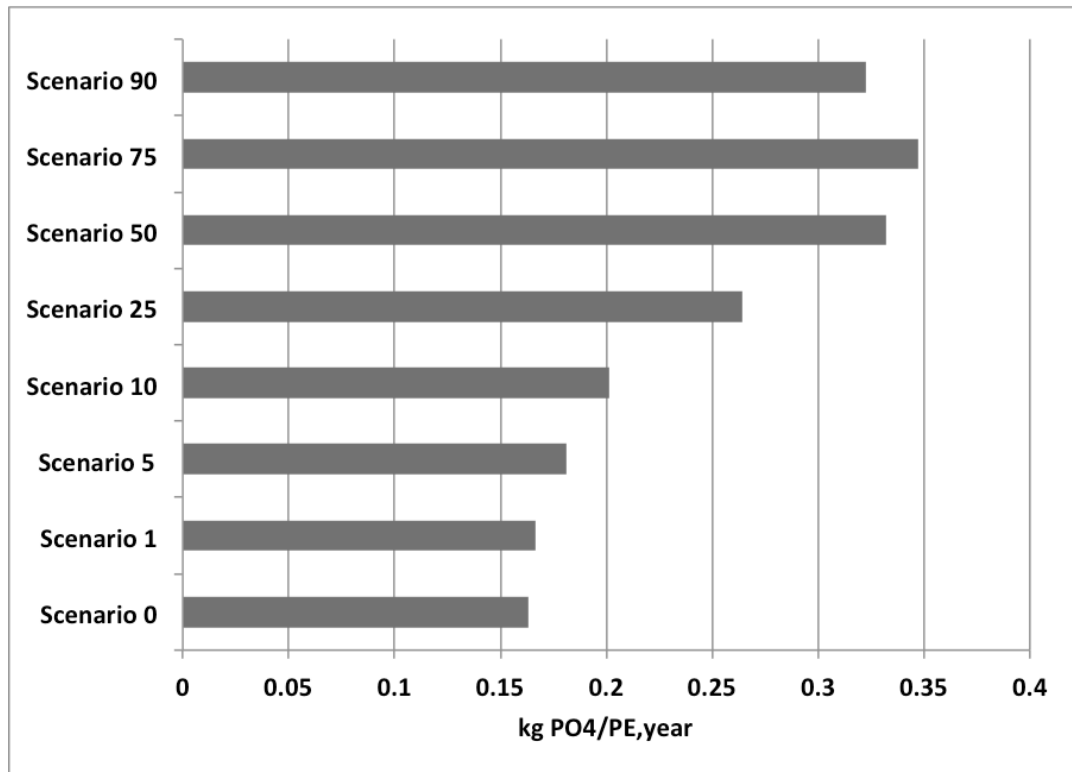


Figure 31: The columns show the amount of PO<sub>4</sub> from both the separated urine and the recovered PO<sub>4</sub> within the MAP that could be recycled to the soil, given in kilograms PO<sub>4</sub> per PE and year.

The recycled PO<sub>4</sub> increases up to scenario 75 with the PO<sub>4</sub> in the urine and modelled PO<sub>4</sub> release. Figure 32 presents the total amount of PO<sub>4</sub> per PE and year that could be recycled to the soil from each scenario from both the separated urine and the recovered PO<sub>4</sub> calculated release from the stored P within the PAOs

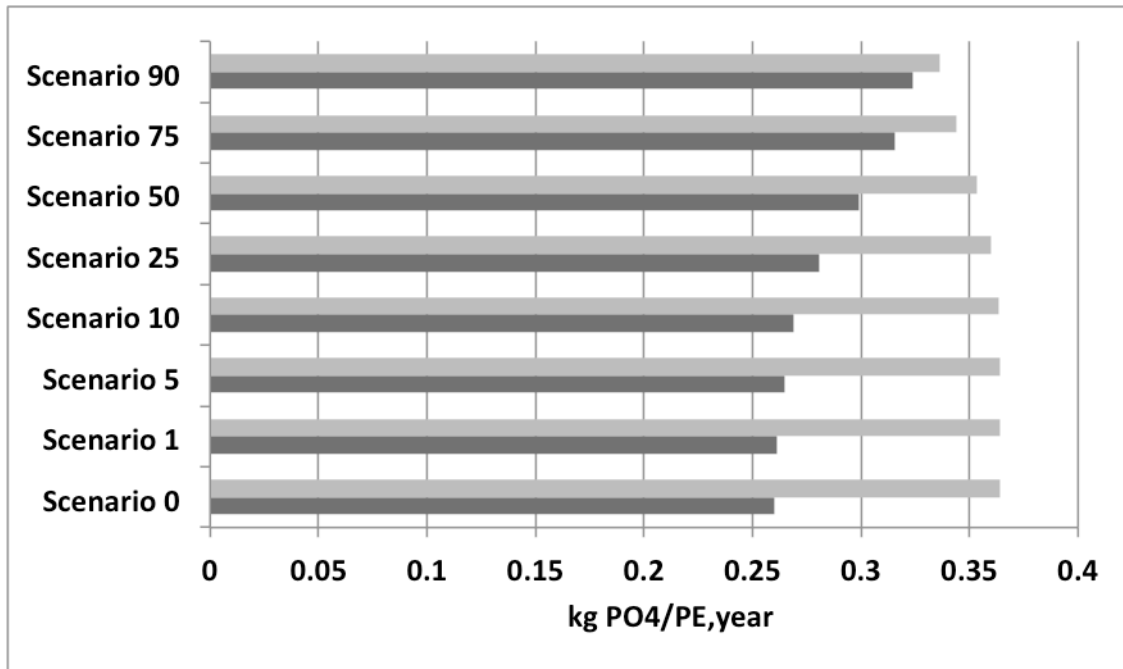


Figure 32: The columns show the amount of PO4 from both the separated urine and the recovered PO4 within the MAP that could be recycled to the soil, given in kilograms PO4 per PE and year. The light grey is calculated with 70% P release, and the dark grey is calculated with a 50% P release efficiency.

The recycled PO4 increases as the urine diversion increases for the calculated 50 % PO4 release and urine. For total recycled PO4 from 70 % PO4 release and PO4 in the urine the change is small between scenario 0 to scenario 25 and then there is a small decrease as the urine diversion increases more.

#### 4.5 RECOVERED N AND AMS PRODUCTION

As mentioned earlier, it was assumed that 70% of the influent TKN to the anaerobic digester would be converted to NH4. In Figure 33 below is the theoretical AMS production from the supernatant from the anaerobic digester presented for each scenario. The whole column represents the AMS production and it is divided in two sections representing the AMS production from the primary sludge (PS) and from the WAS.

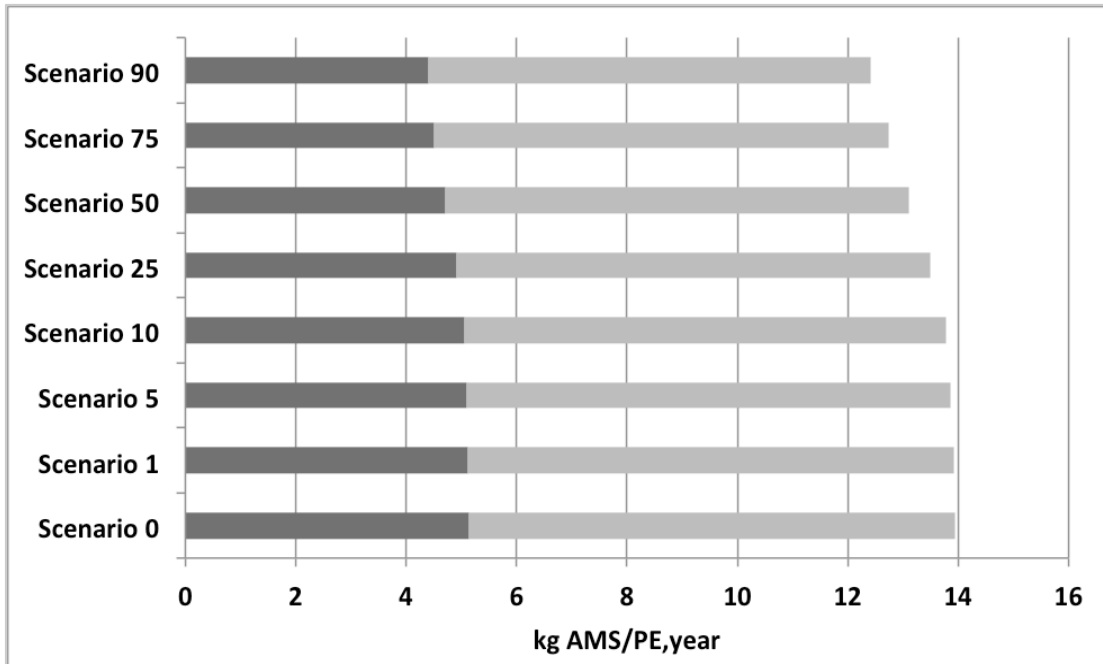


Figure 33: Each column represents the theoretical AMS production from the supernatant from the anaerobic digester for each scenario, given in kilograms AMS per PE and year. The darker part of the column illustrates the amount of AMS produced from the primary sludge and the lighter part is the AMS produced from the waste activated sludge.

Figure 33 show that the amount of AMS produced decreases as the urine diversion increases. The decrease however is quite small; the AMS produced per PE and year varies between 12-14 kg/PE and year for all scenarios. In Figure 34 is the total amount of NH<sub>4</sub> from both the separated urine and within the AMS that could be recycled to the soil for each scenario, given in kilograms NH<sub>4</sub> per PE and year.

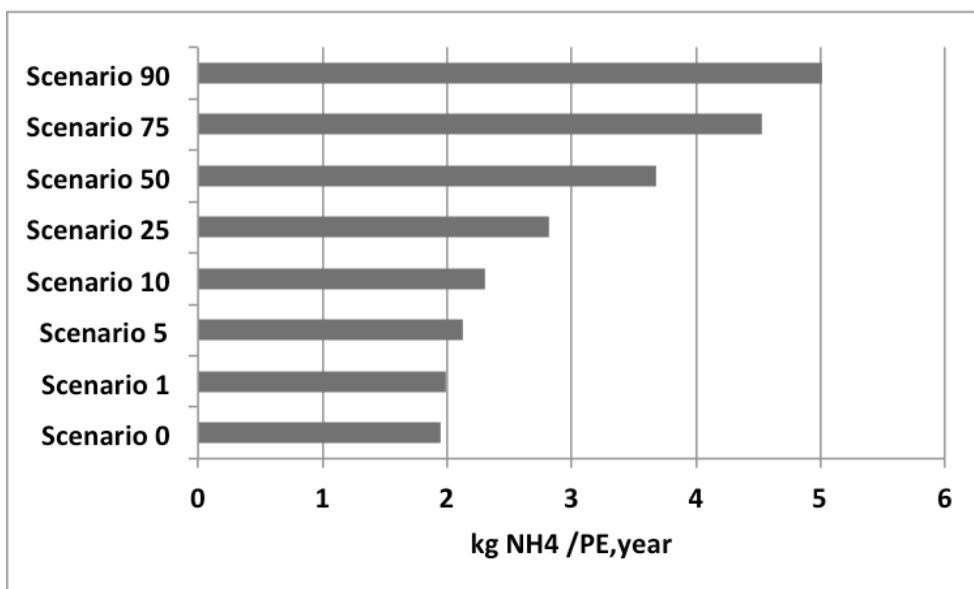


Figure 34: The columns represent the percentage of influent TKN to the modelled WWTP that is recovered as AMS for each scenario.

As seen in Figure 34 the total amount of NH<sub>4</sub> that could be used as fertiliser, from the separated urine and the AMS, increases as the urine separation increases.

#### 4.6 BIOGAS PRODUCTION

The theoretical biogas production was calculated for each scenario and is presented in Figure 35. The production is calculated from the biodegradable COD from both the primary sludge and the excess sludge.

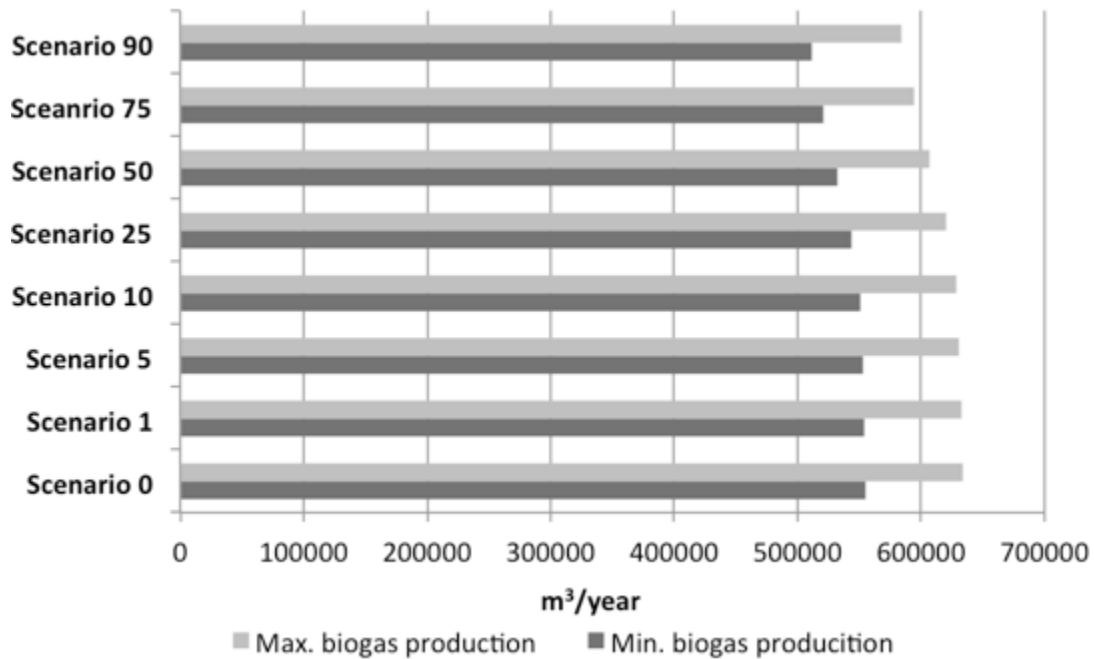


Figure 35: The columns represent the volume biogas that is theoretically possible to produce for each scenario, given in m<sup>3</sup> per year. The darker column shows a biogas production containing 80% methane and the lighter column shows a biogas production with 70% methane.

From Figure 35 it is seen that the biogas production is highest for scenario 0. However the differences are small between scenario 0, with the highest production, and scenario 90, with the smallest production.

## 5 DISCUSSION

### 5.1 INPUT DATA

The input data used for each scenario has been calculated from typical wastewater compositions reported by Jönsson et al. (2005). It is assumed that these values represent the PE in this report. Since urine has the highest concentration of P and N out of all fractions the reduction is also highest for these components when the urine separation increases in the modelled WWTP's catchment area.

Figure 6 and 7 illustrate the fractions of PO<sub>4</sub>:TP and NH<sub>4</sub>:TKN for the original data. The average was also calculated and the final values used in the model was 0.515 for the PO<sub>4</sub>:TP fraction and 0.61 for the NH<sub>4</sub>:TKN fraction. When studying the PO<sub>4</sub>:TP and NH<sub>4</sub>:TKN for each day in the original data set there is a large range of values. These changes of the fractions are not included in the model. Changing the fractions during the simulation could affect the effluent concentrations, efficiency of the EBPR and recovered nutrient. The

calculated fractions for the other scenarios, shown in Table 14, are based on the values chosen for scenario 0. The NH<sub>4</sub>:TKN ratio for scenario 90 resulted in a small, negative value. The limits for a fraction are 0 to 1; the smallest value, 0, was therefore chosen for this fraction. The fact that the equation and original fraction resulted in a negative value for scenario 90 could mean that the values of the fractions for the other scenarios should have been increased slightly.

## 5.2 WWTP MODEL

The modelled WWTP is based on several parameters and simplified models of real processes. The parameters used were based on literature values and from trials when changing them. One unit at the time was calibrated with mass balance calculations and when the error was within +/- 5–10%, as Rieger et al. (2013) recommends, the parameters were set. However, there can be a different set of parameters also resulting in an acceptable error that were not tried but would result in a different outcome due to a different composition of the modelled water and sludge.

The final fractionation, Table 15, could be improved by taking more measured variables into account in the fractionation scheme, other than Q, COD, TSS, TKN, and TP. This would lead to less dependence on fractions. Nobel (2015) however did more laboratory work to define the fractions, and those fractions were considered during the calibration of the fractionation scheme in this report. Henze et al. (2000) recommended increasing the measured TSS with 29% for the modelled TSS. This due to the fact that some part of TSS will not be caught in the filters used to measure the TSS concentration; this part of TSS should be included in the model. However, the mass balances for the whole model were not met when TSS was too high. There were also complications with the return sludge when the TSS correction factor was higher than 1. In the default fractionation schemes from DHI's WEST, this correction factor was not included.

In order for the modelled TP concentration to be correspond to the measured influent concentration was it necessary to reduce the amount of P in the COD, see Table 16. Even the lowest values in the range given by Henze et al. 2000 resulted in a too high TP concentration. But when studying the TP:COD for the original data from Sjölanda and the TP:COD in a typical wastewater presented by Henze et al. (2000) was the TP:COD ratio at Sjölanda half of the value for the typical wastewater. So by the fact of these ratios was the decision made to decrease the default composition factors for P within the COD by 0.5.

The effluent concentrations for all components in scenario 0 are a bit higher than what Sjölanda WWTP has as limits. This implies that the efficiency of the primary clarifier, EBPR and secondary settler was lower in the modelled WWTP than Sjölanda WWTP. This could be due to the low removal percentage of TSS in the primary clarifier, which in this model was 35% but recommendations were approximately 50%. More TSS would be found in the primary sludge if the removal efficiency were better. The EBPR might not be as efficient as it could be in reality, but the parameters for the ASUs in the EBPR were kept to default values because they were considered most reliable. Only one parameter was increased from 4 to 5 g COD/m<sup>3</sup>, the saturation coefficient for acetate. This was done to spare some VFA in the sludge and improve the hydrolysis in ASU\_6 and ASU\_7.

## 5.3 EFFECTS OF URINE SEPARATION ON THE WWTP

There is a significant decrease in incoming TP and TKN concentrations as the urine diversion increases in the WWTP's catchment area. This is shown in Figure 12 and 13, describing the change in influent for each scenario. The change in flow rate, COD and TSS is however

small. This means that the nutrient load in to the WWTP is decreasing. The WWTP could then either increase the PE coupled to the sewage system, if it is dimensioned for a larger flow rate, since the nutrient load is lower. Otherwise more COD could be removed through primary clarifier or as WAS because there is less biomass required to remove the low nutrient load, leading to a smaller COD demand in the ASUs.

Mehta et al. (2015) mentions in their framework that the nutrient accumulation is most important when the concentrations of nutrients are low and the flow rate is high. This means that as the urine separation increases, it is even more important for a well-functioned EBPR to achieve any nutrient recovery. Cullen et al. (2013) reported that the EBPR became more stable when including a hydrolysis unit and MAP recovery method. So the installation of nutrient recovery units could aid the operation of the EBPR. This would aid the nutrient accumulation.

With no change in the parameters and dimensions of the units in the modelled WWTP there is a significant decrease in the effluent TP and TN concentration. The TKN concentration however increases according to Figure 21. This corresponds to what Wilsenach et al. (2003) also observed, and they explained it by the fact that there is a decrease of nitrifying microorganisms in the ASUs as the TKN load in to the WWTP decreases. Also the decrease in effluent concentrations of TP and TN means that the dimensions of the WWTP could be reduced and parameters optimised to lower the operational costs but still achieve an acceptable removal of nutrients. For example, the ASUs areas could be reduced, or the aeration resulting in less energy consumption for the WWTP, without exceeding the effluent limits.

#### **5.4 RECOVERED P AND MAP PRODUCTION**

When studying Figure 26 and Figure 27, describing the PO<sub>4</sub> release of the WAS, it is clear that the modelled PO<sub>4</sub> release is not as efficient as it could be. Baur (2009) recommended a HRT of 36–96 hours if no extra VFA was added. The HRT for the modelled hydrolysis was on average 5 days. It should be sufficient for the PO<sub>4</sub> release. The fact that the PO<sub>4</sub> release is not efficient enough even with an appropriate HRT is probably because a too low VFA concentration in the WAS. Kumpulainen's results (2013) showed that with an efficient EBPR there was no need of an extra VFA source. Thus, the modelled EBPR performance might not be optimal since the VFA concentration in the WAS was too low. It is also possible that the composition of the influent wastewater does not contain enough VFA. The solution to a too low incoming VFA concentration is to add an extra VFA source to the hydrolysis units. Figure 27 shows calculated PO<sub>4</sub> releases with an efficiency of 70% and 50% of the TP into the hydrolysis unit, which are values presented by Ostara and Ekobalans Fenix AB. For the modelled PO<sub>4</sub> release the efficiency is increasing when the urine diversion increases up to 25%. At 25% urine diversion is the efficiency highest. This could be the optimum nutrient and substrate load for the modelled ASU\_6 and ASU\_7 and it is therefore the scenario with the most efficient PO<sub>4</sub> release. When calculating the PO<sub>4</sub> release scenario 0 gave the highest PO<sub>4</sub> amount per year. The differences in this result might be because the performance of the modelled hydrolysis is better when there is a smaller nutrient load into the unit. The increase in performance in turn leads to larger PO<sub>4</sub> release. The increase in performance of the hydrolysis is not accounted for when assuming a PO<sub>4</sub> release from theoretical values such as 50–70% P-release. It could be possible that the calculated hydrolysis should have been adjusted to simulate an improvement of the hydrolysis as the urine diversion increased.

Some parameters in the ASUs were slightly changed to improve the hydrolysis. It was however not enough to reach a sufficient PO<sub>4</sub> release. The volume of the ASU\_6 and ASU\_7 together is 412.5 m<sup>3</sup> and the temperature was kept at 20 °C. The area in reality has to be smaller in order for a WWTP to consider a hydrolysis unit; the unit can be smaller if there is a controlled HRT. In the model is the HRT of an average of 5 days kept by having a large ASU compared to the flow rate. Another possibility is to have a smaller ASU but controlling the flow rate. The temperature of 20 °C in the hydrolysis is not eligible for a WWTP, since that would require heating up the sludge which in turn would increase the energy consumption. Other ways to increase the efficiency of the hydrolysis should be considered.

From Figure 29 and 30, showing the MAP production for each scenario, can the conclusion be drawn that the PO<sub>4</sub> release is very important in order to achieve a sufficient MAP production. The MAP production in Figure 29 and 30 is a theoretical production of MAP, assuming no other limiting reactant than PO<sub>4</sub>. In reality, it is possible that both Mg and N limit the MAP production. A Mg source is usually added, as seen in the comparison of MAP recovery methods, Table 5. The N however, has to be included in the influent to the recovery unit. When studying the N in the supernatant from the dewatering unit prior to anaerobic digester, it was seen that the N probably would be limiting. To solve this, one option is to redirect some of the N-rich supernatant from the anaerobic digester into the MAP producing unit. That would however decrease the AMS production. The calculated MAP productions are based on the PO<sub>4</sub> in the supernatant from the hydrolysis unit. Ekobalans Fenix AB (2017) suggests that the supernatant from the anaerobic digester also is included in the MAP production to increase the PO<sub>4</sub> concentration and MAP production.

Figure 31 and 32 shows the recycled PO<sub>4</sub> from the WWTP's MAP production and the PO<sub>4</sub> in the separated urine. The result differs for the modelled and calculated PO<sub>4</sub> release. When studying the recycled PO<sub>4</sub> from the modelled PO<sub>4</sub> release (Figure 31) and the calculated 50% PO<sub>4</sub> release (Figure 32) the recycled PO<sub>4</sub> from the total system increases as the urine separation increases. The recycled PO<sub>4</sub> from the whole system (separated urine and WWTP) with calculated 70 % PO<sub>4</sub> release however is similar for scenario 0 to scenario 25. The recycled PO<sub>4</sub> decreases for scenarios with more urine diversion than scenario 25.

## **5.5 RECOVERED N AND AMS PRODUCTION**

Figure 33 presents the theoretical production of AMS from the supernatant after the anaerobic digesters as kg AMS per PE and year. It is seen that the amount decreases as the urine diversion increases. But the decrease between scenario 0 and scenario 90 is small. The assumption for this AMS production is that 70% of the TKN going into the anaerobic digester is transformed and available for the ammonia stripping. The anaerobic digester has to be optimised and well functioned for this to be true. The AMS production from the NH<sub>4</sub> in the separated urine increases as the urine separation increases. The recycled NH<sub>4</sub>, from both the separated urine and the supernatant, is shown in Figure 34. This shows that the recycled NH<sub>4</sub> increases as the urine separation increases. This can be explained by the fact that the TKN:TN ratio increases when the urine diversion increases. If as suggested in the discussion of the MAP production that some N is led to the MAP producing unit to increase the MAP production the AMS production will decrease.

## **5.6 BIOGAS PRODUCTION**

The biogas production presented in Figure 35 is the possible production under normal temperature and pressure. These values could be higher or lower depending on the temperature and pressure in the anaerobic digester. Therefore, the values given in Figure 35

should not be considered a fact but instead the figure illustrates the effect of urine separation on the biogas production. Figure 35 shows that the biogas production would not be too affected by an increase in urine diversion since the amount of COD does not decrease a lot. If the parameters for the separation of WAS and PS were changed for the different scenarios, it is possible to increase the COD in the sludge without affecting the efficiency of the EBPR and exceeding the effluent concentration limits. The increase of COD in the sludge would lead to a better biogas production. According to de Lemos Chernicharo (2007) is the nitrate and nitrite limiting the methane production. This is not considered in the calculated biogas production. But when studying the effluents TKN and TN concentration was it shown that the TKN:TN ratio increased when the urine diversion increased. The increase in TKN:TN, and decrease in nitrate and nitrite would then be beneficial for the biogas production. It could be that the decrease of biogas production when the urine diversion increases is even smaller in reality.

## **5.7 METHODS FOR NUTRIENT RECOVERY**

Several options for nutrient recovery at a WWTP were found from the literature study. Only a few could be presented, which were some of those that today exists in full-scale. There is however several more but the information about those, as well as the time frame of this project, were limited. When studying the different P recovery technologies, it was shown that the recovery efficiency was similar for most of them. Questions for more specified information were sent to the companies of each presented technology. Unfortunately, not all the companies responded and therefore the information available for each technology differs.

The methods for producing MAP from the sewage sludge and centrate are similar in many ways. PHOSPAQ is mostly used to produce calcium phosphate but since the lime is not added until the end of the process it could be interesting to look into the possibility of precipitating the P as MAP by adding a Mg source instead of lime. When comparing them in Table 5, is the recovery efficiency from the P-rich water practically the same. There is a larger difference in the removal efficiency for the AMS methods. There are three methods with a higher efficiency: from Ekobalans Fenix AB, CMI Europe Environment and Organics.

The cost for each method has not been established in this report. One could assume that the costs would be approximately the same because of the prices would be adapted according to the site-specific conditions. A request for proposal (RFP) would be needed in order to find out the cost of a nutrient recovery method. Then the site-specific conditions and other specific demands would be considered resulting in an accurate cost analysis. The cost is dependent on the investment costs, and the operational and maintenance costs. It seems for the AMS methods compared in Table 6 that the operational costs would be mainly due to high chemical demand or high energy consumption. For the MAP recovery methods, it seems the operational cost will mainly be due to the chemical demand.

## **5.8 IMPLICATIONS OF THIS STUDY**

The study does not include a thorough calibration and validation with other data sets than the one from Sjölanda WWTP in 2015. The model parameters have not been analysed through a sensitivity analysis. The calibration executed was checking of the mass balance equations, and the set of parameters are based on literature values to achieve an acceptable mass balance. This means that there can be other sets of parameters resulting in an acceptable mass balance but different characteristics of the modelled effluents. The production of MAP, AMS and biogas is theoretical values, which in reality might not be achieved. The figures should be used to show the general effects of urine separation on the WWTP's nutrient recovery and biogasproduction.

## 6 CONCLUSION

As the urine separation increased in the modelled WWTP's catchment area, the influent concentrations of TP and TKN decreased significantly. From scenario 0 with no urine separation, where the average influent TP and TKN concentrations were 4.78 mg/l and 42.3 mg/l, respectively, to average concentration of TP and TKN at 2.4 and 13.7 mg/l for scenario 90 with 90% of the PE using urine separation systems. For the flow rate, COD and TSS concentration, the changes are small.

The decrease in the influent load of TP results in a significant decrease in the effluent concentration. For some scenarios, the effluent TKN concentration increases as the urine separation increased. The TN concentration however decreases. This means that when the urine separation increases in the WWTP's catchment area the TKN:TN ratio increases. For the flow rate, COD and TSS concentrations, the changes are small.

The total MAP production with the modelled PO<sub>4</sub> release is highest for scenario 90. For the calculated PO<sub>4</sub> releases, scenario 0 generates the most MAP. This might be due to the fact that the performance of the modelled hydrolysis increases as the urine diversion increases. But no such adjustment was done for the calculated PO<sub>4</sub> release. The total AMS production is highest for scenario 90 with the highest percentage of urine diversion. This is due to the larger volume of the separated urine and that the TKN:TN ratio in the WWTP increases as the urine diversion increases.

The change in biogas production, when the urine diversion increases, is small. For scenario 0, the biogas production containing 70% methane is slightly above 600000 m<sup>3</sup>/year and for scenario 90 the production is slightly under 600000 m<sup>3</sup>/year.

It is not possible to determine an optimum method for phosphorus recovery out of the parameters studied in this report. The methods recovering P are similar in recovery efficiency, chemical demand and hydraulic retention time. The cost of the method is site-specific. It is hence hard to make a recommendation which method to use.

The methods for nitrogen recovery studied in this report resulted in three methods that seem superior to the others. They had a higher efficiency than the others. The three recommended due to their efficiency is ammonia stripping by Ekobalans Fenix AB, CMI Europe Environment, and Organics. The last mentioned method does not have the same chemical demand as the other two since it is thermally driven, however the energy consumption might be higher. Also for the nitrogen recovery methods is the cost site-specific.

### 6.1 FUTURE STUDIES AND APPLICATIONS

Some suggestions for further studies are:

- A sensitivity analysis of the model.
- A more extensive literature review of different nutrient recovery methods.
- A case study at an existing WWTP with EBPR
- How much can the WWTP save by changing their energy consumption, aeration and other operational parameters when urine diversion in the area increases and still meet the effluent limits? Keep effluent concentrations and flow rate constant for each scenario by changing the parameters and dimensions of the model.
- Study the possibility to include the primary sludge into the MAP production.

- A comparison of the life cycle cost for each nutrient recovery method presented in this report
- Study the hydrolysis unit for PO<sub>4</sub> release further to generate higher PO<sub>4</sub> release and consequently higher PO<sub>4</sub> load.

This report may be used as a guide for WWTP in areas where new development with urine separation solution is planned to see the effects it might have on the WWTP. It is also possible to use the report as a guide before implementing a nutrient recovery technology to determine when it is still profitable even though the urine separation increases in the catchment area. However, to determine the appropriate nutrient recovery method for a WWTP is a request for proposal (RFP) from different providers recommended. Through a RFP to each company site-specifics details can be taken into consideration and a more accurate comparison of the methods can be done.

## REFERENCES

- Angrick, M., Burger, A. & Lehmann, H. (Eds) (2013). *Factor X* [online]. Dordrecht: Springer Netherlands. Available from: <http://link.springer.com/10.1007/978-94-007-5712-7>. [Accessed 2017-11-20].
- Aspegren, H. (1995). *Evaluation of a high loaded activated sludge process for biological phosphorus removal*. Lund: Lund Institute of Technology/Lund University. (1004).
- Aylward, G. & Findlay, T. (2008). *SI Chemical data*. 6. ed Milton, AU: John Wiley & Sons Australia, Ltd.
- Baur, R. J., *Waste activated sludge stripping to remove internal phosphorus*. US7604740B2. 2009-10-20.
- Boehler, M. A., Heisele, A., Seyfried, A., Grömping, M. & Siegrist (2015). Ammonium sulphate recovery from liquid side streams. *Environ Sci Pollut Res*, 22(10), pp 7295–7305.
- Brockmann, M. (2015). *Struvia- Technology for Phosphorus Recovery*. Braunschweig.
- CMI Environment (2017). Expert of Air Stripping solutions. CMI Environment. Available from: <http://www.europe-environnement.com/wp-content/uploads/2017/06/Stripping-EN.pdf>. [Accessed 2018-04-20].
- Colsen (2015). AMFER-Removal of ammonia from digestate & waste water. Colsen. Available from: <http://colsen.nl>. [Accessed 2018-04-20].
- Cullen, N., Baur, R. & Schauer, P. (2013). Three years of operation of North America's first nutrient recovery facility. *Water Science & Technology*, 68(4), p 763.
- DHI. *WEST models guide*. [online] (n.d.) (WEST models guide). Available from: <http://doc.mikepoweredbydhi.help/webhelp/2017/TornadoModels/index.htm>. [Accessed 2018-02-05].
- DHI (2017). *WEST software -WEST optimization*. s.l.
- Egle, L., Rechberger, H., Krampe, J. & Zessner, M. (2016). Phosphorus recovery from municipal wastewater: An integrated comparative technological, environmental and economic assessment of P recovery technologies. *Science of The Total Environment*, 571, pp 522–542.
- Egle, L., Rechberger, H. & Zessner, M. (2015). Overview and description of technologies for recovering phosphorus from municipal wastewater. *Resources, Conservation and Recycling*, 105, pp 325–346.
- Ek, M., Junestedt, C., Larsson, C., Olshammar, M. & Ericsson, M. (2011). *Teknikenkätenskilda avlopp 2009*. Norrköping: SMHI. (SMED; 44).
- Ekobalans Fenix AB (n.d.). Ekobalans- Sustainable Nitrogen Recycling. EkoBalans Fenix AB. Available from: [https://www.ekobalans.se/images/pdf\\_dokument/EkoBalans%20Sustainable%20Nitrogen.pdf](https://www.ekobalans.se/images/pdf_dokument/EkoBalans%20Sustainable%20Nitrogen.pdf). [Accessed 2018-05-07].

Ekobalans Fenix AB (2017). Hållbar återföring av fosfor och kväve.

GNS (n.d.). Digestate Treatment System. GNS. Available from: [http://www.gns-halle.de/downloads/info\\_digestate\\_treatment.pdf](http://www.gns-halle.de/downloads/info_digestate_treatment.pdf). [Accessed 2018-04-20].

Gustavsson, D. (2017). *Flow scheme of conceptual WWTP*. Sweden Water Reseach/VA SYD

Guštin, S. & Marinšek-Logar, R. (2011). Effect of pH, temperature and air flow rate on the continuous ammonia stripping of the anaerobic digestion effluent. *Process Safety and Environmental Protection*, 89(1), pp 61–66.

gypsum, n. *OED Online* Oxford University Press. Available from: <http://www.oed.com.ezproxy.its.uu.se/view/Entry/82888>. [Accessed 2018-05-17].

Held, H. (2017). Veolia- Världsledande och naturlig samarbetspartner. Stockholm. Available from: <http://www.svenskvatten.se/globalassets/utbildning/konferenser-och-seminarier/fosfor-2017/henrik-held-veolia.pdf>. [Accessed 2018-03-15].

Henze, M., Gujer, W., Mino, T., Matsuo, T., Wentzel, M. C., Marais, G. v. R. & Van Loosdrecht, M. C. M. (1999). Activated sludge model no.2d, ASM2D. *Water Science & Technology*, 39(1), pp 165–182.

Henze, M., Gujer, W., Mino, T. & Van Loosdrecht, M. (2000). *Activated sludge models ASM1, ASM2, ASM2d and ASM3*. London: IWA Publishing. ( Scientific and Technical Report; 9).

Hood, B., Gardner, E. & Beal, C. (2009). DOMESTIC URINE SEPARATION CAPTURES PLANT MACRONUTRIENTS. *Water*, p 5.

Jönsson, H., Baky, A., Jeppson, U., Hellström, D. & Kärrman, E. (2005). *Composition of urine, faeces, greywater and biowaste*. Gothenburg: Urban Water. (2005:6).

Kaschka, E. & Weyrer, S. (1999). *PHOSTRIP Handbook*. 4th. ed s.l.: s.n.

Kumpulainen, E. (2013). *Utvärdering och optimering av sidoströmshydrolysen vid Duvbackens reningsverk*. Diss. Uppsala: Uppsala University.

Kvarnström, E., Emilsson, K., Richert Stintzing, A., Johansson, M., Jönsson, H., af Petersens, E., Schönning, C., Christensen, J., Hellström, D., Qvarnström, L., Riddarstolpe, P. & Drangert, J.-O. (2006). *Urine diversion: one step towards sustainable sanitation*. Stockholm: Stockholm Environment Institute. (EcoSanRes Publication Series; 2006–1). ISBN 978-91-975238-9-9.

de Lemos Chernicharo, C. A. (2007). *Anaerobic Reactors* [online]. London: IWA Publishing. Available from: <http://wio.iwaponline.com/cgi/doi/10.2166/9781780402116>. [Accessed 2018-04-27].

Levlin, E. & Hultman, B. (2003). *Phosphorus recovery from phosphate rich side-streams in wastewater treatment plants*. Stockholm: Dep. of Land and Water Resources Engineering,

Royal Institute of Technology.

Liao, P. ., Chen, A. & Lo, K. V. (1995). Removal of nitrogen from swine manure wastewaters by ammonia stripping. *Biosource Technology*, (54), pp 17–20.

Martinello, N. (2013). *Integrating experimental analyses and a dynamic model for enhancing the energy efficiency of a high-loaded activated sludge plant*. Diss. University of Padova.

Mehta, C. M., Khunjar, W. O., Nguyen, V., Tait, S. & Batstone, D. J. (2015). Technologies to Recover Nutrients from Waste Streams: A Critical Review. *Critical Reviews in Environmental Science and Technology*, 45(4), pp 385–427.

Minocha, V. K. & Rao, A. V. . P. (1988). Ammonia removal and recovery from urea fertilizer plant waste. *Environmental Technology Letters*, 9(7), pp 655–664.

Moerman, W., Carballa, M., Vandekerckhove, A., Derycke, D. & Verstraete, W. (2009). Phosphate removal in agro-industry: pilot and full-scale operational considerations of struvite crystallisation. *Proceedings of International Conference on Nutrient Recovery from Wastewater Streams*, London, 2009. London: IWA Publishing. ISBN 978-1-84339-232-3.

Nobel, P. (2105). *High-loaded Activated Sludge-Improvement of a solids retention time controlled system*. Diss. Lund: Lund University.

NuReSys. *Technology*. [online] (n.d.) (NuReSys-Recovers Natures Essentials). Available from: <http://www.nuresys.be/technology.html>. [Accessed 2018-03-11].

Olsson, G., Nielsen, M., Lynggaard Jensen, A., Yuan, Z. & Steyer, J.-P. (2005). *Instrumentation, Control and Automation in Wastewater systems*. London: IWA Publishing. (15).

Organics (n.d.a). ODSL11 Ammonia stripping systems. Organics. Available from: <https://www.organics.co.uk/DataSheets/ODSL11%20Ammonia%20stripping%20systems.pdf>. [Accessed 2018a-04-20].

Organics (n.d.b). ODSP09 Thermally-driven ammonia stripping. Organics. Available from: <https://www.organics.co.uk/DataSheets/ODSP09%20Thermally-driven%20ammonia%20stripping.pdf>. [Accessed 2018b-04-20].

Ostara Nutrient Recovery Technologies Inc. *Nutrient management solutions*. [online] (2017a) (Ostara). Available from: <http://ostara.com/nutrient-management-solutions/>. [Accessed 2018-02-06].

Ostara Nutrient Recovery Technologies Inc. (2017b). OSTARA Pearl. Ostara Nutrient Recovery Technologies Inc. Available from: [http://ostara.com/wp-content/uploads/2017/11/EU\\_Ostara\\_Pearl\\_Handout\\_171027.pdf](http://ostara.com/wp-content/uploads/2017/11/EU_Ostara_Pearl_Handout_171027.pdf). [Accessed 2018-02-06].

Ostara Nutrient Recovery Technologies Inc. (2017c). OSTARA WASSTRIP. Ostara Nutrient Recovery Technologies Inc. Available from: [http://ostara.com/wp-content/uploads/2017/04/Ostara\\_WASSTRIP\\_Handout\\_170411.pdf](http://ostara.com/wp-content/uploads/2017/04/Ostara_WASSTRIP_Handout_170411.pdf). [Accessed 2018-02-06].

Paques (n.d.). PHOSPAQ-Sustainable phosphorus recovery. Paques. Available from: <https://en.paques.nl/mediadepot/4124db800971/WEBbrochurePHOSPAQ.pdf>. [Accessed 2018-02-12].

Rieger, L., Gillot, S., Langergraber, G., Ohtsuki, T., Shaw, A., Takács, I. & Winkler, S. (2013). *Guidelines for using activated sludge models*. London: IWA Publishing. (Scientific and Technical Report; 22).

Salehi, S., Cheng, K. Y., Heitz, A. & Ginige, M. P. (2018). Re-visiting the Phostrip process to recover phosphorus from municipal wastewater. *Chemical Engineering Journal*, 343, pp 390–398.

Schultz, C. (2009). Sustainable Solution for Phosphate and Ammonium Removal. *Pollution Solution* [online], (September 2009). Available from: <https://www.pollutionsolutions-online.com/article/water-wastewater/17/paques/sustainable-solution-for-phosphate-and-ammonium-removal/490>.

Smolders, G. J. F., Van der Meij, J., Van Loosdrecht, M. C. M. & Heijnen, J. J. (1994). Model of the anaerobic metabolism of the biological phosphorus removal process: stoichiometry and pH influence. *Biotechnology and bioengineering*, 43(6), pp 461–470.

Steen, I. (1998). Phosphorus availability in the 21st century Management of a non-renewable resource. *Phosphorus & Potassium*, (217).

Svenskt Vatten (2013). *Avloppsteknik 2 Reningsprocessen*. 3rd. ed Stockholm: Svenskt Vatten AB.

Takacs, I., Patry, G. G. & Nolasco, D. (1991). A dynamic model of the clarification-thickening process. *Water Research*, 25(10), pp 1263–1271.

Tchobanoglous, G., Stensel, H. D., Tsuchihashi, R., Burton, F., Abu-Orf, M., Bowden, G. & Pfrang, W. (2014a). Chapter 1 Introduction to Wastewater Treatment and Process Analysis. *Wastewater Engineering Treatment and Resource Recovery*. 5th, International ed. ed, pp 1–56. New York: McGraw-Hill Education. ISBN 978-1-259-01079-8.

Tchobanoglous, G., Stensel, H. D., Tsuchihashi, R., Burton, F., Abu-Orf, M., Bowden, G. & Pfrang, W. (2014b). Chapter 2 Wastewater Characteristics. *Wastewater Engineering Treatment and Resource Recovery*. 5th, International ed. ed, pp 57–181. New York: McGraw-Hill Education. ISBN 978-1-259-01079-8.

Tchobanoglous, G., Stensel, H. D., Tsuchihashi, R., Burton, F., Abu-Orf, M., Bowden, G. & Pfrang, W. (2014c). Chapter 7 Fundamentals of biological treatment. *Wastewater Engineering Treatment and Resource Recovery*. 5th, International ed. ed, pp 551–674. New York: McGraw-Hill Education. ISBN 978-1-259-01079-8.

Tchobanoglous, G., Stensel, H. D., Tsuchihashi, R., Burton, F., Abu-Orf, M., Bowden, G. & Pfrang, W. (2014d). Chapter 15 Plant recycle flow treatment and nutrient recovery. *Metcalf & Eddy I AECOM. Wastewater Engineering Treatment and Resource Recovery*. 5th, International ed. ed, pp 551–674. New York: McGraw-Hill Education. ISBN 978-1-259-01079-8.

Vaclav, S. (2000). Phosphorus in the environment: Natural flows and human interferences. *Annual review of Energy and the Environment*, 25.

Veolia Water Technologies (2015). Struvia- Sustainable recycling of phosphorus from wastewater. Veolia Water Technologies. Available from: [http://technomaps.veoliawatertechnologies.com/processes/lib/municipal/3351,150354\\_Mkt\\_Mun\\_Brochure\\_STRUVIA\\_EN\\_.pdf](http://technomaps.veoliawatertechnologies.com/processes/lib/municipal/3351,150354_Mkt_Mun_Brochure_STRUVIA_EN_.pdf). [Accessed 2018-03-15].

Wahlberg, E. (2006). Determine the Effect of Individual Wastewater Characteristics and Variances on Primary Clarifier Performance. *Water Intelligence Online*, 5(0), pp 9781843397243–9781843397243.

Water Environment Federation (2005). *Clarifier Design*. 2nd. ed s.l.: McGraw-Hill.

Wilsenach, J. & Van Loosdrecht, M. (2003). Impact of separate urine collection on wastewater treatment systems. *Water Science & Technology*, 48(1), pp 103–110.

Zarebska, A., Romero Nieto, D., Christensen, K. V., Fjerbæk Søtoft, L. & Norddahl, B. (2015). Ammonium Fertilizers Production from Manure: A Critical Review. *Critical Reviews in Environmental Science and Technology*, 45(14), pp 1469–1521.

#### **Personal communication**

Gustavsson, D. (pers.contact). Through meetings and emails during 2017-2018. Sweden Water Research/VA SYD.

## APPENDIX

### A. MODELLED VS. MEASURED INFLUENT FOR SCENARIO 0

In the figure below, Figure A1 is the measured flow compared with the flow generated by the model for the scenario with no urine diversion. The diamonds illustrated the measured data and the grey line the modelled influent flow.

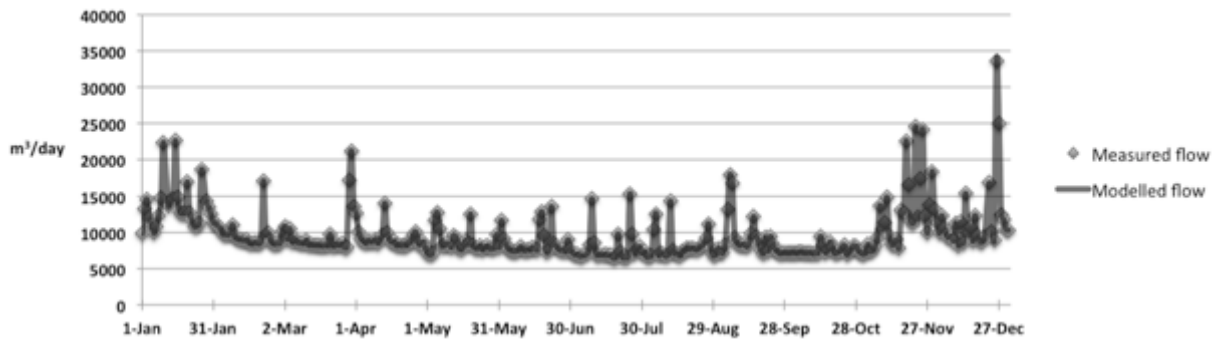


Figure A1: The graph shows the measured influent flow rate to Sjölanda in 2015, marked with grey diamonds. The grey line illustrates the modelled influent flow rate to the modelled WWTP for scenario 0 with no urine diversion. The flow rate is given in  $m^3$  per day.

In the Figure A1 it is clearly seen that the modelled influent flow rate follows the same pattern as the measured data. In the figure below, Figure A2, is the measured COD compared with the influent COD generated by the model for the scenario with no urine diversion.

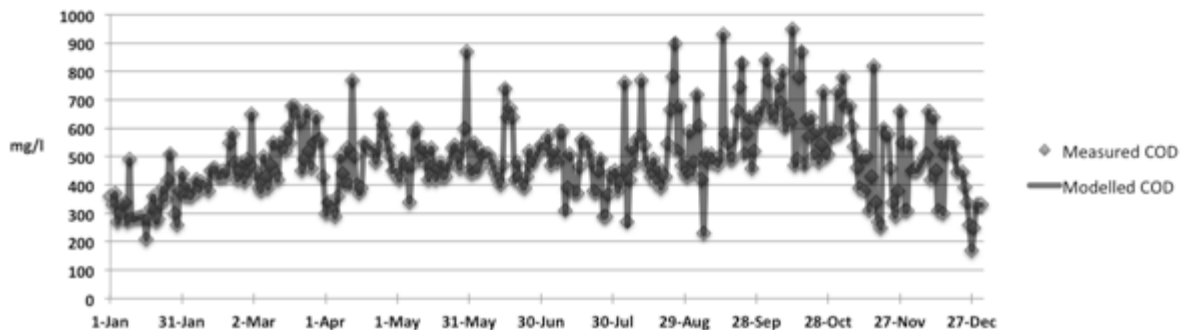


Figure A2: The graph shows the measured influent concentration of COD to Sjölanda in 2015, marked with grey diamonds. The grey line illustrates the modelled influent concentration of COD to the modelled WWTP for scenario 0 with no urine diversion. The concentration is given in mg per litre.

The pattern of the influent measured COD concentration is also represented in the modelled influent COD. In Figure A3 is the measured TSS compared with the TSS generated by the model for the scenario with no urine diversion. The modelled TSS concentration corresponds well with the measured.

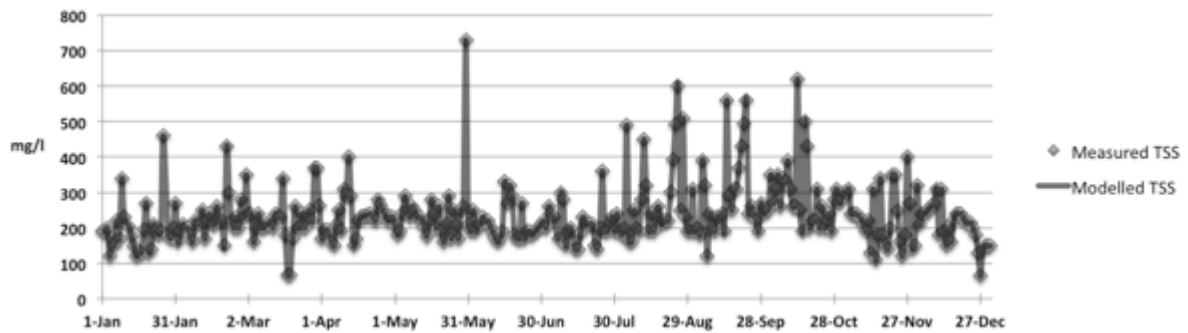


Figure A3: The graph shows the measured influent concentration of TSS to Sjölunda in 2015, marked with grey diamonds. The grey line illustrates the modelled influent concentration of TSS to the modelled WWTP for scenario 0 with no urine diversion. The concentration is given in mg per litre.

In the figure below, Figure A4, is the measured TKN concentration compared with the TKN generated by the model for the scenario with no urine diversion. Both the measured TKN and the modelled TKN follows the same pattern.

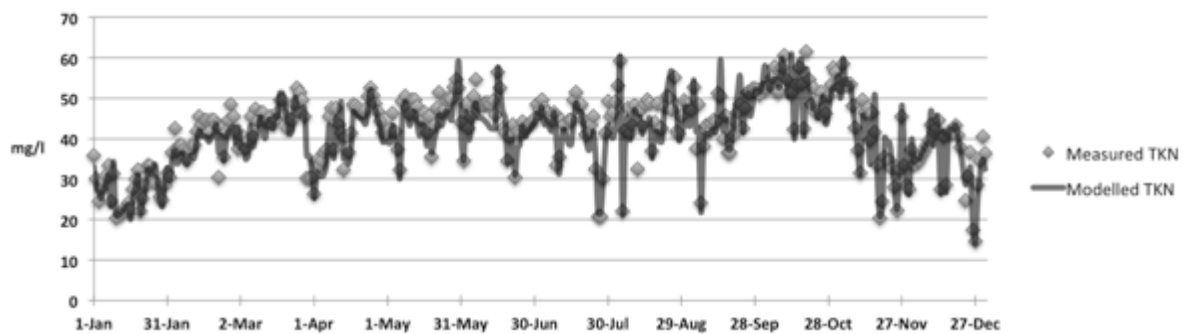


Figure A4: The graph shows the measured influent concentration of TKN to Sjölunda in 2015, marked with grey diamonds. The grey line illustrates the modelled influent concentration of TKN to the modelled WWTP for scenario 0 with no urine diversion. The concentration is given in mg per litre.

In the figure below, Figure A5, is the measured TP concentration, given in mg/l, compared with the TP generated by the model for the scenario with no urine diversion.

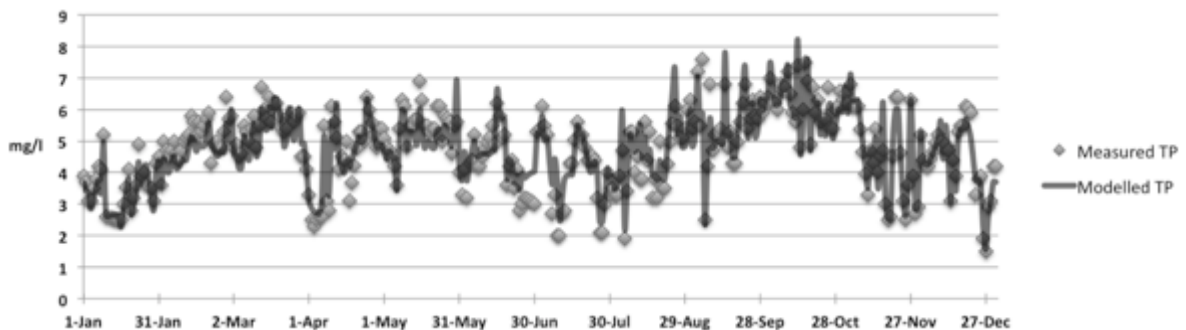


Figure A5: The graph shows the measured influent concentration of TP to Sjölunda in 2015, marked with grey diamonds. The grey line illustrates the modelled influent concentration of TP to the modelled WWTP for scenario 0 with no urine diversion. The concentration is given in mg per litre.

The modelled TP concentration corresponds well with the measured data.

## B. INPUT DATA FOR SCENARIO 0

Date	#t #d	Water m3/d	COD g/m3	TSS g/m3	TKN g/m3	TP g/m3
01/01/15	1	9832,1	360,0	190,0	35,9	3,9
02/01/15	2	13215,6	330,0	190,0	30,1	3,7
03/01/15	3	14573,6	370,0	200,0	24,6	3,1
04/01/15	4	11959,7	270,0	120,0	27,6	3,1
05/01/15	5	11067,9	300,0	170,0	29,5	3,5
06/01/15	6	9915,2	330,0	150,0	30,8	3,8
07/01/15	7	10857,1	340,0	220,0	33,4	4,2
08/01/15	8	12306,5	270,0	170,0	24,5	4,1
09/01/15	9	14693,7	490,0	340,0	31,4	5,2
10/01/15	10	22415,5	280,0	230,0	20,4	2,6
12/01/15	11	13633,4	282,5	203,3	21,3	2,6
13/01/15	12	14368,0	285,0	176,0	22,2	2,6
14/01/15	13	14602,8	287,5	148,3	23,2	2,5
15/01/15	14	22667,5	290,0	120,0	24,1	2,5
16/01/15	15	14871,6	210,0	130,0	22,2	2,5
17/01/15	16	12743,6	280,0	130,0	27,5	3,0
18/01/15	17	12618,1	320,0	194,3	30,1	3,5
19/01/15	18	12732,3	360,0	270,0	32,3	4,1
20/01/15	19	16937,4	270,0	130,0	22,0	2,8
21/01/15	20	12748,3	280,0	140,0	25,3	3,2
22/01/15	21	11720,7	330,0	210,0	28,4	3,6
23/01/15	22	10840,5	390,0	190,0	33,5	4,9
24/01/15	23	10898,2	350,0	180,0	33,3	3,9
25/01/15	24	11182,0	420,0	190,0	30,1	4,0
26/01/15	25	18663,8	510,0	460,0	29,0	3,6
28/01/15	26	14263,0	300,0	180,0	25,6	3,5
29/01/15	27	13488,5	260,0	170,0	24,9	3,1
30/01/15	28	12508,2	380,0	200,0	28,5	4,3
31/01/15	29	11385,4	440,0	270,0	31,5	4,5
01/02/15	30	11205,2	360,0	160,0	30,5	3,6
02/02/15	31	10830,7	400,0	190,0	36,5	5,0
03/02/15	32	10590,0	360,0	210,0	42,5	4,7
04/02/15	33	9791,6	360,0	200,0	37,2	4,5
05/02/15	34	9774,2	390,0	200,0	38,5	4,7
06/02/15	35	9697,8	420,0	180,0	38,5	5,0
07/02/15	36	9900,7	380,0	160,0	37,5	4,6
08/02/15	37	11046,9	410,0	220,0	34,5	4,4
09/02/15	38	9405,0	405,0	215,0	37,6	4,7
10/02/15	39	9168,6	400,0	210,0	38,5	5,0
11/02/15	40	9031,3	380,0	250,0	38,5	5,1

12/02/15	41	9014,3	450,0	170,0	41,8	5,2
13/02/15	42	8913,5	460,0	220,0	45,5	5,8
14/02/15	43	8991,8	460,0	240,0	43,5	5,6
15/02/15	44	8540,5	430,0	210,0	44,5	5,2
16/02/15	45	8423,8	430,0	210,0	44,5	5,6
17/02/15	46	8533,0	450,0	260,0	41,5	5,3
18/02/15	47	8590,9	430,0	220,0	44,5	5,5
19/02/15	48	8432,6	450,0	220,0	44,5	5,7
20/02/15	49	8710,4	550,0	150,0	43,5	5,9
21/02/15	50	17101,0	580,0	430,0	30,5	4,3
22/02/15	51	9633,5	480,0	300,0	42,5	4,9
23/02/15	52	9922,9	420,0	220,0	35,5	5,0
24/02/15	53	8913,7	450,0	200,0	41,5	4,8
25/02/15	54	8448,4	480,0	230,0	44,5	4,8
26/02/15	55	8416,1	410,0	200,0	48,5	5,3
27/02/15	56	8545,9	490,0	280,0	45,5	6,4
28/02/15	57	8468,5	440,0	230,0	41,5	5,7
01/03/15	58	10203,7	650,0	350,0	37,5	5,8
02/03/15	59	10819,6	460,0	240,0	38,5	4,8
03/03/15	60	9069,1	440,0	240,0	40,5	4,9
04/03/15	61	10534,6	390,0	160,0	37,5	4,5
05/03/15	62	8684,9	380,0	200,0	39,3	4,6
06/03/15	63	9113,9	500,0	240,0	45,5	5,5
07/03/15	64	8743,3	430,0	200,0	40,5	5,3
08/03/15	65	8583,9	390,0	200,0	47,3	5,0
09/03/15	66	8548,5	470,0	210,0	44,4	5,4
10/03/15	67	8468,3	550,0	210,0	46,5	5,8
11/03/15	68	8931,5	440,0	220,0	46,4	4,8
12/03/15	69	8283,0	420,0	200,0	44,4	5,5
13/03/15	70	8328,0	550,0	240,0	44,5	6,7
14/03/15	71	8248,1	550,0	230,0	45,5	6,0
15/03/15	72	8264,3	520,0	230,0	43,5	5,7
16/03/15	73	8221,4	600,0	340,0	44,5	6,4
17/03/15	74	8180,5	550,0	180,0	46,5	5,6
18/03/15	75	8171,7	680,0	68,0	49,5	6,2
19/03/15	76	8223,0	680,0	68,0	49,5	6,2
20/03/15	77	8189,6	650,0	168,8	45,9	5,8
21/03/15	78	9760,0	620,0	260,0	42,5	5,4
22/03/15	79	8183,5	450,0	200,0	44,5	5,3
23/03/15	80	8175,7	490,0	200,0	44,5	5,4
24/03/15	81	8386,7	660,0	240,0	48,5	5,8
25/03/15	82	8237,5	520,0	200,0	52,5	5,9
26/03/15	83	8468,0	460,0	240,0	51,5	5,6
27/03/15	84	7989,6	550,0	250,0	49,5	5,8
28/03/15	85	7930,2	640,0	220,0	45,5	5,9
29/03/15	86	17185,0	560,0	370,0	30,2	4,5

30/03/15	87	21197,1	560,0	370,0	30,2	4,5
31/03/15	88	13525,0	430,0	263,9	30,5	4,1
01/04/15	89	12634,4	300,0	170,0	26,3	3,3
02/04/15	90	10014,4	340,0	192,7	34,5	2,5
03/04/15	91	9154,3	340,0	195,0	33,5	2,3
04/04/15	92	8821,0	310,0	180,0	34,5	2,5
05/04/15	93	8563,1	290,0	160,0	36,5	2,6
06/04/15	94	8830,1	360,0	150,0	37,3	2,6
07/04/15	95	8733,4	500,0	210,0	45,4	5,5
08/04/15	96	8711,0	440,0	250,0	47,5	3,1
09/04/15	97	8998,5	400,0	190,0	37,4	2,8
10/04/15	98	8504,1	530,0	310,0	47,5	6,1
11/04/15	99	9088,6	400,0	290,0	43,5	5,6
12/04/15	100	9602,4	770,0	400,0	41,5	5,1
13/04/15	101	14033,0	500,0	290,0	32,3	4,1
14/04/15	102	9983,3	400,0	150,0	40,4	4,5
15/04/15	103	8990,7	370,0	170,0	36,5	4,4
16/04/15	104	8695,6	390,0	220,0	41,5	5,0
17/04/15	105	8747,4	550,0	230,0	48,5	3,1
18/04/15	106	8215,4	542,5	232,7	48,0	3,7
19/04/15	107	8269,1	535,0	235,3	47,5	4,2
20/04/15	108	8205,2	527,5	237,7	47,0	4,8
21/04/15	109	8216,8	520,0	240,0	46,5	5,3
22/04/15	110	8158,5	480,0	230,0	47,2	5,3
23/04/15	111	8638,8	530,0	220,0	50,5	5,0
24/04/15	112	8685,1	650,0	280,0	52,5	6,4
25/04/15	113	9648,5	612,5	265,3	50,7	6,0
26/04/15	114	10043,0	575,0	250,3	48,7	5,6
27/04/15	115	8512,0	537,5	235,3	46,6	5,2
28/04/15	116	8295,4	500,0	220,0	44,4	4,8
29/04/15	117	8713,6	450,0	230,0	41,5	5,4
30/04/15	118	7892,1	450,0	230,0	41,5	5,4
01/05/15	119	7143,7	435,0	204,4	42,1	5,1
02/05/15	120	6938,6	420,0	180,0	42,5	4,8
03/05/15	121	7111,1	490,0	190,0	46,2	4,7
04/05/15	122	11702,5	480,0	241,1	41,7	4,4
05/05/15	123	12765,7	470,0	290,0	37,4	4,2
06/05/15	124	10512,0	340,0	250,0	32,3	3,6
07/05/15	125	8164,2	470,0	230,0	49,1	5,4
08/05/15	126	8186,3	590,0	260,0	50,5	6,3
09/05/15	127	8475,8	600,0	250,0	47,5	6,1
10/05/15	128	8236,2	490,0	230,0	46,1	4,8
11/05/15	129	7991,2	530,0	230,0	49,5	5,5
12/05/15	130	9522,8	530,0	227,5	49,5	5,5
13/05/15	131	9300,0	475,0	201,7	47,9	5,7
14/05/15	132	7847,4	420,0	176,3	45,5	5,7

15/05/15	133	7608,7	530,0	220,0	44,5	6,9
16/05/15	134	8098,5	470,0	280,0	46,5	6,3
17/05/15	135	8892,1	420,0	240,0	41,4	5,5
18/05/15	136	8412,6	460,0	200,0	45,5	5,5
19/05/15	137	12531,3	480,0	260,0	35,4	5,3
20/05/15	138	8210,2	430,0	190,0	43,2	5,4
21/05/15	139	7880,6	430,0	160,0	47,5	5,4
22/05/15	140	7791,8	470,0	210,0	51,5	6,1
23/05/15	141	8206,3	480,0	290,0	46,5	6,1
24/05/15	142	7633,8	530,0	170,0	47,2	5,0
25/05/15	143	7978,3	540,0	250,0	49,3	5,8
26/05/15	144	8114,5	500,0	208,1	49,9	5,7
27/05/15	145	7827,9	460,0	170,0	49,8	5,6
28/05/15	146	7784,1	530,0	250,0	52,8	4,6
29/05/15	147	7876,8	600,0	260,0	54,5	5,5
30/05/15	148	9708,8	870,0	730,0	52,5	5,6
31/05/15	149	7929,9	450,0	210,0	44,1	4,0
01/06/15	150	11609,8	440,0	190,0	34,4	3,3
02/06/15	151	9083,3	550,0	250,0	48,5	4,1
03/06/15	152	8248,2	450,0	190,0	42,4	3,2
04/06/15	153	7741,8	460,0	210,0	45,3	4,3
05/06/15	154	7543,8	520,0	210,0	50,5	4,4
06/06/15	155	7445,8	500,0	230,0	54,5	5,2
07/06/15	156	7427,2	510,0	220,0	48,3	4,2
08/06/15	157	7526,5	510,0	220,0	48,3	4,2
09/06/15	158	7996,3	487,5	204,1	48,7	4,5
10/06/15	159	7596,8	465,0	188,9	48,9	4,7
11/06/15	160	7526,4	442,5	174,1	48,8	4,9
12/06/15	161	7651,2	420,0	160,0	48,5	5,1
13/06/15	162	7570,9	400,0	170,0	49,4	5,5
14/06/15	163	7908,2	470,0	190,0	45,9	4,9
15/06/15	164	7749,4	740,0	330,0	56,5	6,2
16/06/15	165	7608,2	640,0	270,0	52,5	5,8
17/06/15	166	11720,9	670,0	320,0	42,5	5,1
18/06/15	167	12802,1	640,0	290,0	41,5	5,2
19/06/15	168	9563,2	420,0	180,0	34,5	3,6
20/06/15	169	7262,5	480,0	170,0	40,5	4,2
21/06/15	170	7618,2	430,0	170,0	43,5	4,4
22/06/15	171	13521,7	400,0	270,0	30,5	3,5
23/06/15	172	8432,6	390,0	170,0	41,5	4,1
24/06/15	173	8169,2	430,0	190,0	41,4	2,8
25/06/15	174	7703,6	520,0	190,0	44,3	3,0
26/06/15	175	7563,2	470,0	180,0	42,5	3,2
27/06/15	176	7620,3	487,5	187,4	43,2	3,2
28/06/15	177	7369,4	505,0	194,9	43,8	3,1
29/06/15	178	8961,6	522,5	202,4	44,4	3,1

30/06/15	179	7588,4	540,0	210,0	44,9	3,0
01/07/15	180	7207,5	540,0	220,0	48,5	5,3
02/07/15	181	6960,6	530,0	200,0	47,1	5,4
03/07/15	182	6959,6	570,0	260,0	49,5	6,1
04/07/15	183	6719,5	470,0	240,0	47,5	5,5
05/07/15	184	6762,5	520,0	230,0	46,5	5,2
07/07/15	185	7084,3	480,0	170,0	44,3	2,7
08/07/15	186	8294,1	590,0	300,0	46,5	3,3
09/07/15	187	14608,2	590,0	280,0	33,5	2,0
10/07/15	188	8561,1	310,0	150,0	35,5	2,0
11/07/15	189	6928,0	390,0	190,0	44,5	2,7
12/07/15	190	6898,6	510,0	200,0	43,5	2,8
14/07/15	191	6927,3	370,0	140,0	44,5	4,3
15/07/15	192	6943,9	370,0	140,0	44,5	4,3
16/07/15	193	6840,7	465,0	183,5	49,5	5,0
17/07/15	194	6879,6	560,0	230,0	51,5	5,6
18/07/15	195	6489,2	550,0	210,0	48,5	5,2
19/07/15	196	6531,5	550,0	210,0	48,5	5,2
20/07/15	197	9771,2	515,0	211,0	44,7	4,8
21/07/15	198	7323,3	480,0	210,0	41,0	4,4
22/07/15	199	6563,8	380,0	150,0	41,7	4,4
23/07/15	200	6638,8	370,0	140,0	43,5	4,5
24/07/15	201	6510,8	450,0	200,0	45,5	4,4
25/07/15	202	15287,5	490,0	360,0	32,5	3,2
26/07/15	203	9706,4	290,0	190,0	20,7	2,1
27/07/15	204	7041,1	290,0	190,0	20,7	2,1
28/07/15	205	7706,6	365,0	215,0	30,1	3,0
29/07/15	206	8027,5	440,0	230,0	41,4	4,0
30/07/15	207	7153,3	430,0	190,0	49,2	3,3
31/07/15	208	7367,2	450,0	240,0	45,5	3,5
01/08/15	209	6693,0	380,0	190,0	46,5	3,3
02/08/15	210	6724,8	410,0	180,0	49,0	3,3
03/08/15	211	6752,9	450,0	200,0	53,1	3,9
04/08/15	212	10382,8	760,0	490,0	59,3	4,7
05/08/15	213	12532,4	270,0	160,0	22,1	1,9
06/08/15	214	6883,0	420,0	160,0	41,9	3,4
07/08/15	215	7215,8	530,0	250,0	47,5	5,3
08/08/15	216	7022,3	470,0	200,0	41,4	5,3
09/08/15	217	6753,6	560,0	190,0	43,2	4,0
10/08/15	218	6898,2	570,0	280,0	48,3	4,5
11/08/15	219	14303,0	770,0	450,0	32,4	3,8
12/08/15	220	7546,0	540,0	320,0	47,0	3,8
13/08/15	221	7070,0	480,0	190,0	43,1	5,6
14/08/15	222	7012,8	460,0	240,0	48,5	4,4
15/08/15	223	6748,4	430,0	190,0	49,5	5,3
16/08/15	224	7366,2	490,0	240,0	48,9	3,2

17/08/15	225	7507,2	410,0	260,0	36,9	3,8
18/08/15	226	7886,5	460,0	210,0	44,0	3,2
19/08/15	227	7745,9	390,0	220,0	48,7	5,0
20/08/15	228	7868,6	430,0	220,0	42,6	3,5
21/08/15	229	7722,0	430,0	220,0	42,6	3,5
22/08/15	230	7622,0	547,5	301,3	47,9	4,3
23/08/15	231	7850,2	665,0	391,8	50,4	5,0
24/08/15	232	8177,5	782,5	491,3	50,2	5,6
25/08/15	233	8399,7	900,0	600,0	47,1	6,1
26/08/15	234	9249,5	520,0	250,0	55,1	5,5
27/08/15	235	11179,8	680,0	510,0	41,8	5,1
28/08/15	236	7966,4	470,0	230,0	41,2	5,1
29/08/15	237	6844,1	440,0	190,0	45,5	5,4
30/08/15	238	6915,1	430,0	190,0	49,4	6,0
31/08/15	239	7754,9	590,0	310,0	48,9	6,3
01/09/15	240	7377,3	440,0	190,0	48,4	5,4
02/09/15	241	7147,0	480,0	200,0	46,9	5,6
03/09/15	242	8226,2	720,0	180,0	52,8	7,2
04/09/15	243	13145,1	610,0	390,0	37,5	5,5
05/09/15	244	17953,7	420,0	320,0	48,5	7,6
06/09/15	245	16778,9	230,0	120,0	24,1	2,5
07/09/15	246	9179,5	510,0	240,0	38,1	4,2
08/09/15	247	8599,6	480,0	200,0	43,3	6,8
09/09/15	248	8265,9	510,0	190,0	41,3	4,7
10/09/15	249	8291,8	480,0	230,0	43,9	5,2
11/09/15	250	8367,0	490,0	230,0	44,5	5,3
12/09/15	251	8063,0	470,0	240,0	44,2	5,4
13/09/15	252	8395,0	500,0	190,0	51,3	5,0
14/09/15	253	9811,7	930,0	560,0	50,4	6,8
15/09/15	254	12169,5	580,0	290,0	39,9	4,8
16/09/15	255	9394,8	550,0	250,0	45,6	5,3
17/09/15	256	8850,9	490,0	310,0	36,6	4,3
18/09/15	257	7500,8	490,0	310,0	36,6	4,3
19/09/15	258	7124,0	575,0	369,8	40,7	5,0
20/09/15	259	9308,8	660,0	431,4	44,0	5,6
21/09/15	260	7400,8	745,0	494,8	46,6	6,2
22/09/15	261	9420,0	830,0	560,0	48,5	6,8
23/09/15	262	8355,8	510,0	240,0	42,5	5,4
24/09/15	263	7663,8	580,0	260,0	47,5	5,7
25/09/15	264	7403,9	640,0	240,0	51,5	6,3
26/09/15	265	7128,7	460,0	220,0	51,5	5,8
27/09/15	266	7162,3	520,0	190,0	52,3	5,7
28/09/15	267	7212,1	650,0	270,0	52,4	6,4
29/09/15	268	7169,9	630,0	240,0	52,1	5,9
30/09/15	269	7164,1	670,0	250,0	50,9	6,2
01/10/15	270	7219,7	680,0	250,0	52,6	6,4

02/10/15	271	7212,3	840,0	350,0	52,5	7,0
03/10/15	272	7151,0	770,0	270,0	52,5	6,2
04/10/15	273	7260,7	640,0	310,0	53,1	6,2
05/10/15	274	7289,4	660,0	350,0	55,1	6,0
06/10/15	275	7184,9	630,0	260,0	57,7	6,8
07/10/15	276	7190,8	750,0	340,0	51,7	6,6
08/10/15	277	7183,4	690,0	330,0	51,6	6,7
09/10/15	278	7175,8	800,0	390,0	57,5	7,2
10/10/15	279	7089,8	600,0	310,0	60,5	6,5
11/10/15	280	7226,6	650,0	260,0	54,5	5,9
12/10/15	281	7127,9	620,0	260,0	51,5	5,6
13/10/15	282	9411,3	950,0	620,0	51,5	7,4
14/10/15	283	8312,1	470,0	250,0	42,3	4,8
15/10/15	284	7243,1	490,0	190,0	53,3	6,0
16/10/15	285	7573,2	780,0	500,0	57,5	7,5
17/10/15	286	8663,1	870,0	430,0	53,5	6,9
18/10/15	287	7986,0	470,0	200,0	42,5	4,9
19/10/15	288	7164,3	630,0	220,0	61,5	6,7
20/10/15	289	7237,1	570,0	220,0	54,5	5,9
21/10/15	290	7338,7	640,0	310,0	48,5	6,3
22/10/15	291	7826,8	500,0	200,0	52,5	5,6
23/10/15	292	8207,6	590,0	260,0	46,5	5,7
24/10/15	293	6968,3	480,0	200,0	49,5	5,7
25/10/15	294	7272,8	540,0	220,0	51,4	6,7
26/10/15	295	7684,0	730,0	240,0	45,5	5,4
27/10/15	296	8106,0	500,0	190,0	46,1	5,4
28/10/15	297	8094,9	510,0	280,0	50,5	6,0
29/10/15	298	7457,5	600,0	310,0	53,3	6,1
30/10/15	299	7168,7	570,0	270,0	57,5	6,6
31/10/15	300	7025,1	580,0	280,0	56,5	6,3
01/11/15	301	7176,9	730,0	300,0	54,0	6,5
02/11/15	302	8325,1	580,0	300,0	52,7	6,2
03/11/15	303	7440,3	780,0	310,0	58,5	6,8
04/11/15	304	7494,3	680,0	240,0	53,5	6,1
05/11/15	305	8143,7	680,0	240,0	53,5	6,1
06/11/15	306	9371,9	680,0	240,0	53,5	6,1
07/11/15	307	13723,9	607,5	234,8	48,1	5,4
08/11/15	308	10415,8	535,0	224,7	42,7	4,7
09/11/15	309	11356,9	462,5	209,8	37,1	4,0
10/11/15	310	14808,9	390,0	190,0	31,5	3,3
11/11/15	311	9567,5	500,0	220,0	49,5	4,7
12/11/15	312	8372,0	380,0	130,0	46,5	4,3
13/11/15	313	8314,5	500,0	310,0	47,5	5,4
14/11/15	314	8985,0	310,0	110,0	39,5	4,0
15/11/15	315	7876,7	430,0	180,0	46,5	4,5
16/11/15	316	13005,5	820,0	340,0	41,5	4,7

17/11/15	317	12749,9	340,0	180,0	33,5	3,0
18/11/15	318	22618,1	270,0	150,0	20,5	2,5
19/11/15	319	16539,5	250,0	140,0	24,5	2,6
20/11/15	320	11454,1	600,0	200,0	35,5	4,5
21/11/15	321	11309,6	580,0	350,0	34,5	6,4
22/11/15	322	24636,7	580,0	350,0	34,5	6,4
23/11/15	323	12058,0	460,0	247,0	32,7	4,6
24/11/15	324	17346,8	340,0	160,0	28,0	3,1
25/11/15	325	24239,4	290,0	120,0	22,2	2,5
26/11/15	326	12342,0	380,0	180,0	32,2	3,6
27/11/15	327	9927,3	660,0	400,0	45,5	6,3
28/11/15	328	13827,5	550,0	270,0	33,5	3,9
29/11/15	329	18398,8	310,0	140,0	28,5	2,7
30/11/15	330	13191,2	310,0	150,0	27,5	2,9
01/12/15	331	11336,9	550,0	320,0	37,3	5,2
02/12/15	332	9922,7	450,0	210,0	33,5	4,4
03/12/15	333	12303,3	450,0	240,0	34,5	4,2
04/12/15	334	10544,4	450,0	240,0	34,5	4,2
05/12/15	335	9672,5	465,0	247,5	35,7	4,4
06/12/15	336	9305,9	480,0	255,1	37,0	4,7
07/12/15	337	9478,5	495,0	262,5	38,2	4,9
08/12/15	338	8900,0	510,0	270,0	39,5	5,2
09/12/15	339	11225,5	660,0	310,0	43,5	5,0
10/12/15	340	8120,1	420,0	180,0	41,5	4,8
11/12/15	341	11393,5	640,0	310,0	42,5	4,9
12/12/15	342	8541,9	450,0	190,0	44,5	4,7
13/12/15	343	15344,3	310,0	150,0	27,5	3,1
14/12/15	344	9820,2	550,0	200,0	40,5	4,4
15/12/15	345	10718,8	300,0	160,0	28,5	3,9
16/12/15	346	8821,1	510,0	220,0	41,5	5,3
17/12/15	347	12326,3	550,0	240,0	41,5	5,5
18/12/15	348	9561,1	550,0	240,0	41,5	5,5
19/12/15	349	8739,5	550,0	240,0	43,3	6,1
20/12/15	350	8681,0	497,5	228,7	40,8	6,1
21/12/15	351	9382,2	445,0	214,9	38,0	5,9
23/12/15	352	16809,3	445,0	214,9	24,7	3,3
24/12/15	353	10018,8	392,5	198,7	30,6	3,8
25/12/15	354	8853,0	340,0	180,0	36,5	3,9
26/12/15	355	33623,3	260,0	130,0	17,5	1,9
27/12/15	356	25053,0	170,0	65,0	14,7	1,5
28/12/15	357	12453,8	250,0	140,0	28,5	2,9
29/12/15	358	11783,6	330,0	150,0	34,5	3,1
30/12/15	359	10436,8	330,0	150,0	40,4	4,2
31/12/15	360	10330,7	330,0	150,0	36,5	4,2